

Christoph Lauterbach

Potential, system analysis and preliminary design of low-temperature solar process heat systems



Christoph Lauterbach

Potential, system analysis and preliminary design
of low-temperature solar process heat systems

This work has been accepted by the Faculty of Mechanical Engineering of the University of Kassel as a doctoral thesis for acquiring the academic degree of Doktor der Ingenieurwissenschaften (Dr.-Ing.). The research was executed at the Group of Solar and System Engineering, Institute of Thermal Engineering.

Supervisor: Prof. Dr. Klaus Vajen, University of Kassel
Co-Supervisor: Prof. Dr. Víctor Martínez Moll, University of the Balearic Islands

Examiners: Dr. Ulrike Jordan, University of Kassel
Prof. Dr. Jens Knissel, University of Kassel

Defense day: 28th February 2014

Bibliographic information published by Deutsche Nationalbibliothek
The Deutsche Nationalbibliothek lists this publication in the Deutsche Nationalbibliografie;
detailed bibliographic data is available in the Internet at <http://dnb.dnb.de>.

Zugl.: Kassel, Univ., Diss. 2014
ISBN 978-3-86219-742-2 (print)
ISBN 978-3-86219-743-9 (e-book)
URN: <http://nbn-resolving.de/urn:nbn:de:0002-37430>

© 2014, kassel university press GmbH, Kassel
www.uni-kassel.de/upress

Printing Shop: Print Management Logistics Solutions GmbH & Co. KG, Kassel
Printed in Germany

Abstract

The industrial sector is very promising for the use of solar thermal technology, since it accounts for a large share of the total final energy consumption (e.g. 27 % in Germany in 2010) and it predominantly uses the consumed energy as thermal energy (74 % in Germany in 2010). In order to develop this area of application, it is necessary to understand which industrial sectors have the highest potential, which processes within these sectors are most suitable for the integration of solar heat as well as to quantify the possible contribution to the industrial heat demand. For this thesis, the industrial heat consumption in Germany is analyzed, which leads to the selection of the 11 most promising sectors within industry. These are Chemicals, Food and beverages, Motor vehicles, Paper, Fabricated metal, Machinery and equipment, Rubber and plastic, Electrical equipment, Textiles, Printing and Wood. The theoretical potential of solar heat for industrial processes below 300 °C in Germany adds up to 134 TWh per year, the technical potential (considering efficiency measures, limited roof area and a solar fraction) being 16 TWh per year or 3.4 % of the overall industrial heat demand.

Solar thermal systems can achieve higher system yields in industrial applications compared to domestic ones. At the same time, systems can be more complex in industrial applications. In order to design and operate solar process heat systems efficiently and to exploit the large potential, possible faults of such systems and their impact have to be evaluated. In this thesis, an implemented solar process heat system is methodically analyzed based on measurements and simulations with a validated model. Several faults are identified and their influence, as well as the influence of a reduced load on the system yield is evaluated. The analysis shows that a reduced load is most influential. Further, the most important impact factors on the system performance are identified: the collector parameters (η_0 , a_1) and load characteristics (mass flow, temperature).

The design of solar process heat systems is in many cases very demanding, hence costly. This high effort is a major barrier for a further development of solar heat for industrial applications. The decision to install solar thermal systems is in most cases based on solar heat generation cost. Collector field and heat store size are the most important figures for the estimation of the overall cost of a solar thermal system. Therefore, a simple approach for dimensioning the collector field and heat store is developed in this thesis in order to enable manufacturers and planners on one hand and costumers on the other hand to make a decision in favor or against a solar process heat system. In addition to investment cost, the specific system yield, which is determined for selected process heat applications in this thesis, is necessary to calculate solar heat generation cost. Finally, indications on the necessary accuracy of the load profile are provided to help to reduce effort in the design phase.

Zusammenfassung

Die Industrie stellt aufgrund ihres großen Anteils am Endenergieverbrauch von z.B. 27 % in Deutschland und der Tatsache, dass ein Großteil (74 % in Deutschland im Jahr 2010) davon als thermische Energie benötigt wird, ein aussichtsreiches Anwendungsfeld für die Nutzung thermischer Solarenergie dar. Für die verstärkte Nutzung thermischer Solarenergie in der Industrie ist es erforderlich, die aussichtsreichsten Wirtschaftszweige und industriellen Prozesse für die Nutzung thermischer Solarenergie zu identifizieren und ihren möglichen Beitrag zu Deckung des industriellen Wärmeverbrauchs zu quantifizieren. Für die vorliegende Arbeit wurde der Wärmeverbrauch der Industrie in Deutschland analysiert und darauf aufbauend die 11 aussichtsreichsten Wirtschaftszweige identifiziert. Diese sind die Chemische Industrie, das Ernährungsgewerbe, die Automobilindustrie, das Papiergewerbe, die Herstellung von Metallerzeugnissen, der Maschinenbau, die Gummi- und Kunststoffverarbeitung, elektrische Ausrüstungen, das Textilgewerbe, das Druckgewerbe und das Holzgewerbe. Das theoretische Potential für die Nutzung solarer Prozesswärme in Deutschland unter 300 °C beträgt ca. 134 TWh pro Jahr. Das technische Potential (berücksichtigt Effizienzmaßnahmen, begrenzte Dachflächen und solarer Deckung) liegt bei 16 TWh pro Jahr oder 3,4 % des industriellen Wärmebedarfs. Thermische Solaranlagen können in industriellen Anwendungen grundsätzlich höhere Systemerträge erzielen als in Anwendungen in Ein- und Mehrfamilienhäusern, wobei die Komplexität bei der Bereitstellung von Prozesswärme meist höher ist. Um Solaranlagen zur Prozesswärmebereitstellung effizient auslegen und betreiben zu können, müssen mögliche Fehler identifiziert und ihr Einfluss auf den Systemertrag untersucht werden. Für die vorliegende Arbeit wurde eine Pilotanlage zur Prozesswärmebereitstellung anhand von Messdaten und Simulationen mit einem validierten Model systematisch untersucht. Diverse Fehler wurden identifiziert und ihr Einfluss sowie die Auswirkung einer reduzierten Last auf den Systemertrag wurden untersucht. Die Analyse zeigt, dass eine reduzierte Last den größten Einfluss hat. Weitere wichtige Faktoren wie z.B. Kollektorparameter (η_0 , a_1) wurden identifiziert. Die Auslegung von Solaranlagen zur Prozesswärmebereitstellung ist oftmals aufwändig und daher teuer, was eine wesentlich Hürde für die verstärkte Nutzung solarer Prozesswärme darstellt. Die Entscheidung für die Installation einer Solaranlage basiert meistens auf den solaren Wärmegestehungskosten. Um diese zu berechnen, sind hauptsächlich die geplante Kollektorfläche und das Speichervolumens nötig. Daher wurde für diese Arbeit ein einfacher Ansatz zur Vorauslegung von Kollektorfläche und Speicher erarbeitet, um eine schnelle Entscheidung für oder gegen eine Solaranlage zur Prozesswärmebereitstellung zu ermöglichen. Zusätzlich zu den Investitionskosten ist der jährliche Systemertrag, der in der vorliegenden Arbeit für wichtige Anwendungen solarer Prozesswärme ermittelt wird, entscheidend, um solare Wärmegestehungskosten zu berechnen. Schließlich werden Hinweise für die Planung zur notwendigen Genauigkeit des Lastprofils gegeben, die den Aufwand in der Planungsphase reduzieren können.

Acknowledgements

Writing this dissertation has been a tough academic and personal challenge as well as a great experience. It would not have been completed without the support of many people, who I owe my gratefulness.

At first, I would like to thank Prof. Dr. Klaus Vajen for his supervision. He supported the research for this thesis and the associated research projects and was always available for fruitful discussions. At the same time, he gave me the freedom for independent research and to develop myself scientifically and personally. Further, I would like to thank Prof. Dr. Víctor Martínez Moll for being the second supervisor of this thesis, his valuable comments and the pleasant collaboration within IEA SHC Task 49. I also thank Dr. Ulrike Jordan and Prof. Dr. Jens Knissel for agreeing to be part of the examination committee.

I also owe thanks to Roland, Claudius and Philipp of FSAVE Solartechnik and Klaus-Peter Reinl and Peter Schollinger of the Hütt Brewery for their great support within the research project which was the basis for this thesis. I further thank all colleagues at the Group of Solar and System Engineering. Thanks to Corry, Katrin, Janybek and Markus for helpful discussions and support by answering several questions along the way. I thank Oleg and Stefan for endless and very patient simulation support. Thanks also to Philipp, Benedikt and Christian for being partners for discussion and sharing problems and uncertainties. Thanks to Mustafa for introducing me to walking fish, Ruslan for cheering me up on many working days and Meike for her manifold support. Thank you to Kerstin, Martin, Pasquale, Shardad and Stefan for supporting my work with their master theses. I also thank Dominik for proofreading.

Thank you to all the friends who always supported and motivated me and to Marie for proofreading and improving my English.

A special thanks goes to my office mate and friend Bastian. You played a decisive role in the development and completion of this thesis. Thank you for all the discussions, for always supporting me at work and for sharing great times outside the office.

Many thanks to my parents Astrid and Reinhold for their love and constant, unconditional support and my brother Stefan for the encouragement while finishing our dissertations.

Last but not least, I thank my girlfriend Sonja. Your love, support and patience helped me a lot especially in the final and crucial phase of this thesis.

Contents

Abstract	III
Zusammenfassung	V
Acknowledgments	VII
1. Introduction	1
1.1. Background and motivation	1
1.2. Objectives and structure	3
2. Related literature	5
2.1. Potential of solar heat for industrial processes	5
2.2. Analysis and performance of large solar thermal (process heat) systems	7
2.3. Design approaches for solar process heat systems	10
3. Potential of solar heat for industrial processes in Germany	13
3.1. Methodological approach	14
3.2. Industrial heat demand in Germany	16
3.3. Potential for Germany and Europe	21
3.4. Promising industrial sectors and processes	23
3.5. Conclusion	30
4. System analysis of a low-temperature solar process heat system	31
4.1. Pilot plant at a brewery	32
4.1.1. System description	32
4.1.2. Uncertainties of measurement	35
4.1.3. Performance	35
4.1.4. Operational experience	37
4.1.5. Component analysis	38
4.2. Validation of simulation model	43
4.2.1. Simulation model	43
4.2.2. Validation results	44
4.3. System analysis with simulations	45
4.3.1. Identified faults and influence on system performance	46
4.3.2. Global sensitivity analysis	48
4.3.3. Local sensitivity analysis of load and influential parameters	50
4.4. Conclusion	53

5. Preliminary design of low-temperature solar process heat systems	55
5.1. Integration and applications of solar process heat systems	56
5.2. System configuration, parameters and control	60
5.3. Selected locations	62
5.4. Load profiles.....	63
5.5. Dimensioning of collector field.....	67
5.5.1. Influence of process temperature	69
5.5.2. Influence of collector type	72
5.5.3. Influence of orientation and slope.....	75
5.5.4. Influence of load profile and store volume	76
5.5.5. Simulated design values.....	79
5.6. Dimensioning of heat store.....	84
5.7. Utilization and yield for selected process heat applications.....	90
5.7.1. Influence of load profile.....	90
5.7.2. Utilization and yield.....	94
5.8. Summary and conclusion	97
6. Summary and conclusion.....	99
6.1. Summary and implications of the results	99
6.2. Limitations and suggestions for future research.....	103
Nomenclature.....	105
References	108
List of figures	115
List of tables.....	116
Annex.....	117
A TRNSYS types	117
B Load profiles	118
C Design values for dimensioning of collector field.....	120
D Detailed results for dimensioning of heat store	121
E Detailed results for utilization and yield	125
F Publications	128

1. Introduction

1.1. Background and motivation

Since a large share of today's energy consumption is for thermal uses, renewable heating technologies are especially important to reduce greenhouse gas emissions. Heat demand has a share of 56 % of the total final energy consumption in Germany. Process heat has a major share (37 %) of this heat consumption besides space heating (55 %) and domestic hot water (8 %). Within the industrial sector, even 74 % of the final energy consumption is needed to mainly provide process heat, but also space heating and hot water (BMW, 2010). In 2010, renewable heating technologies provided a share of 9.5 % of the German heat supply, whereas biomass accounted for 90 % and only 4 % was provided by solar thermal systems. Because of a limited potential of biomass, an extended use of solar and geothermal heat plays an important role for the reduction of greenhouse gas emissions and independence of fossil fuels (Nitsch et al., 2010).

Today, solar thermal systems are almost exclusively used for providing hot water, space heating, and the heating of swimming pools. The conditions for the use of solar thermal are favorable in the industrial sector because in many cases the load is constant over the year and existing heat store capacity might be used. However, process heat generation is a rather unexploited application for solar thermal systems (STS) compared to domestic applications like hot water generation, space heating, or heating of swimming pools. Only a few hundred systems were installed in industrial companies worldwide, so solar thermal systems in industry have a negligible share of 0.02% compared to the installed capacity worldwide (Vannoni et al., 2008).

Nevertheless, several studies for the use of solar heat for industrial processes determined a large potential for this application. Taibi et al. (2012) estimate that 1,555 TWh (5.6 EJ) per year could be provided by solar thermal systems in industry worldwide by 2050. In other studies, the possible contribution of solar thermal technology is estimated between 3.2 and 4.4 % of the overall heat demand in industry (Müller et al., 2004; Schweiger et al., 2001; Vannoni et al., 2008; van de Pol et al., 2001). Compared to conventional applications of solar thermal systems for domestic hot water (DHW) and space heating, solar process heat represents a considerable market.

Solar thermal systems can achieve higher system yields in industrial applications compared to domestic applications under certain boundary conditions, such as low process temperature and constant load. However, systems can be more complex in industrial applications, because of the variety of heat consumers and temperature levels. This leads to

a larger variety of components and hydraulic setups. Several publications state that implemented solar process heat systems fall behind the predicted performance (Anthrakidis et al., 2010; Karagiorgas et al., 2001; Kutscher and Davenport, 1980; Wutzler et al., 2011). Even for large STS for domestic applications several faults and a lack of performance is documented (Croy and Wirth, 2006; Croy et al., 2011; Drück and Schenke, 2007; Peuser et al., 2001). In order to design and operate solar process heat systems efficiently and to exploit its large potential, possible faults of such systems need to be identified and their impact on the system yield as the most important performance indicator has to be evaluated.

The design of solar process heat systems is in many cases demanding, hence costly. This significant effort is a major barrier for a further development of solar heat in the industrial sector as manufacturers and planners of such systems take risks developing a design for a system which possibly will not be sold and installed. The decision for installing a solar thermal system is in most cases based on the solar heat generation cost. Collector field and storage size are the most important figures for the estimation of the overall cost of a solar thermal system. Therefore, a simple approach for dimensioning collector field and heat store is necessary to enable manufacturers and planners on one hand and customers on the other hand to make a decision in favor or against a solar process heat system. In addition to the investment cost, the specific system yield which is determined for selected process heat applications in this thesis is necessary to calculate solar heat generation cost. Finally, indications on the necessary accuracy of the load profile can help to reduce the effort in the design phase.

Already in 1983, Brown (1983) discussed the prospects of solar heat for industrial processes after a minimum of 22 solar thermal systems for either space heating, cooling, DHW or process heat had been installed in industry between 1975 and the end of 1980 in the USA. The expectation for solar process heat becoming a large market was high but declined considerably after 1978 because fuel prices stabilized and energy conservation was considered. Brown (1983) identified four issues to be crucial for the prospects of solar heat for industrial processes: performance and cost of solar process heat systems (1), actual and expected cost of energy supply and energy conservation (2), attitude, financial possibilities and technical receptivity of industrial market (3) and evolution of solar equipment industry (4).

Today, 30 years later, the same issues are still prevailing for the prospects of solar process heat except that established solar equipment providers exist. This thesis shall contribute to the first issue by ensuring and improving the performance of solar thermal systems in industry and reducing cost associated with design and feasibility of such systems.

1.2. Objectives and structure

Following research objectives are pursued within this thesis:

1. How is the industrial heat demand distributed across different temperature levels, how large is the potential contribution of solar heat for a sustainable heat supply in industry and which are suitable industrial sectors and processes to be supplied with solar heat?
2. Which are possible faults of low-temperature solar thermal systems in industry, how is their impact on system performance and which are the most important impact factors on the overall system performance?
3. Which important process heat applications exist below 100 °C, how can systems for such applications be pre-dimensioned and what are typical annual system yields of these systems to be considered for an economic feasibility assessment?

Section 2 of this thesis introduces the literature related to the three research objectives. Major results or approaches of relevant publications are described and their consideration for this thesis is illustrated.

Related to the first research objective, Section 3 investigates the potential of solar heat for industrial processes in Germany. Initially, methodological approaches for potential studies in the field of solar process heat are introduced using two comprehensive studies as examples and the approach for this thesis is illustrated. Further on, the section analyzes the industrial heat demand in Germany and calculates the shares of the relevant temperature levels. In addition, the determination of the potential of solar heat for industrial processes in Germany and a calculation of a theoretical as well as a technical potential are explained. Finally, this section analyzes suitable industrial sectors and identifies suitable processes for the integration of solar heat. Section 3 is based on a peer-reviewed paper derived from this thesis (Lauterbach et al., 2012a). Parts of this section were also published in (Lauterbach et al., 2010; Lauterbach et al., 2011b; Lauterbach et al., 2011c). The research for this section was performed in a research project titled “SOPREN – Solar process heat and energy efficiency” funded by the German Federal Ministry for the Environment, Nature Conservation and Nuclear Safety, contract No. 0329601T. The project contained three main work packages: the potential study described in this section, the demonstration of solar thermal systems in industrial applications (especially the solar process heat system at a brewery described in Section 4 of this thesis) and the development sector concept for the utilization of solar heat in breweries. This sector concept is described in detail in the Dissertation of Bastian Schmitt (Schmitt, 2014).

With respect to the second research objective, Section 4 describes the system analysis of a low-temperature solar process heat system which was built at a brewery in Germany. At first, the section describes the integration of the STS in the hot water supply of the brewery, the system configuration, its performance, the analysis of its components and the gained operational experience. Different faults which occurred during operation are identified and described. Afterwards, the section introduces the developed simulation model and illustrates the results of validation. This simulation model was used to quantify the impact of each individual fault. Further, the section explains the system analysis with simulations. A global and local sensitivity analysis were performed in order to identify and evaluate the most important impact factors on the overall system performance. Finally, Section 4.4 presents the conclusion. Section 4 is based on a paper in a peer-reviewed journal derived from this thesis (Lauterbach et al., 2014). Parts of this section were also published in (Lauterbach et al., 2012b; Schmitt et al., 2010; Schmitt et al., 2012b). The research for this section was also performed in the framework of the research project “SOPREN – Solar process heat and energy efficiency”.

Related to the third research objective, Section 5 explains the principles of integration of solar thermal systems in industrial processes and identifies major applications of solar process heat systems. Additionally, the section describes the configuration of the simulation model used to derive design values and the selected locations for the simulation study. Furthermore, the section presents an approach for the pre-dimensioning of the collector field and heat store and evaluates the influence of several impact factors on the design. The section further illustrates the results of simulations to determine the system yield of selected process heat applications. Finally, Section 5.6 provides the conclusion. Parts of Section 5.1 were published in (Lauterbach et al., 2011a; Schmitt et al., 2011). An exhaustive list of publication that results from this work can be found in the Annex. The research for this section was partly performed in a research project titled “SolFood – Solar heat for the food industry” funded by the German Federal Ministry for the Environment, Nature Conservation and Nuclear Safety, contract No. 0325541A.

Finally, Section 6 summarizes the main findings of this thesis, illustrates and discusses the results and limitations and provides suggestions for future research.

2. Related literature

This section introduces literature related to the three main topics of this thesis. Major results or approaches of relevant publications are described and their consideration for this thesis is illustrated.

2.1. Potential of solar heat for industrial processes

Studies about the potential of solar heat for industrial processes were performed for different countries or regions in the past. This section summarizes the results and findings regarding temperature distribution of industrial heat demand, suitable sectors and processes as well as quantitative potential whereas Section 3.1 presents a comparison of methodological approaches.

Schweiger et al. (2001) determined the potential for solar heat at low (<60 °C) and medium (60 to 160 °C) temperatures for Spain and Portugal. 34 case studies in industrial enterprises were the basis on which the temperature distribution of heat demand was determined of which the share of low and medium temperature heat demand of the whole sector was calculated. More than half of the enterprises belonged to the sector Food and beverages and few case studies were performed in Paper (4), Textiles (6), Leather (2), and one each in Cork and Motor vehicles. The analysis of temperature levels showed that more than 60 % of the heat demand is needed below 160 °C except for Paper industry and that in some sectors almost the total heat demand is below 60 °C. The authors determined the technical potential by estimating the available roof area (which was the limiting figure in most cases) for each analyzed enterprise and assuming a maximum solar fraction of 60 %. Schweiger et al. determined the technical potential at 3.4 % of the industrial heat demand in Spain and 4.4 % in Portugal. They found Food and beverages to be the most promising sector for the use of solar heat. Chemicals, Paper, Motor vehicles, Tobacco, Leather, and Textiles are also mentioned as suitable for the application of solar heat.

Van de Pol et al. (2001) identified promising sectors for the application of STS in the Netherlands. These are Food and beverages, Paper, Textiles, and Industrial laundries. The authors analyzed the energy demand and typical processes within the sectors to determine the share which could be supplied by solar heat. The focus was on hot water for processes below 60 °C whereas DHW and boiler make-up water were not considered. They calculated a potential (not clearly referred to as technical potential) of 3.2 % of the industrial heat demand (Vannoni et al., 2008). The use of waste heat is mentioned as a major barrier for the spread of solar heat for industrial processes. Additional barriers

mentioned are the lack of sufficient and suitable roof area and competing technologies such as combined heat and power (CHP) and heat pumps.

Vannoni et al. (2006) describe the results of a potential study regarding solar heat for industrial processes in Greece, Wallonia (Belgium) and a few industrial sectors in Germany. For Greece, the authors identified a potential for hot water preparation in seven sectors (Chemicals, Food and beverages, Tobacco, Paper, Textiles, Leather and Transport equipment). For Germany, the potential was investigated for Food and beverages, Textiles and Paper. The authors only estimated a technical potential for Paper recycling and Bottle washing in breweries due to the lack of data for other sectors. They estimated a theoretical potential of 181 GWh/a for paper recycling and calculated a technical potential of 60 GWh/a by assuming a solar fraction of 30 %. They further assumed a specific solar system yield of 400 kWh/(m²a) and calculated a market volume of 150,000 m² collector area (aperture or gross area not specified) for paper recycling. The technical potential (167 GWh/a) and market volume (557,000 m²) for bottle washing in breweries was estimated identically, assuming a specific solar system yield of 300 kWh/(m²a). For Wallonia (Belgium), the study mentions following suitable sectors: Chemicals, Food and beverages, Paper, Textiles and Tobacco.

A publication by Kovacs et al. (2003) describes an investigation regarding the potential of solar heat for industrial processes in Sweden. The authors estimate the limit for feasible application of STS in industry at 150 °C because of the climatic conditions in Sweden. They see the highest potential in the sectors of Food and beverages and Machinery and equipment.

Kalogirou (2003) studied the potential of solar heat for industrial processes in Cyprus through a simulation study. The author simulated the yield of STS for different temperatures levels. He identified suitable sectors and applications based on heat demand and temperature levels. Kalogirou found that the sector Food and beverages, as well as, drying and washing processes in general to be suitable for the use of solar heat and mentions that solar heat for industrial processes has a great potential without providing a quantitative figure.

Müller et al. (2004) calculated the low (<100 °C) and medium temperature (<250 °C) heat demand by adding the demand for space heating (not for DHW) and steam generation for all industrial sectors in Austria. The authors selected following suitable sectors: Chemicals, Food and beverages, Rubber and plastics, Textiles and Prefabricated concrete components. They excluded the ones with a low heat demand or high waste heat potential. The theoretical potential is defined as low and medium temperature heat demand of the mentioned sectors and heat demand of processes of washing, cleaning and surface treatment of metals across all sectors. Müller et al. calculated the technical potential (3.9 %

of the industrial heat demand) by deducting the existing renewable share of 15 % of the heat supply and a further 60 % due to possible efficiency measures and restrictions regarding economic feasibility. In addition, they assumed an average solar fraction of 40 % for process heat applications (20 % for space heating).

McLeod et al. (2005) published a study on the potential of solar process heat for the Australian State of Victoria. They estimated the industrial and service sectors' heat demand at 53 % of the final energy consumption based on statistics about the shares of the different fuels. A technical potential for industry is not clearly declared. Within the study the following industrial sectors are mentioned as suitable for the application of solar thermal systems: Chemicals, Food and beverages, Machinery and equipment, Textiles, and Paper.

Vannoni et al. (2008) investigated the potential of solar heat in industry for Italy by estimating the available roof and facade area. They estimated the available area by using employee-specific data on available areas and a reduction of 80 % for roofs and 93 % for facades due to availability. The authors calculated a technical potential of 3.7 % of the industrial heat demand for Italy. Vannoni et al. mention the following industrial sectors to be suitable for the application of solar process heat: Chemicals, Food and beverages, Motor vehicles, Textiles, Paper, Tobacco and Leather.

According to Taibi et al. (2012) solar thermal has a global potential of approximately 1,555 TWh (5.6 EJ) per year by 2050. Almost 50 % of the potential is seen in the Food and beverages sector. Further promising sectors are Machinery and equipment, Mining and quarrying, Textiles and Leather, and Transport equipment. The authors state that the potential has a roughly equal regional distribution between OECD countries, China and the rest of the world. Further, Taibi et al. found that solar process heat is close to economic feasibility in regions with good radiation but needs substantial cost reduction for Central Europe and other areas with lower solar resources.

2.2. Analysis and performance of large solar thermal (process heat) systems

Regarding the system behavior and performance of large STS for domestic applications Peuser et al. (2001) describe the results of a demonstration project in Germany between 1978 and 1983 evaluating 141 solar thermal systems for domestic hot water and heating of swimming pools. In a second phase of the program, large solar thermal systems with a collector area of more than 100 m² were monitored in detail. Peuser evaluated typical failures of 98 representative systems in terms of application, system design and components. The most common failures (almost 50 % of the systems) were leakages of the collector loop or damage of its isolation. Additionally, collector defects often occurred

(e.g. condensation inside the collector and damage of its cover). Regarding the design, expansion vessels which were too small for periods of stagnation turned out to be the most common failure. Further, the authors assume that the control system failed (at least partly) in 40 to 50 % of the installations.

Heimrath (2004) performed a simulation-based analysis of STS, heat distribution network and building for solar assisted space heating of multifamily houses. Heimrath states that the design of the heat distribution network has the strongest thermal impact on the efficiency of the STS. The author found that system-specific parameters like e.g. UA-value of the charging and discharging heat exchangers and inlet height of its return can have an immense impact on the solar fraction which is used as the target function.

Croy and Wirth (2006) and Drück and Schenke (2007) jointly analyzed six large STS for domestic hot water and space heating (combisystems) with collector areas between 46 and 220 m² in Germany. All systems were monitored in detail and optimized after a short period of operation. The authors detected a wrong hydraulic setup of the system in 5 cases in which the return flows of the different heat consumers were combined. This led to a mixing of temperature levels. Some pipes were also connected to the wrong store of several stores or at a wrong height. Further, the authors detected faults in the control of two systems. They describe that immense uncertainties regarding the design of large combisystems existed at the time of the publication in 2006, which is still true for solar industrial process heat systems today. Additionally, the authors conclude that many combisystems incorporate failures and have lower performance than predicted in the design phase.

Building upon the results of Peuser et al. (2001), Croy et al. (2011) analyzed the state of the art of large STS for DHW and district heating built in Germany between 1988 and 2005. The systems analyzed in (Peuser et al., 2001) were considered after 15 years of operation and compared to more recent installations (1 to 10 years of operation). Most of the failures described in (Peuser et al., 2001) regarding the collector were reduced and several (like e.g. damages of the collector cover) did not occur anymore. Further failures like leakages of solar loop and solar loop isolation were reduced substantially. On the other hand, problems with the system control increased compared to the earlier study. A failure which occurred in about 10 % of the systems was a reduced performance of the heat exchangers. The authors also analyzed the long term performance of eight STS after 7 to 12 years of operation and compared it to the design value. The system yield of these systems was between 38 and 90 % (63 % on average) of its design values. The authors state that a deviation of the real load compared to the expected one during the design was a major reason for the low performance. They conclude that determining the load is a crucial issue for predicting the performance of an STS.

Kutscher and Davenport, (1980) collected operating data of six solar process heat systems in 1979 regarding their behavior and performance. The actual annual energy system efficiencies ranged from 8.1 % to 19.7 % which was between 25 % and 50 % of the predicted performance. This was because the STS could not be fully utilized and the system's excessive thermal losses, but not due to failures of certain components.

Nagaraju et al. (1999) describe the performance of a solar thermal system with a collector field of 2,560 m² (aperture or gross area not specified) and four stores with a volume of 57.5 m³ each in India. The system is used to heat 110 m³ of water daily from 22 to 85 °C for an egg powder plant. The system performance was evaluated for months with varying irradiation. The system utilization ratio (used/ incident solar energy as in Equation 2) was 56 % in January on days with good irradiation of 6 kWh/(m²d) and between 45 % and 58 % in other months. Further, the authors estimate the heat losses of the store at around 3.5 % on a day with typical operation after determining heat losses of 6 % within a 24 h period with no discharge.

Eskin (2000) performed an experimentally validated simulation study of a solar process heat system using parabolic trough collectors at a textile plant in Turkey. He used one month of monitoring data to validate the daily simulations of the system. Eskin states that the behavior of solar process heat systems strongly depends on the load profile and thus models the heat load of the textile plant. Nevertheless, the author did not vary the load profile in the presented simulation study to support the statement.

Bokhoven et al. (2001) present operational experience of two large solar thermal systems in the Netherlands. One system with $A_{col} = 1,200 \text{ m}^2$ (aperture or gross area not specified) and $V_{store} = 1,000 \text{ m}^3$ was used for agricultural drying and a drain back system ($A_{col} = 2,379 \text{ m}^2_{ap}$, $V_{store} = 1,000 \text{ m}^3$) to prepare hot water at 65 °C for a confectionary factory. The experience with the first system focuses on the design of a large store below ground water level. The investigation of the second one focuses on scaling up the drain back concept. Nothing is mentioned about the performance of neither system.

Karagiorgas et al. (2001) present a study about ten solar process heat installations in Greece in the 1990s. The system utilization (used/ incident solar energy) of five systems (for which monitoring data was available) ranged between 7.3 % and 26.5 % (average 18 %) on a typical day of operation. In one case, the utilization ratio was that low because of a poor insulation of heat store and an undersized solar heat exchanger. In the case of another system, high heat losses occurred because the solar loop was not insulated. Finally, one system was oversized which led to a low system utilization.

Wutzler et al. (2011) describe the monitoring results of a solar thermal system with $A_{col} = 736 \text{ m}^2_{ap}$ and two stores with $V_{store} = 55 \text{ m}^3$ each at a brewery in Germany. The

system is used to provide space heating, DHW and heating of a bottle washing machine. The collector utilization ratio for July 2010 was 40 %, the system utilization ratio was 27 %. 21 % of the heat charging the store is lost to the ambient in summer. In March, the system had a collector utilization ratio of 35 % and a system utilization ratio of 18 %. 40 % of the charged heat was lost from the store to the ambient. The system utilization ratios are 20.7 % and 19.4 % respectively for two annual monitoring periods.

Anthrakidis et al. (2010) published a paper dealing with operational experience of a solar thermal system with $A_{\text{col}} = 400 \text{ m}^2$ (aperture or gross area not specified) and five stores with $V_{\text{store}} = 1.5 \text{ m}^3$ each to heat an electroplating process in Germany. They indicate that the operation was not optimal as five stores were installed in a parallel setup and are charged differently. Sometimes, the stores were even cooled by the solar thermal system if a heated store is charged by low temperatures from the collectors.

2.3. Design approaches for solar process heat systems

Gordon and Rabl (1982) developed a method for designing STS for process heat applications for constant daytime loads on every day of the year. The method is given in explicit equations but limited to the case of a completely constant load using correlations for the annually energy collection by the principal collector types. The authors found the economic optimum to be a slightly oversized collector field with dumping of excess energy during times of peak insolation. This fact was considered for the design approach developed in Section 5.2 of this thesis as an average “good” summer day is used for the simulation study.

Collares-Pereira et al. (1984) present a method for design and optimization of solar industrial process hot water systems with storage. A single-pass open-loop system is compared to a multi-pass closed loop system. The design is only appropriate if the fluid heated by the STS is discarded after being used in the process. Further, the process water is stored directly (as the system is open) which is not possible in many cases due to hygienic considerations.

Kutscher et al. (1982) published a comprehensive design guide for solar process heat systems in the USA. The authors describe the preliminary design of STS for industry besides several other sections on e.g. system configurations, controls and installation. They explain the calculation of the annual performance of an STS for preliminary design. This is done in a step by step procedure starting with the annual energy collection of the collector field and the introduction of loss factors (for piping, store losses etc.) determined by detailed system simulations. Indirect (including a heat exchanger) hot water or air systems are considered, as well as, mixed tank recirculation systems which include a heat store, and

steam systems. The necessary calculation seems quite complex for practical use although the preliminary design method gets along without simulation.

Benz et al. (1998) designed two STS for a bottle washing machine in a brewery and a spray dryer in a dairy in Germany. They do not present general design rules but describe a design with detailed TRNSYS simulations.

Schweiger et al. (2000) performed a simulation study for solar process heat applications for 5 different sites in Spain and Portugal. They determined the system yield for 4 different collector types (flat plate, evacuated tube and evacuated flat plate, compound parabolic concentrator (CPC)) for a process heat demand always higher than the energy delivered by the collector field. This is done for different process temperatures from 60 to 200 °C. The results help to estimate typical system yields for solar process heat applications. Such typical yields are presented in Section 5.7 of this thesis for various boundary conditions.

Aidonis et al. (2004) performed a similar simulation study with TSOL simulation software (Dr. Valentin EnergieSoftware GmbH, 2013) for processes at different temperature ranges (20/70°C; 30/80°C; 40/90°C). They considered various European locations for a flat plate collector (FPC) and an evacuated tube collector (ETC) with specific parameters to evaluate the solar gains of solar process heat applications. An available load utilization (ALU) is introduced to achieve results which are independent of system size. It is defined as load (in MWh) per m² of collector area (ALU = 1 means for 1 MWh of load 1 m² collector area is installed). The approach of decoupling simulation results from system size with a specific available load is considered for this thesis in Section 5. The authors found that ALU has a large influence on solar gains beside the temperature range.

Aidonis et al. (2005b) provide recommendations regarding the suitability of a load profile. They state that a load profile to achieve sufficient yield for feasibility of an STS needs heat demand 75 % of the year including summer, 5 days per week and an average daily load in summer larger than for the rest of the year. The authors recommend a solar fraction between 10..50 % and to consider space restrictions for the dimensioning of the collector field. Further, they recommend a value of 50 l/m² (aperture or gross area not specified) for the heat store and less for low solar fractions.

In another study, Aidonis et al. (2005a) provide a nomogram based on system simulations for a dyeing process to simplify the dimensioning of solar thermal systems. The nomogram shows a solar fraction and specific solar yield for a utilization ratio (daily hot water demand of the process per m² collector).

Kulkarni et al. (2008) followed a design-space-approach for dimensioning an STS for industrial applications. This is done for an STS consisting of a concentrating collector, a pressurized hot water store and a discharge heat exchanger. The design space is the region

bounded by constant solar fraction curves traced on a collector area vs. store volume diagram. This diagram is always valid for one chosen solar fraction and shows all possible design combinations of collector area and store volume. Therefore, the design space approach requires the choice of a solar fraction as a starting point which is not always feasible for solar process heat applications. Further, a new design space has to be developed as soon as any boundary condition changes which makes the approach not very feasible for practical use.

Hess and Oliva (2011) followed the same approach as Aidonis et al. (2005a) mentioned above. The authors created nomograms for convective drying with hot air, heating of industrial baths, and preheating of fresh- and boiler feed water. However, the possible application of these nomograms is limited since their validity is limited to a specific application (e.g. dyeing) with a fixed temperature, at a defined location and with a given load profile. If one (or even more) of these variable changes, the nomogram can only be used to create a new one for the respective boundary condition.

VDI 6002 (2004) presents an approach for dimensioning for large STS for DHW preparation ($>20\text{m}^2_{\text{ap}}$). The approach is to design the collector field for a summer day with good irradiation. This approach leads to an economically favorable system size as an energy excess of the STS in summer is prevented. Further recommendations for the size of heat store are provided. The approach of dimensioning the collector field for a good summer day is considered for preliminary design for process heat applications in Section 5 of this thesis.

3. Potential of solar heat for industrial processes in Germany

Potential studies for the use of solar heat for industrial processes (SHIP) were carried out in the past for different countries or regions. A comprehensive study for Spain and Portugal identifies several sectors and processes to be suitable for the use of solar heat (Schweiger et al., 2001). A similar study was performed for Austria (Müller et al., 2004). Further potential studies were performed for Victoria (Australia) (McLeod et al., 2005), Italy (Vannoni et al., 2008), the Netherlands (van de Pol et al., 2001), Sweden (Kovacs et al., 2003), and Cyprus (Kalogirou, 2003) as described in Section 2.1. Vannoni et al. (2006) describe the results of a study for Greece, Wallonia (Belgium) and a few industrial sectors in Germany.

So far, no comprehensive potential study was done for Germany. Furthermore, no detailed analysis of the industrial heat demand below 300 °C exists. Therefore, this section tries to close the knowledge gap regarding distribution of temperature levels of the industrial heat demand. This is crucial for the application of solar thermal systems in industry. Furthermore, the potential contribution of solar heat for a sustainable heat supply in industry has to be quantified. Finally, the suitable industrial sectors and processes have to be identified to facilitate the prioritized application of solar heat in industry.

For this thesis the industrial heat demand in Germany was analyzed and different sources were combined to determine the shares of temperature levels below 300 °C and the quantitative potential of solar heat for industrial processes. The most promising industrial sectors and processes for the application of solar process heat were selected based on their heat demand below 300 °C and on waste heat potential. Results of prior studies verified this selection.

Section 3.1 introduces methodological approaches for potential studies in the field of solar process heat, using two comprehensive studies as examples. Subsequently, the approach for this thesis is illustrated. Section 3.2 analyzes the industrial heat demand in Germany and calculates the shares of relevant temperature levels. Section 3.3 explains the determination of the potential of solar heat for industrial processes in Germany and the calculation of a theoretical as well as a technical potential. Finally, Section 3.4 analyzes suitable industrial sectors and identifies suitable processes for the integration of solar heat.

This section is based on a peer-reviewed paper derived from this thesis (Lauterbach et al., 2012a). Parts of this section were also published in (Lauterbach et al., 2010) and (Lauterbach et al., 2011c).

3.1. Methodological approach

Prior potential studies in the field of solar heat for industrial processes differ significantly regarding their approach to select suitable industrial sectors and processes and their way to determine a quantitative potential. In some studies the potential is determined based on the energy and heat demand of industrial sectors, one uses the available roof area and others calculate the potential on the basis of case studies in selected industrial companies. For the choice of a suitable approach for the investigation within this thesis the approaches of prior studies were analyzed and compared. Generally, it can be distinguished between a top-down and a bottom-up approach.

For the top-down approach, data (e.g., distribution of heat demand or available roof area) of the entire industry is analyzed to select suitable sectors and calculate a quantitative potential. This approach was followed by the comprehensive potential study for Austria in 2004 (Müller et al., 2004). In a first step, the energy demand of the industry in Austria was analyzed and low (<100 °C) and medium temperature (<250 °C) heat demand was calculated by adding the demand for space heating and steam generation for all industrial sectors. Hot water consumption is not mentioned, which only leads to a minor uncertainty because its share in industry is rather low.

At first, suitable sectors were selected to determine a theoretical potential. Therefore, sectors with low heat demand or high waste heat potential were excluded. The sectors of Chemicals, Food and beverages, Rubber and plastic, Textiles, and Prefabricated concrete components were selected. Further, the processes of washing, cleaning and surface treatment of metals are mentioned as suitable for the use of solar heat. The low and medium temperature heat demand of the mentioned sectors and processes is defined as the theoretical potential. This theoretical potential is divided in a short-term (<100 °C) and a mid-term (<250 °C) potential because at the time of the study, collector technology for process heat generation at temperatures above 100 °C was neither technically mature nor available on the market.

The technical potential was calculated by deducting the renewable share of 15 % of the heat supply and a further 60 % due to possible efficiency measures and restrictions regarding economic feasibility. In addition, an average solar fraction of 40 % for process heat applications and 20 % for space heating was assumed by the authors. The figures for efficiency measures and solar fraction are not explained in detail.

For a bottom-up approach, selected industrial companies are analyzed and the results are used to determine suitable sectors and a quantitative potential using statistics of the overall industrial heat demand or number and size of companies. This approach was followed in the potential study for Spain and Portugal (Schweiger et al., 2001). The aim of this study

was to determine the potential for solar heat at low (<60 °C) and medium (60 to 160 °C) temperatures. In a first step almost 1,700 enterprises were contacted by mail or called. In total 59 answers were received and finally case studies were performed in 34 industrial enterprises in Spain and Portugal. More than half of the enterprises belong to the sector Food and beverages and few case studies were done in Paper (4), Textiles (6), Leather (2), and one each in Cork and Motor vehicles. The temperature distribution of the heat demand of each sector was determined on the basis of these case studies and the share of low and medium temperature heat demand of the whole sector was calculated. A theoretical potential is not clearly defined. The technical potential was determined by estimating the available roof area for each enterprise analyzed and assuming a maximum solar fraction of 60 %. The available roof area was the limiting factor in most cases.

Comparing the two approaches, the advantage of a top-down approach is a coherent distribution of the industrial heat demand, which is the necessary basis to calculate a theoretical potential. This is, however, only true, if the used data can be verified. The calculation of the distribution of the industrial heat demand with a bottom-up approach incorporates, as the above mentioned example shows, a high uncertainty unless a large number of companies are studied. In order to determine the temperature distribution and a theoretical potential, the top-down approach seems to be the better choice as the feedback to questionnaires is typically very low. Figures for restrictions as e.g., limited roof area or possible efficiency measures as well as a solar fraction are necessary in order to calculate a technical potential. In case of a top-down approach one relies on assumptions for these figures, as the above example shows.

Using a bottom-up approach, the figures can be estimated with a much better certainty, however only if the number of enterprises studied is sufficient. Nevertheless, the results of case studies have to be verified with literature. As the execution of a large number of case studies needs high resources, this could be replaced by studying case studies and built examples from literature, possibly combined with a few additional case studies.

The choice for one of the described approaches also depends on the availability of data regarding the overall industrial heat demand and its temperature distribution. As comprehensive data is available for Germany from studies for technologies such as CHP and heat pumps, a top-down approach was chosen for the analysis within this thesis.

The first step was the analysis of the industrial heat demand and the calculation of the shares of the relevant temperature levels, as explained in detail in Section 3.2. Afterwards, the theoretical potential was calculated. This was defined as the heat demand at temperatures below 300 °C of all industrial sectors except the ones with a high waste heat potential like e.g. Basic metals. Furthermore, the technical potential was determined by considering a restricted roof area and possible efficiency measures, as well as an average

solar fraction, as described in Section 3.3. A reduction for existing renewable heat was not considered as this is incorporated in the solar fraction and biomass can also be used to provide higher temperatures or to cover the heat demand in winter. By assuming an average energy yield per square meter of collector, the necessary collector area could be calculated, which also indicates the possible market size. Furthermore, the most promising sectors were selected using their overall heat demand below 300 °C and waste heat potential as criteria. Finally, the selected sectors were analyzed to identify suitable processes for the use of solar heat.

3.2. Industrial heat demand in Germany

The final energy consumption in Germany was 2,414 TWh in 2009, the industrial sectors share was around 640 TWh, representing 27 %. The heat demand, including process heat, space heating, and DHW, is of high importance as it accounted for 74 % of final energy consumption in industry, as shown in Figure 3-1 (BMWi, 2010).

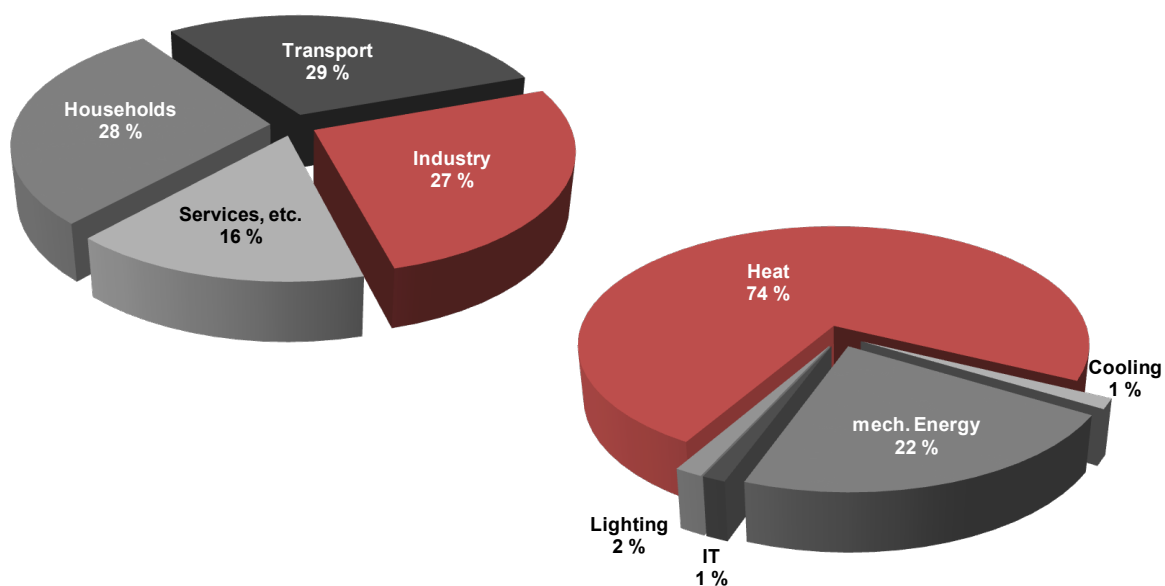


Figure 3-1: Final energy consumption in Germany and distribution within industry in 2007 (BMWi, 2010).

Today, the heat supply is mainly provided by fossil fuels. The fuel with the largest share is natural gas with 47 % followed by coal with 21 %. Oil and electricity have a share of 8 % each, district heat 7 % and renewables 5 %. Other fuels have a share of 4 % (BMWi, 2010). In order to determine the theoretical potential for solar heat in industrial processes, a thorough analysis of the industrial heat demand and its temperature levels is necessary. Table 3-1 shows the industrial heat demand in Germany for 2009 sorted by the temperature level.

This data was calculated by using employee-specific heat demand figures from (Eikmeier et al., 2005), which have been determined by investigating about 150 representative energy consumers and about 90 typical buildings. As the number of analyzed companies and buildings is quite high, it can be assumed that employee-specific heat demand figures are reasonably reliable. Further the numbers of employees for 2009 per sector from the German Federal Statistical Office were used (DeStatis, received 2011).

Table 3-1: Breakdown of industrial heat demand for the year 2009 (DeStatis, received 2011; Eikmeier et al., 2005).

Industrial sector (NACE Rev.2 Code)	HW	SH	Process heat [TWh]				Sum	Share*
			<100°C	100 ..500°C	500 ..1000°C	>1000°C		
Food products and beverages (10/11)	0.3	8.3	11.8	14.6	0	0	35.0	7.5 %
Tobacco products (12)	0.0	0.0	0.0	0.0	0	0	0.1	0.0 %
Textiles (13)	0.1	1.2	2.0	0	0	0	3.3	0.7 %
Wearing apparel (14)	0.0	0.1	0.2	0	0	0	0.3	0.1 %
Leather and related products (15)	0.0	0.1	0.2	0	0	0	0.3	0.1 %
Wood and wood products (16)	0.0	0.3	1.5	0.4	0	0	2.1	0.5 %
Paper and paper products (17)	0.1	2.4	2.7	9.9	0	0	15.1	3.2 %
Printing and reprod. of recorded media (18)	0.0	0.4	0.2	2.7	0	0	3.3	0.7 %
Chemicals and chemical products (20/21)	0.2	6.7	13.5	20.9	44.7	11.0	96.9	20.7 %
Rubber and plastic products (22)	0.1	1.6	0.9	3.5	0	0	6.1	1.3 %
Non-metallic mineral products (23)	0.1	3.5	1.2	1.8	26.9	55.8	89.3	19.0 %
Basic metals (24)	0.2	4.4	0.9	2.7	31.5	123.5	163.1	34.8 %
Fabricated metal products (25)	0.9	6.3	2.3	1.8	1.0	2.4	14.8	3.2 %
Computer, electronic, optical products (26)	0.1	0.9	0.3	0.2	0.1	0.3	2.0	0.4 %
Electrical equipment (27)	0.3	2.4	0.9	1.1	0.3	0.8	5.8	1.2 %
Machinery and equipment (28)	0.6	4.5	1.6	1.2	0.6	1.7	10.3	2.2 %
Motor vehicles and trailers (29)	1.0	7.3	2.7	2.0	1.0	2.8	16.8	3.6 %
Other transport equipment (30)	0.1	0.9	0.3	0.2	0.1	0.3	2.0	0.4 %
Furniture and other goods (31/32)	0.0	0.7	0.4	1.0	0.0	0.1	2.4	0.5 %
Sum	4.2	52.0	43.6	64.2	106.2	198.7	468.9	100 %
Share*	1 %	11 %	9 %	14 %	23 %	42 %	100 %	
Figure from (BMW, 2010)	5.7	49.4			418.6		473.7	

*of the overall industrial heat demand; Mineral oil (19) not listed as demand is covered by own production; all numbers without unit in TWh; HW: hot water; SH: space heating.

To verify the calculated industrial heat demand, the last line of Table 3-1 shows the aggregated values for hot water, space heating and process heat for 2009 from the official energy statistics of the German Federal Ministry of Economics and Technology (BMW, 2010). The comparison with calculated values shows a good accordance of figures for the total industrial heat demand with a deviation of only 1 %. The values for process heat and space heating also accord well with the calculated values, only for hot water there is a deviation of 26 %, which is, however, of minor importance for the overall heat demand.

Three industrial sectors (Chemicals, Non-metallic mineral products and Basic metals) dominate the industrial heat demand in Germany and had a total share of nearly 75 % of the industrial heat demand in 2009. Additional sectors with relevant shares are Food and beverages, Motor vehicles, Paper, Fabricated metal, and Machinery and equipment. These five sectors have an aggregated share of almost 20 %.

Regarding the temperature level, Table 3-1 shows that high temperatures above 500 °C had a large share of 65 % of the industrial heat demand. Processes with high temperatures are mainly found in heavy industries like Basic metals and Non-metallic mineral products. A share of 14 % was consumed in the medium temperature range of 100 to 500 °C, 21 % in the low temperature range which includes process heat at low temperatures, space heating and hot water.

The sectors Chemicals and Food and beverages had by far the highest share in the low temperature range for process heat below 100 °C, space heating and hot water with 20 % each. In order to determine the potential for the use of solar heat for industrial processes in Germany, the heat demand below 300 °C is especially important, as for the temperature ranges of 100 to 200 °C and 200 to 300 °C different advanced systems and components are necessary. Therefore, the temperature range from 100 to 500 °C was further divided. Figure 3-2 shows a breakdown of industrial heat demand by temperature level from 100 to 500 °C for Chemicals, Food and beverages, and an average of other sectors (Hofer, 1994).

Hofer (1994) determines the shares of industrial heat demand differently for sectors with highly standardized production processes like e.g., Non-metallic mineral products and inhomogeneous sectors, e.g. Food and beverages. In case of standardized production processes, the energy demand and necessary temperature for every process step is analyzed and the temperature distribution is calculated based on the production volume. For inhomogeneous sectors the overall energy and heat demand is taken from official statistics and case studies are performed to derive the temperature distribution of their heat demand.

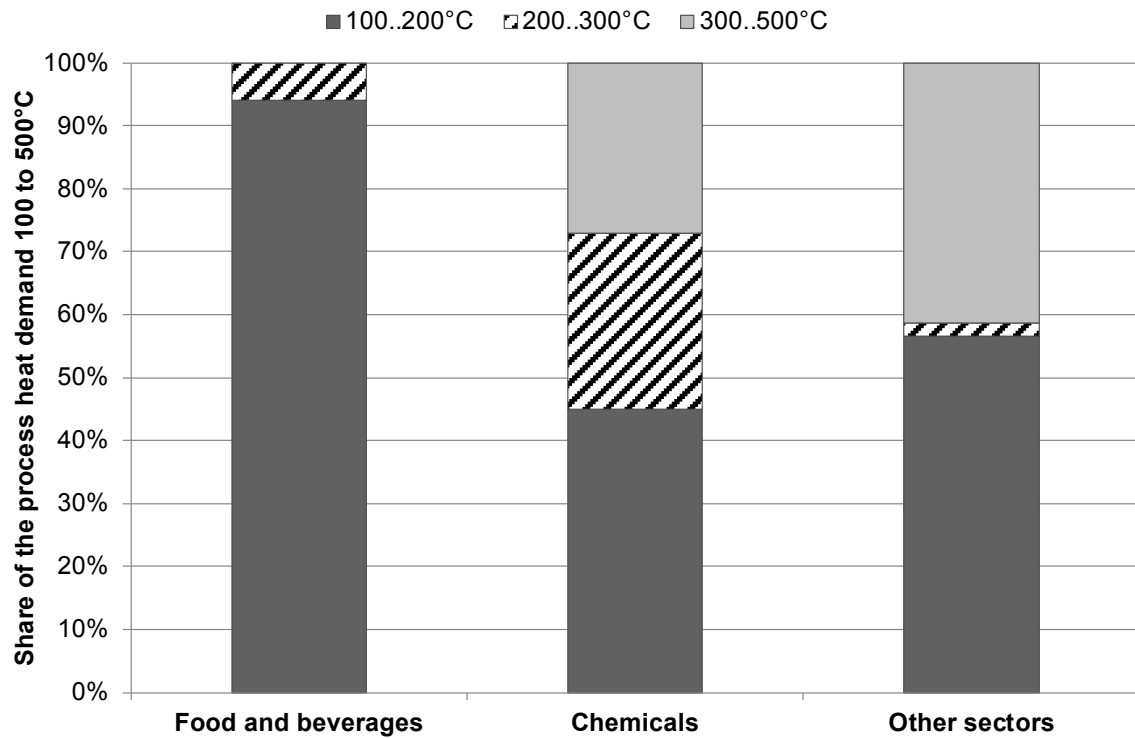


Figure 3-2: Breakdown of the industrial process heat demand between 100 and 500 °C (own figure derived from (Hofer, 1994)).

As the classification of industrial sectors was different at the time of (Hofer, 1994) it was not possible to derive a temperature distribution for all sectors. Therefore, only Food and beverages and Chemicals are displayed separately as they are most important, whereas for the other sectors an average is used. This incorporates an uncertainty for the temperature distribution. Nevertheless, Food and beverages and Chemicals have a share of 55 % of the 100 to 500 °C temperature range as shown in Table 3-1.

Further, the distribution for Paper, which has a share of 15 % of the 100 to 500 °C temperature range, was verified within the analysis done for Section 3.4. Although this distribution is not completely correct for individual sectors as for Printing, it seems acceptable to use the average distribution for other sectors. The distribution of Figure 3-2 was used to calculate the distribution of temperatures within the 100 to 500 °C temperature range of Table 3-1.

Table 3-2, which is sorted by the heat demand below 300 °C, shows the detailed distribution. 21 % of the industrial heat demand is in the temperature range lower than 100 °C for process heat, space heating and hot water, which is very promising for the application of solar heat, as the efficiency of solar thermal systems declines with rising temperatures. An additional 8 % are in the temperature range of 100 to 200 °C. The share of the industrial heat demand in the temperature range of 200 to 300 °C is significantly

smaller. The sectors of Chemicals and Food and beverages have by far the highest shares of heat demand below 300 °C.

Table 3-2: Breakdown of the industrial heat demand with detailed temperature distribution between 100 and 500 °C.

Industrial sector (NACE Rev.2 Code)	HW	SH	Process heat [TWh]					Sum	Sum <300°C
			<100°C	100 ..200°C	200 ..300°C	300 ..500°C	>500°C		
Chemicals and chemical products (20/21)	0.2	6.7	13.5	9.5	5.9	5.5	55.7	96.9	35.7
Food products and beverages (10/11)	0.3	8.3	11.8	13.7	0.9	0.0	0.0	35.0	35.0
Motor vehicles and trailers (29)	1.0	7.3	2.7	1.1	0.0	0.8	3.7	16.8	12.2
Paper and paper products (17)	0.1	2.4	2.7	5.6	0.2	4.1	0.0	15.1	11.0
Fabricated metal products (25)	0.9	6.3	2.3	1.0	0.0	0.8	3.4	14.8	10.6
Machinery and equipment (28)	0.6	4.5	1.6	0.7	0.0	0.5	2.3	10.3	7.5
Basic metals (24)	0.2	4.4	0.9	1.5	0.1	1.1	154.9	163.1	7.0
Non-metallic mineral products (23)	0.1	3.5	1.2	1.0	0.0	0.7	82.7	89.3	5.9
Rubber and plastic products (22)	0.1	1.6	0.9	2.0	0.1	1.4	0.0	6.1	4.7
Electrical equipment (27)	0.3	2.4	0.9	0.6	0.0	0.5	1.1	5.8	4.3
Textiles (13)	0.1	1.2	2.0	0.0	0.0	0.0	0.0	3.3	3.3
Printing and reprod. of recorded media (18)	0.0	0.4	0.2	1.5	0.1	1.1	0.0	3.3	2.2
Wood and wood products (16)	0.0	0.3	1.5	0.2	0.0	0.2	0.0	2.1	2.0
Furniture and other goods (31/32)	0.0	0.7	0.4	0.6	0.0	0.4	0.2	2.4	1.8
Computer, electronic, optical products (26)	0.1	0.9	0.3	0.1	0.0	0.1	0.4	2.0	1.5
Other transport equipment (30)	0.1	0.9	0.3	0.1	0.0	0.1	0.4	2.0	1.4
Leather and related products (15)	0.0	0.1	0.2	0.0	0.0	0.0	0.0	0.3	0.3
Wearing apparel (14)	0.0	0.1	0.2	0.0	0.0	0.0	0.0	0.3	0.3
Tobacco products (12)	0.0	0.0	0.0	0.0	0.0	0.0	0.0	0.1	0.1
Sum	4.2	52.0	43.6	39.3	7.5	17.4	304.9	468.9	146.6
Share*	1 %	11 %	9 %	8 %	2 %	4 %	65 %	100 %	31 %

*of the overall industrial heat demand; all numbers without unit in TWh; HW: hot water; SH: space heating.

The majority of heat demand in Germany is needed at temperatures above 500 °C with a share of 65 %, of which 78 % is used in Basic metals and Non-metallic mineral products. A possible uncertainty of this high temperature heat demand would change the presented shares. Assuming e.g. a negative 10 % deviation in the heat demand over 500 °C of Basic metals and Non-metallic mineral products leads to an increased share of the overall low temperature (<100 °C) heat demand from 21 to 22.4 %.

In contrast to this temperature distribution, Werner (2006) states that a third of the industrial heat demand in Europe is at temperatures lower than 100 °C and almost 60 % at temperatures below 400 °C. These figures were determined by applying a temperature distribution for the German industry (ARGE Fernwärme e.V., 2000) to the energy balances of other countries (International Energy Agency, accessed 2011). An explanation for the deviation in temperature distribution might be the minor role of several industries with low

temperature heat demand as e.g. Food and beverages, Textiles, Wearing apparel and Wood in Germany compared to the average of Europe (Eurostat, accessed 2011).

Other references support the temperature distribution determined in this study. Forschungsstelle fuer Energiewirtschaft e.V. (1999) states that a comparably low heat demand exists for process temperatures between 200 and 800 °C in Germany and about one third of the heat demand is needed at temperatures below 200 °C. Lambauer et al. (2008) investigate the potential of heat pumps to provide heat up to 100 °C in the German industry. The industrial heat demand below 100 °C, which is defined as the technical potential, is calculated with 108 TWh for 2006. This result also supports the values of Table 3-2, where the heat demand below 100 °C sums up to 100 TWh, and according to BMWi (2010) the energy demand in industry decreased by about 11 % from 2006 to 2009.

3.3. Potential for Germany and Europe

The theoretical potential of solar heat for industrial processes in Germany was determined by adding the sum of process heat below 300 °C and the demand for space heating and hot water for all industrial sectors, except Basic metals and Non-metallic mineral products. These sectors were not considered as they have by far the highest waste heat potential due to the dominant heat consumption above 500 °C. This leads to a theoretical potential of 134 TWh per year. In order to calculate the technical potential further restrictions were taken into account.

First of all, the heat demand in many industrial enterprises can often easily be reduced by heat recovery measures, such as an economizer for the steam boiler or the use of waste heat from supply of cold and compressed air. Heat integration of several processes can further reduce the heat demand. In addition, a fraction of the required heat has to be supplied by electricity due to operational reasons. Finally, in many cases sufficient space is not available for the installation of solar thermal systems (Schweiger et al., 2001) and many roofs in industry are not capable of carrying additional static loads. In (Müller et al., 2004) it is assumed that a share of 60 % of the theoretical potential for low and medium temperature processes cannot be used because of mentioned restrictions. Although this assumption cannot be fully verified it is also considered for this study as the described reasons support that major restrictions exist for the use of solar heat for industrial processes.

A solar fraction is documented for six solar process heat systems in Germany: Three systems provide heat for surface treatment and electroplating, two in Food and beverages and one for a paint shop. The average solar fraction of these systems is 32 % (O.Ö. Energiesparverband, 2011a). Within (Schweiger et al., 2001) 25 systems were dimensioned

for case studies and suggested to participating companies. The average solar fraction of these systems was 29 %. Six further case studies were carried out in (Müller et al., 2004) with an average solar fraction of 40 %. Furthermore, for the potential study for the Netherlands (van de Pol et al., 2001) a solar fraction of 30 % was assumed. Therefore, an average solar fraction of 30 % was assumed in this thesis to determine the technical potential. Applying the figures for efficiency measures, restricted roof area and average solar fraction to the theoretical potential of 134 TWh per year, the technical potential for solar heat in industry in Germany can be estimated at 16 TWh per year or 3.4 % of the total industrial heat demand.

As the heat demand presented in Table 3-1 and Table 3-2 was verified with figures from official statistics and the references given in Section 3.2 support the temperature distribution, it can be concluded that the theoretical potential represents a reliable figure. In order to estimate the technical potential, a reduction of the theoretical potential due to possible efficiency measures and an average solar fraction were assumed. Both figures incorporate an uncertainty, the higher being the reduction for efficiency measures and available roof area, as the assumption of solar fraction is justified by several references. A reduced or increased value for efficiency measures and available roof area to 50 % or 70 % would lead to a technical potential of 20 or 12 TWh per year, respectively. This variation shows that the technical potential represents an estimate rather than a definite figure.

In order to compare the estimated potential with prior potential studies, Figure 3-3 shows the technical potential for Austria (Müller et al., 2004), Italy (Vannoni et al., 2008), the Netherlands (van de Pol et al., 2001), Portugal, and Spain (Schweiger et al., 2001). As the figure shows, it is in a range between 3 and 4.5 % of the industrial heat demand in the particular region and about 16.7 TWh per year for these five countries in total (Vannoni et al., 2008). For the European Union (EU25) a potential of 72 TWh per year or 3.8 % of the industrial heat demand in the EU25 is given in (Vannoni et al., 2008). The calculated potential for Germany is within the range of prior studies, although additional industrial sectors were considered for this study. On one hand this can be explained by a lower solar fraction compared to e.g., (Müller et al., 2004). On the other hand, the additional sectors have only a very small share of the overall heat demand.

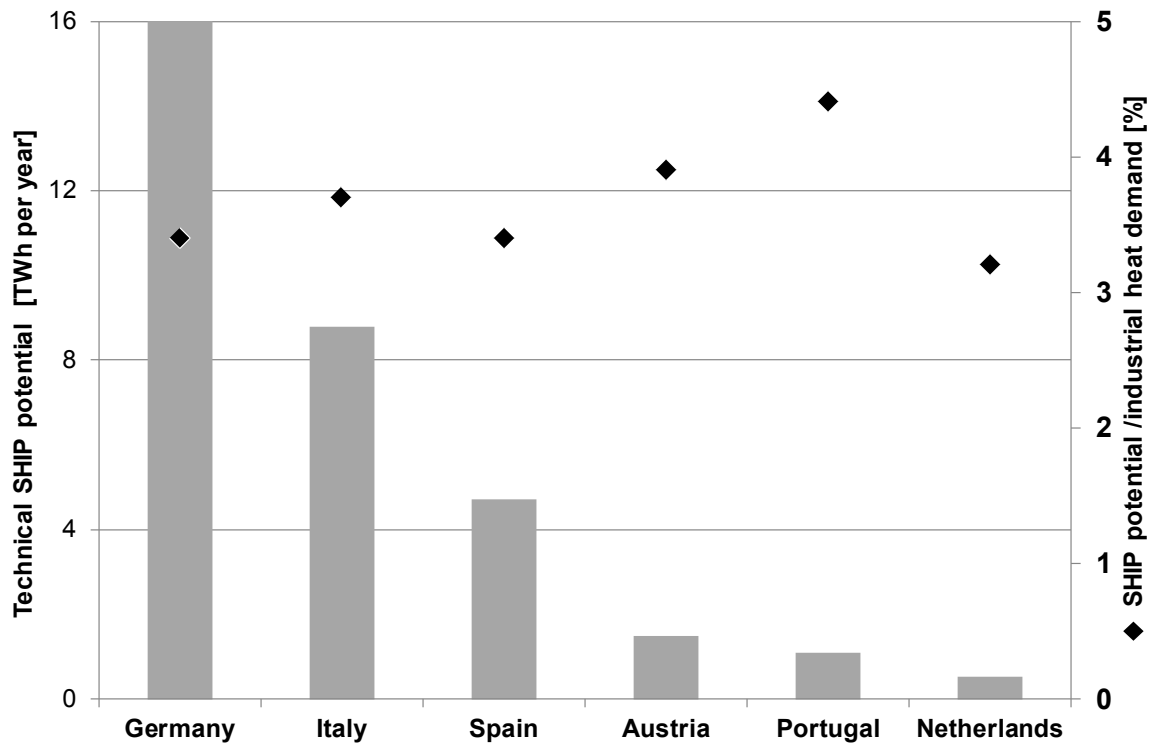


Figure 3-3: Technical potential of solar heat for industrial processes in European countries.

The absolute number of 16 TWh per year represents by far the highest potential of solar heat for industrial processes in European countries, as shown in Figure 3-3. Solar thermal collectors with about 25 GW_{th} (35 million m²) would be necessary to develop the technical potential, assuming an average annual solar system yield of 450 kWh/(m²a). For the EU25 in total about 110 GW_{th} (155 million m²) would be needed which represents a substantial market for solar thermal systems.

3.4. Promising industrial sectors and processes

Within this section the most promising sectors for the use of solar heat are selected. Further, selected sectors are analyzed and suitable processes are identified.

A first selection of promising sectors was done by considering their heat demand below 300 °C, as Figure 3-4 shows. Out of the sectors of Table 3-2, six sectors with a heat demand of less than 2 TWh below 300 °C were excluded. Although Furniture and other goods has almost the same heat demand below 300 °C than Wood, it summarizes many different sub-sectors and was therefore excluded. In a second step, the sectors of Basic metals and Non-metallic mineral products were excluded because of their assumed high waste heat potential. Figure 3-4 indicates that the selected sectors represent a substantial

share of the industrial heat demand. In total, these 11 sectors consume about 88 % of the industrial heat demand below 300 °C in Germany, including space heating and hot water.

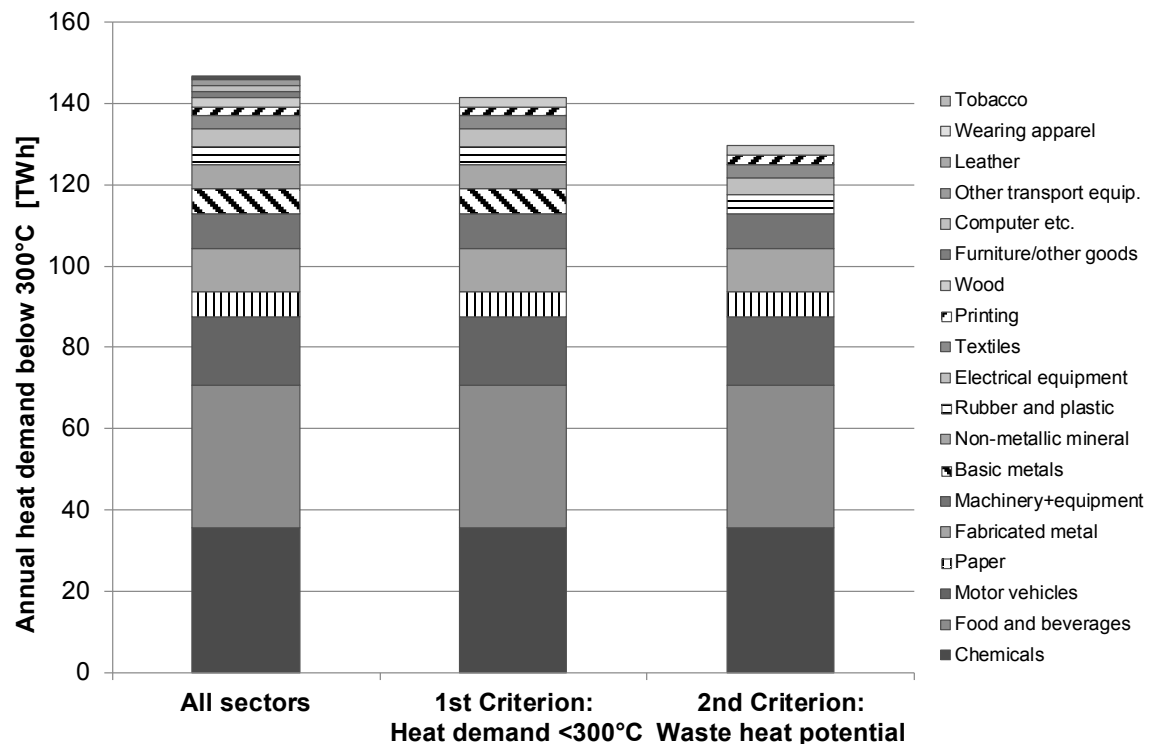


Figure 3-4: Heat demand below 300 °C of all and the selected promising sectors.

Prior potential studies that were performed in the past for different countries or regions identified several industrial sectors and processes as suitable for the application of solar thermal systems. Besides the studies for Austria (Müller et al., 2004) and Spain and Portugal (Schweiger et al., 2001), which are described in Section 3.1, further potential studies identifying suitable sectors are available for Victoria (Australia) (McLeod et al., 2005), Italy (Vannoni et al., 2008), the Netherlands (van de Pol et al., 2001), Sweden (Kovacs et al., 2003), and for Greece, Wallonia (Belgium) as well as a few industrial sectors in Germany (Vannoni et al. 2006, 2006). Table 3-3 summarizes the sectors referred to as suitable in prior studies.

The relevance of individual sectors and hence the temperature levels of the industrial heat demand can vary strongly in different countries. Nevertheless, the necessary temperatures and processes within a sector and thus the promising sectors are transferable because production processes can be assumed to be similar across different countries. Therefore, the results of previous studies support the selection of promising sectors for Germany.

Table 3-3: Suitable sectors mentioned in prior potential studies in the field of solar heat for industrial processes.

Industrial sector	Austria	Greece	Germany	Italy	Spain and Portugal	Netherlands	Victoria (Australia)	Wallonia (Belgium)
Chemicals	X	X		X	X		X	X
Food and beverages	X	X	X	X	X	X	X	X
Paper		X	X	X	X	X	X	X
Motor vehicles		X	x	X	X			
Machinery and equipment							X	
Rubber and plastic	X							
Textiles	X	X		X	X	X	X	X
Prefabricated concrete components	X							
Tobacco		X		X	X			X
Leather		X		X	X			

Following, selected sectors are analyzed and suitable processes for the integration of solar heat are identified. The sectors of Motor vehicles, Machinery and equipment, and Electrical equipment are not covered, as a large share of its heat demand is for space heating and DHW and suitable processes are very similar to Fabricated metal. The sector of Printing is not analyzed in detail as only one major process, which is the drying of paper just below 200 °C, uses heat in this sector. The selection of sectors is based on the heat demand below 300 °C and its waste heat potential. More research such as case studies are necessary regarding the possible use of waste heat especially in the sectors of Motor vehicles, Fabricated metal, Machinery and equipment but also in Chemicals as they all have a certain high temperature heat demand. The question arises if high temperatures are needed at the same production sites as low temperature processes. The results of prior studies also show that some sectors are mentioned as suitable only in a few or a single study, which shows the need for further investigation.

The sector of **Chemicals** has the highest quantitative potential for the application of solar heat because of its large heat demand. Although a large share of the heat is needed at high temperatures, there is still a considerable heat demand at low (<100 °C) and medium (<300 °C) temperatures. The sector has a share of 24 % of the heat demand of the 11 selected sectors at temperatures below 100 °C. At medium temperatures (100 to 300 °C) the share is 36 %. The average energy costs are in the range of 4 to 5 % of the total manufacturing costs, which shows the importance of energy usage. This share depends strongly on the subsector (VCI, 2009). Especially the production of ammonia and petrochemicals, e.g. production of polypropylene, are very energy intensive, whereas the

subsector of pharmaceuticals needs less energy. Potential processes for the integration of solar heat are cooking at temperatures of 85 to 110 °C, distillation (110 to 300 °C), biochemical processes at low temperatures (<60 °C), preheating and polymerization processes (Schnitzer et al., 2006). Due to very complex production facilities and the possible use of waste heat, a deeper analysis of this sector is necessary to identify the most suitable application areas for solar heat.

The sector of **Food and beverages** is mentioned as suitable in all prior potential studies. It has about the same shares of the heat demand at low and medium temperatures of the promising sectors as has Chemicals. Within Food and beverages, the major share of the heat is needed at low temperatures below 100 °C, accounting for 58 % (incl. hot water and space heating). Additional 42 % are consumed between 100 and 300 °C. Due to the fact, that no consistent data of the heat demand of the subsectors is available, data for the overall energy demand was considered here to identify the most promising subsectors (DeStatis, 2009). Although the sugar industry has the highest share of the energy demand of Food and Beverages, the potential is limited, because production takes place mainly in autumn and winter, and combined heat and power is used extensively. Milk production, slaughtering and meat production, and fruit and vegetable processing have a considerable heat demand and therefore seem promising for the use of solar heat. Further subsectors which appear suitable are beer production, mineral water, feed, and malt. Common processes are pasteurization of liquid goods at 65 to 100 °C, cooking at 100 °C in meat processing, blanching of vegetables or meat (65 to 95 °C), drying and evaporation at 40 to 130 °C in fruit and vegetable processing and cleaning of products and production facilities in all subsectors at 60 to 90 °C.

The sector of **Paper** has a share of 12 % of the heat demand below 300 °C of the selected sectors. Within the paper industry about two-thirds of the heat demand is needed at temperatures between 100 and 500 °C, mainly for drying processes. Still, one-third of the heat demand is consumed at temperatures below 100 °C. The temperature distribution of Table 3-2 shows a high heat demand at temperatures between 100 and 200 °C and 300 and 500 °C. Drying cylinders using steam at temperatures of 130 to 200 °C are widely used. Further, directly fired drying hoods, operating at around 400 °C, are frequently installed in tissue production (hygiene paper). The average share of energy costs is about 11 % of the total manufacturing costs and can sometimes reach up to 25 % (Vogt et al., 2008). This shows the high importance of energy efficiency and the utilization of renewable energy in this sector. Besides drying, de-inking of recycled paper and preheating of boiler feed water represent promising applications for solar thermal energy in this industry sector. Further suitable processes are cooking and bleaching.

The sector of **Fabricated metal** has a share of 8 % of the heat demand below 300 °C of the selected sectors. Low temperature heat below 100 °C, including process heat, space

heating and hot water accounts for 64 % of the total heat demand. Still, processes at temperatures higher than 300 °C also account for 28 % of the heat demand. According to WKO (2003) energy costs are only 0.3 to 1.6 % of the total manufacturing costs within the sector. Especially for coating processes the required heat is at low temperatures. For example the processes degreasing, electroplating and pickling require temperatures below 100 °C. Drying is a common process that requires hot air at about 120 °C. Similar processes can be found in the sectors of Motor vehicles, Machinery and equipment, and Electrical equipment.

43 % of the heat needed in **Rubber and plastic** is at temperatures below 100 °C and 40 % at 100 to 300 °C. According to BMWi (2010) the share of energy costs is 3 %. Besides the supply of hot water and space heating, drying of plastic pellets is a potential process for solar thermal energy. The pellets are air-dried at temperatures from 50 to 150 °C to ensure quality. Another possible application is preheating of pellets before processing, e.g. by extrusion or injection molding.

Manufacturing of **Textiles** consumes 4 % of heat demand below 300 °C of the 11 selected sectors. The heat demand is mainly limited to temperatures below 100 °C. In contrast to the numbers of Table 3-1, the analysis showed that a few processes with temperatures higher than 100 °C exist in this sector. Within the textile industry, washing at 40 to 90 °C, drying, and a large number of finishing processes like bleaching at 70 to 100 °C, desizing at 80 to 90 °C and coloring at 40 to 120 °C are the main consumers of process heat. At a rough estimate up to 25 to 50 % (Müller et al., 2004) of heat needed in the textiles sector could be covered by solar thermal energy. This represents a considerable potential, although the sectors' share of the industrial heat demand is quite low.

The **Wood sector** consumes only 2 % heat demand below 300 °C of the 11 selected sectors. The most important subsectors regarding energy and heat consumption are the manufacture of (veneer-) plywood and lumber mills. A large part of the heat demand (82 %) is needed at temperatures below 100 °C. Drying of raw wood before processing represents the most important process for the integration of solar heat. Besides this, processes like steaming, cooking and pickling are promising due to low or moderate temperatures.

The potential for individual sectors is important to examine which sectors are most promising for the application of solar heat. Figure 3-5 shows the technical potential of the 11 selected sectors, which was determined in the same way as the overall potential in Section 4.

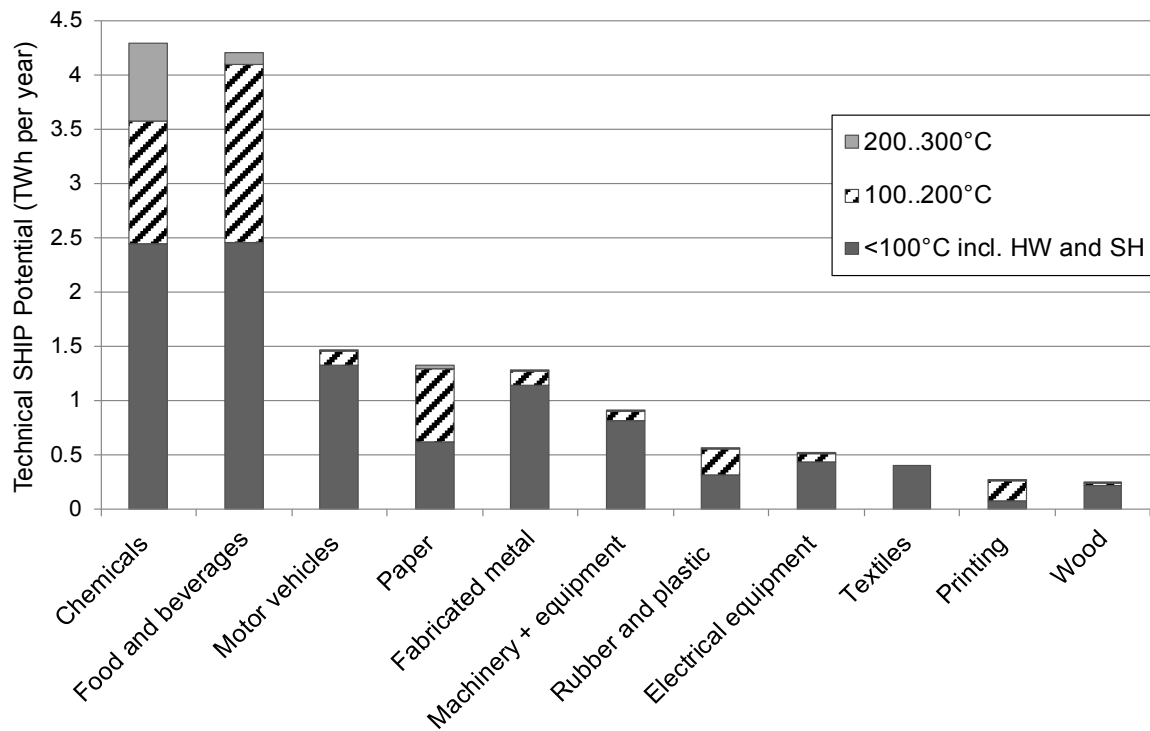


Figure 3-5: Technical potential for the use of solar process heat of the eleven selected sectors divided in temperature ranges.

Besides the calculated potential, the temperature distribution for each individual sector is visible in Figure 3-5, which is important in order to assess the most promising sectors. For Motor vehicles, Fabricated metal, Machinery and equipment, and Electrical equipment a large share of the potential is heat demand for space heating and DHW. Chemicals and Food and beverages have by far the highest potential of all sectors, whereas the integration of solar heat in processes of Food and beverages seems easier due to lower complexity of the production processes and therefore offers the higher short-term potential, as Taibi et al. (2012) state.

The analysis of industrial sectors shows that various processes are suitable for the use of solar heat. Figure 3-6 shows an overview of the processes identified as suitable for the integration of solar heat in this thesis, as they all take place at low or medium temperatures. The selection of processes was verified with other studies (Aidonis et al., 2005a; Müller et al., 2004; Schweiger et al., 2001). As the figure shows, various processes suitable for the use of solar heat can be found in several of the selected sectors.

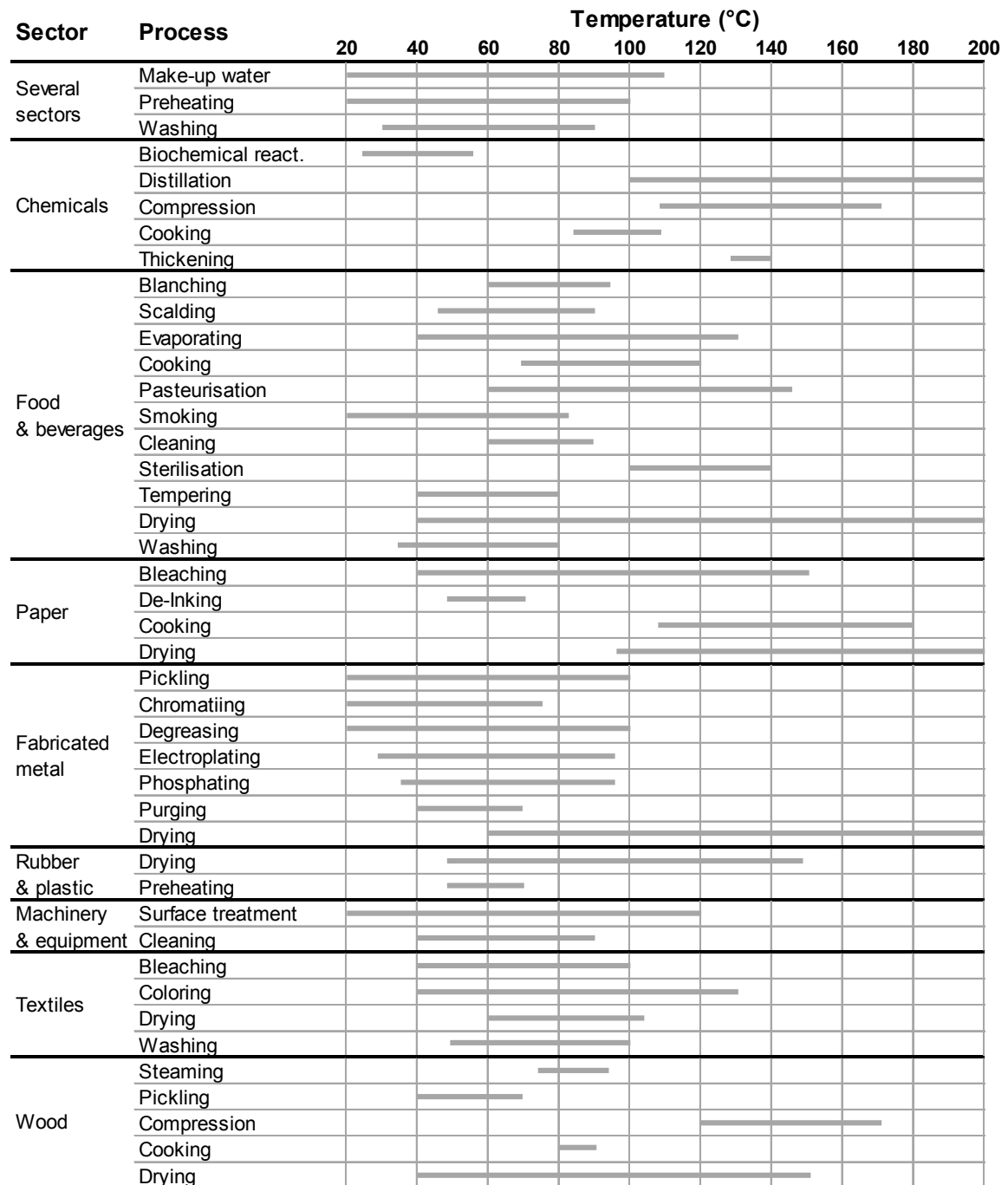


Figure 3-6: Promising processes for the integration of solar heat, identified for this thesis and verified with (Aidonis et al., 2005a; Müller et al., 2004; Schweiger et al., 2001).

3.5. Conclusion

At first, this section analyzed the temperature distribution of the industrial heat demand in Germany. An overview of the heat demand below 300 °C in Germany is presented, which is crucial to assess the potential not only of solar thermal but also of CHP and heat pumps in industry.

The analysis of the temperature distribution of the industrial heat demand shows that the most important temperature ranges for the application of solar process heat in Germany are below 100 °C and between 100 and 200 °C. Further collector developments should focus on cost reduction for standard collectors used below 100 °C and development of cost effective process heat collectors up to 200 °C as well as demonstration projects in this temperature range. Steam production on supply level is a promising application for solar process heat in regions with a high share of direct insolation as the effort for integration can be reduced compared to integration on process level. As almost all steam networks are operated at pressures corresponding to temperatures lower than 200 °C, this temperature range should be a major focus for future developments. As a high share of the low temperature heat demand is for space heating, the combination of solar thermal systems with CHP and heat pumps needs to be investigated.

A theoretical potential of solar heat for industrial processes in Germany of 134 TWh per year, and a technical potential of 16 TWh per year were determined. In future, the experience of additional solar thermal systems in industry will help to achieve more reliable figures, e.g. efficiency measures and solar fraction, to estimate the technical potential. The share of the theoretical potential which can be technically developed, and to a certain extend also the theoretical potential itself, always depend on the available and feasible solar thermal technology. Still, it can be concluded that a substantial technical potential for the use of solar heat and therefore a good possibility to reduce greenhouse gas emissions exists in Germany. Nevertheless, increased efficiency of high temperature processes is crucial to lower the greenhouse gas emissions of industry substantially.

Finally, the most promising industrial sectors were identified and analyzed regarding suitable processes. Some of the selected sectors surely offer broad possibilities for the use of solar heat, whereas in others the restrictions of energy efficiency might reduce the theoretical potential substantially. The sectors of Chemicals and Food and beverages have the highest potential for the use of solar heat. In Chemicals, the possibilities for the use of waste heat has to be investigated in more detail, since a large amount of heat is consumed at temperatures above 500 °C. Considering its big share of the industrial heat demand at low temperatures, the results of the prior studies and the variety of suitable processes, the sector of Food and beverages has the highest short-term potential for the use of solar thermal energy in industry.

4. System analysis of a low-temperature solar process heat system

As shown in Section 2, the system behavior and performance of large STS for domestic applications has been extensively studied in the past. Common failures of early large scale STS were leakages of the collector loop, damage of its isolation, condensation inside the collector, damage of its cover, too small designed expansion vessels and failures of the control system (Peuser et al., 2001). Wrong hydraulic setups in terms of combined return flows for different heat consumers and failures of control were identified for some STS by Croy and Wirth (2006) and Drück and Schenke (2007). The authors conclude that many combisystems incorporated failures and have a lower performance than predicted in design phase. Heimrath (2004) also proved the strong thermal impact of the design of heat distribution networks on the efficiency of the STS. In later STS, most of the failures described in (Peuser et al., 2001) regarding the collector and solar loop were reduced substantially. Nevertheless, problems with the system control increased and a common failure of reduced performance of the heat exchangers was identified. Overall, the system yield of the analyzed STS was between 38 and 90 % (63 % in average) of its design values (Croy et al., 2011).

Some publications are also available regarding the behavior and performance of solar process heat systems. Several authors show that the predicted performance could not be reached by the later installed STS (Anthrakidis et al., 2010; Karagiorgas et al., 2001; Kutscher and Davenport, 1980; Wutzler et al., 2011). The reasons include excessive thermal losses, oversized systems, and wrong hydraulic setups.

Up to now, no detailed analysis of a realized STS in industry is available based on measurements and simulations with a validated model. Furthermore, the most important factors that influence the performance of such a system have neither been identified nor been quantified. The objective of this section is to identify possible faults that may occur in an STS in industry and to evaluate their impact on its performance. In addition, important factors that influence the overall system performance are identified and their influence is evaluated. In addition, the section describes the complex interaction between energy efficiency measures (especially heat recovery) with the integration of an STS in an industrial process.

An STS for process heat generation built at a brewery in Germany was analyzed as an example for this thesis. At first, Section 4.1 describes the integration of the STS in the hot water supply of the brewery, the system configuration, its performance, gained operational experience, and analysis of its components. Afterwards, Section 4.2 introduces the

developed simulation model and illustrates the results of validation. Further, Section 4.3 explains the system analysis with simulations. Finally, Section 4.4 provides the conclusion. This section is based on a paper in a peer-reviewed journal derived from this thesis (Lauterbach et al., 2014). Parts of this section were also published in and (Lauterbach et al., 2011b; Schmitt et al., 2010; Schmitt et al., 2012b).

4.1. Pilot plant at a brewery

The studied brewery in Germany produces approximately 6,200 m³ of beer per year and has an annual final energy consumption of 5 GWh. About 80 % of the energy is supplied by natural gas and used to provide process heat, hot water and space heating. All heat consumers are connected to a steam network that is fed by a boiler with a nominal capacity of 2.6 MW_{th}. The production process is operated in one shift on five days per week. During summer, the amount of produced beer increases by a factor of 1.3 compared to the winter period. Based on their production capacity, technical installations and energy consumption, the brewery is a representative example of a small to medium enterprise in the central European brewing sector.

4.1.1. System description

The developed concept for the brewery combines an energy efficiency measure with an improved heat recovery and the utilization of solar thermal energy. The initial state of the hot water supply of the brewhouse is shown in Figure 4-1.

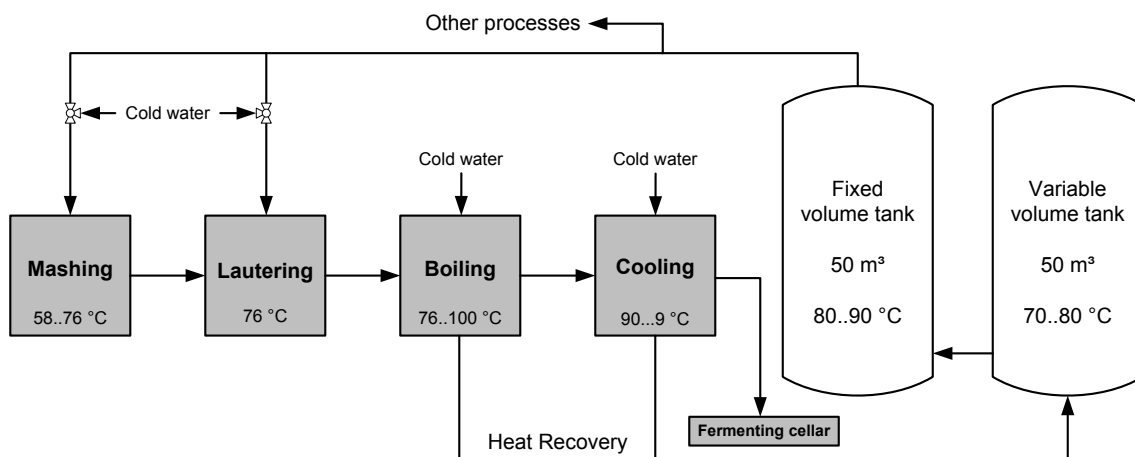


Figure 4-1: Initial state of the hot water supply of the brewhouse. The process steps in the brewhouse are shown in grey.

Two tanks are installed for the hot water supply of the whole brewery. One has a constant fluid volume of 50 m³, in the other it is possible to store a variable amount of water up to 50 m³. This is necessary because of the fluctuating streams of incoming hot water from heat recovery and outgoing water to supply several process steps. The temperature level in the fixed volume tank is at 80 to 90 °C and slightly higher compared to the variable volume tank at 70 to 80 °C. The hot water needed for mashing and lautering is provided by the fixed volume tank. To supply the required temperature, the water is cooled down by mixing with cold water of 10 °C. Additionally, this tank supplies the bottle filling hall with hot water of 80 °C, used for cleaning of installations and filters.

The tanks are fed by two heat recovery installations. During the boiling and cooling process steps, brewing water at 10..15 °C is heated up to 80 °C by heat recovery and fed into the variable volume tank. In order to increase energy efficiency, wort boiling at atmospheric pressure was replaced by an efficient vacuum boiling technology that led to energy savings of approximately 30 % at this process step. An additional heat exchanger was installed to preheat the wort close to boiling temperature after lautering, saving a part of the steam required for heating the wort before boiling. Further, the heat recovery during wort boiling is used to additionally heat up the fixed volume tank instead of heating cold water up to 80 °C (as shown in Figure 4-2).

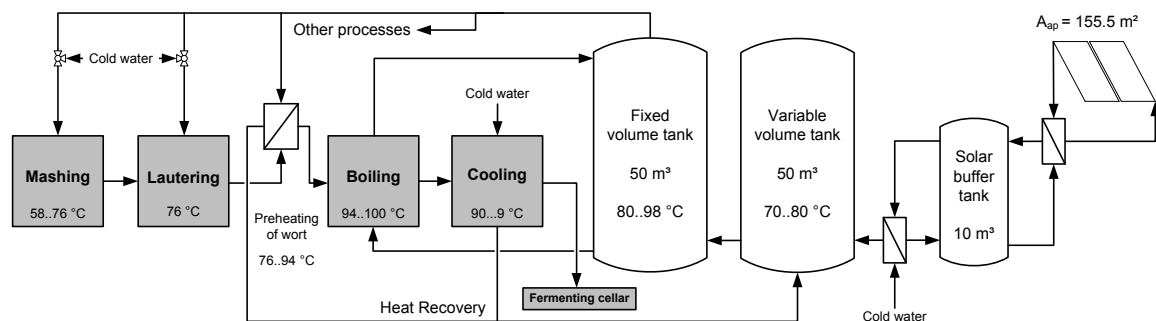


Figure 4-2: Improved hot water supply of the brewhouse with integrated STS. The heat recovery from boiling is used to heat the fixed volume tank. Heat from the upper part of the fixed volume tank is used to preheat the wort before boiling which leads to less available hot water and the possibility to integrate an STS.

Therefore, water from the lower part of the tank is heated up from 80 to 98 °C and stored in the upper part of the tank. The hot water from the upper part of the fixed volume tank is then taken to preheat the wort and fed into the variable volume tank afterwards. This modification resulted in a more efficient heat recovery since the waste heat is utilized at a higher temperature level. This has two consequences: (i) steam for heating up the wort before boiling is saved, and (ii) the available amount of hot water from heat recovery is reduced, so that it can be provided by solar energy at a lower temperature level. Thus, an

STS was integrated to heat up cold water of 15 °C that is fed into the variable volume tank, depending on its filling level. This design leads to a simple system control and high expected solar gains.

The hot water supply of the brewhouse was modeled in the transient system simulation software TRNSYS 17 (Klein et al., 2009) by creating profiles for all hot water streams of the production process and simulation of both tanks. The design approach in the simulation study was to determine the maximum amount of energy that can be delivered by the STS while avoiding stagnation in summer. The simulation with the developed load profiles showed that a large amount of hot water is required at night time and during morning hours. Therefore, the variable volume tank has to be fed with solar heated water particularly during the early morning hours. Hence it was decided to install an additional solar heat store for the STS, as shown in Figure 4-3. This design ensures a high specific system yield. The collector field aperture area is $A_{ap} = 155.5 \text{ m}^2$ and a volume of the solar heat store is $V_{store} = 10 \text{ m}^3$.

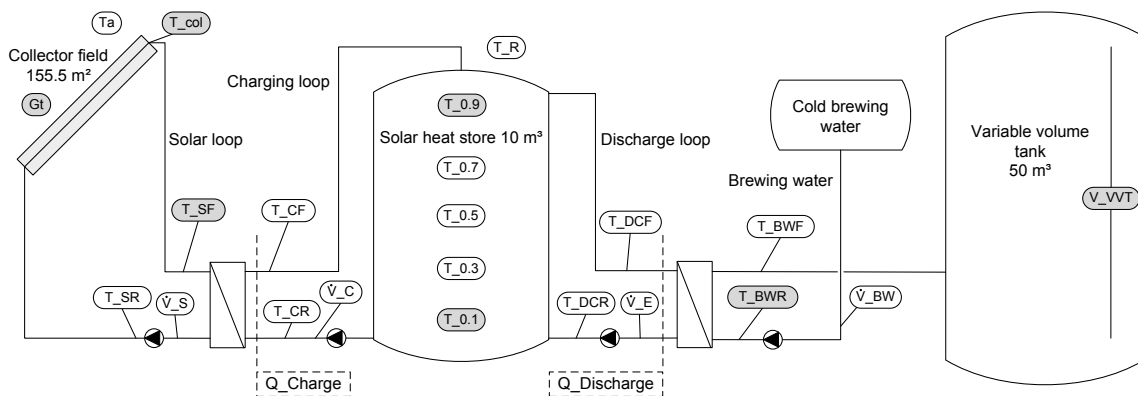


Figure 4-3: Hydraulic scheme of the STS with monitoring sensors; the grey colored sensors are used not only for monitoring but also for control; dashed lines show positions of heat balances.

The collector array consists of 22 Thüsol S 7.69 (ITW, 2009) collectors with a gross area of 169 m² (aperture area = 155.5 m²). The roof has an orientation of 40° south-west at a slope of 28°. Monitoring and control sensor locations are shown in Figure 4-3, where the grey colored sensors are used for both, control and monitoring. The solar loop is controlled by the temperature difference (7 and 3 K) between the collector and the lowest temperature in the store. The secondary charging loop is controlled identically, using the solar flow temperature (T_{SF}) instead of the collector temperature. The solar heat store is discharged if the filling level of the variable volume tank falls below 70 % (and as long as it remains below 75 %) and the temperature in the upper part of the solar heat store exceeds 40 °C. When both conditions are fulfilled, the pumps in discharging and brewing water loop are

switched on. Night cooling of the solar heat store is activated on weekends if $T_{0.1}$ is higher than 70 °C and the filling level of the variable volume tank is more than 70 %.

Heat balances are calculated at the two positions marked in Figure 4-3. Measurements of the mass flow in the solar loop are difficult due to the properties and uncertainties of the concentration of the water-glycol mixture, so the heat quantity in the solar loop was not considered. The temperature sensors of the brewing water return flow (T_{BWR}) is located too far from the heat exchanger with part of the piping outside the buildings, so that the heat quantities for charging (Q_{Charge}) and discharging ($Q_{Discharge}$) of the store are used in the following.

4.1.2. Uncertainties of measurement

It is necessary to calculate heat flows to evaluate the performance of the STS and validate the simulation model. The temperatures within the system are measured with resistance temperature sensors (Pt-1000, class A) connected with two leads. The uncertainty of these sensors is $\pm (0.15 + 0.002 \cdot |T|)$ °C (DIN EN 60751, 2009), leading at 50 °C to a deviation of ± 0.25 K. The multi-jet flow meters used within the STS have an uncertainty margin of ± 3 % (Aquametro, 2012). According to error propagation (Taylor, 1997), the resulting maximum error for heat flows is 4 % when combining the uncertainty margins for volume flow and temperatures ($T_{flow} = 70$ °C; $T_{return} = 20$ °C). The hemispheric irradiance on the collector plane is measured and used as an input for the simulation model. The irradiance sensor is a Kipp & Zonen CMP 6 pyranometer that has an uncertainty given by the manufacturer of less than 5 % for each day (Kipp & Zonen, 2011) with an uncertainty of $10 \text{ W} \pm 4$ % estimated by de Keizer (2012) for a single radiation measurement.

4.1.3. Performance

The described system has been monitored since June 1st, 2010 with a measurement interval of one minute. The utilization ratio of the charging loop is the first performance indicator used for the evaluation. It is defined as the ratio between heat quantity charging the solar heat store and the total irradiation on the collector field during the same period.

$$\bar{\eta}_{charge} = \frac{\text{Heat quantity charging the store (} Q_{Charge} \text{)}}{\text{Total irradiation on collector field (} H_t \text{)}} \quad (1)$$

The heat quantity charging the store (Q_{Charge}) is used to calculate the energy delivered to the solar buffer because it can be measured with higher accuracy compared to the solar loop as water instead of water-glycol is used. As thermal losses in the heat exchanger are

very small, this does not lead to a major deviation (Mies et al., 2006). The second performance indicator is the system utilization ratio, defined as the ratio of heat quantity discharging the store to total irradiation on the collector field during the same period.

$$\bar{\eta}_{\text{sys}} = \frac{\text{Heat quantity discharging the store (Q_Discharge)}}{\text{Total irradiation on collector field (Ht)}} \quad (2)$$

In 2011 the total specific irradiation on the collector field was 1.167 kWh/(m²_{ap}a) and 373 kWh/(m²_{ap}a) were delivered to the solar heat store resulting in a collector loop utilization ratio of 32 %, as shown in Table 4-1.

Table 4-1: Heat quantities for charging, discharging and night cooling of the STS and utilization ratio for 2011; the pump in the discharge loop is also switched on during night cooling to increase the heat losses of the store.

Energy quantity / utilization ratio	Abbreviation	Total [MWh]	Specific [kWh/m ² _{ap}]
Irradiation on collector plane	Ht	181	1167
Heat charging the store	Q_Charge	58	373
Heat discharging the store	Q_Discharge	48	311
Night cooling: charging loop	NC_Charge	1.2	8
Night cooling: discharging loop	NC_Discharge	0.5	3
Charging loop utilization ratio	$\bar{\eta}_{\text{charge}}$	32.0 %	32.0 %
System utilization ratio	$\bar{\eta}_{\text{sys}}$	26.6 %	26.6 %

In 2011, 311 kWh/(m²_{ap}a) was delivered to the brewing water resulting in a system utilization ratio of 27 %. Figure 4-4 shows the monthly total irradiation on the collector field, the energy delivered to the solar heat store and the brewing water as well as the monthly collector loop and system utilization ratio.

During the design of the system, a collector yield of 475 kWh/(m²_{ap}a) and system yield of 446 kWh/(m²_{ap}a) were calculated on the basis of detailed simulations. With an annual irradiation on the collector plane of 1076 kWh/(m²_{ap}a) the resulting utilization ratios were 43 % for the solar loop and almost 42 % for the whole system. As the values for utilization ratios and specific collector and system yield show, the system performance is below the expectations as the predicted utilization ratios are not reached in any month of 2011. Further, the difference between both ratios and thus the losses of piping and heat store are higher than predicted in the design. Following, the reasons for this low performance are investigated.

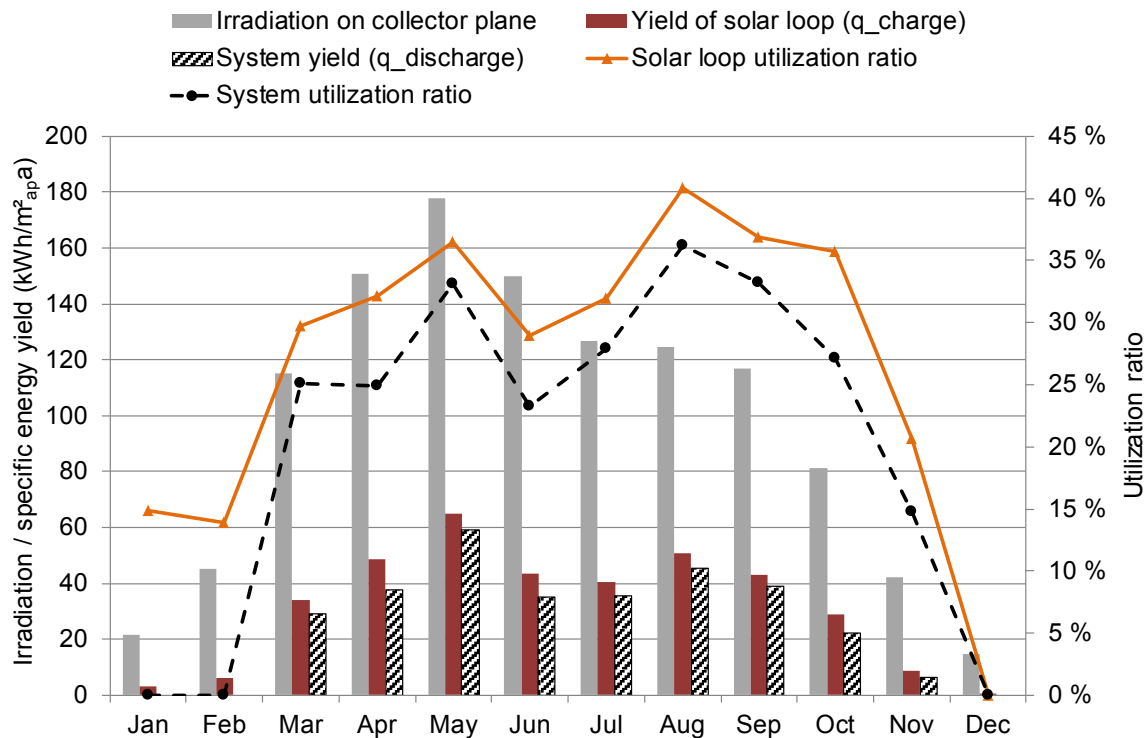


Figure 4-4: Measured irradiation on collector plane, specific collector and system yield; solar loop and system utilization ratio for 2011.

4.1.4. Operational experience

After the start-up, the monitoring of the STS showed a lot of manual interference in the discharge control. Although the filling level of the variable volume tank was below 70 % and solar heated water could be fed in, the brewing water pump was turned off manually by operational staff in the brewhouse. This resulted in an infrequent discharge of the solar heat store, extensive periods of stagnation and a relatively low utilization of the STS. Figure 4-5 shows a typical production week with undesired manual interference in the discharge control.

As Figure 4-5 shows, the brewing water pump is manually switched off before the filling level reaches the limit of 75 %, which is the control criterion to switch off the pump. The operational staff claimed “long term experience with correct filling levels” of the variable volume tank as a reason for the manual interference. As the manual switch off of the pump is not transferred to the control, the pump in the discharge loop operates until the filling level reaches 75 % and the solar heat store is more or less fully mixed. As the lower part of the solar heat store is heated up, the efficiency of the STS system decreases and accordingly stagnation can occur in summer. The system analysis with simulations described in Section 4.3.1 shows that the manual interference has a high impact on the

system yield. The system yield rose by 21 % after implementing automated control in the simulation model, as shown in Figure 4-9.

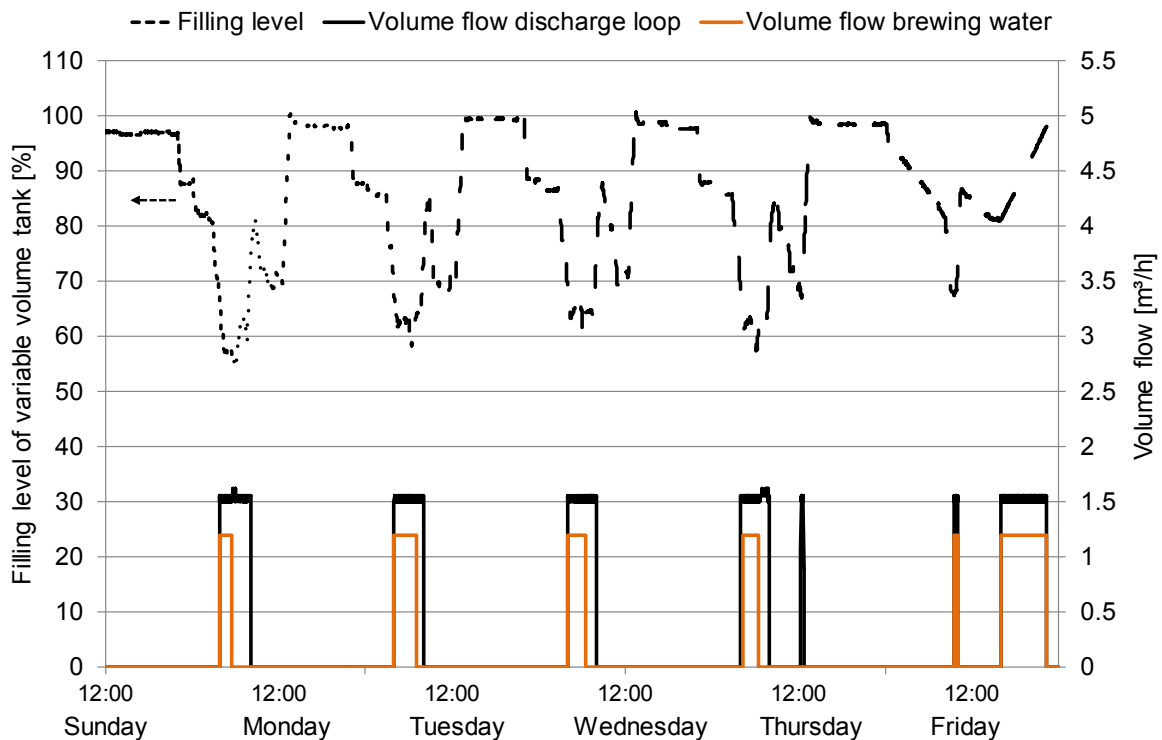


Figure 4-5: Filling level of the variable volume tank and volume flows of discharge and brewing water loop for a week in April 2011.

Another reason for low performance of the STS is the operation of the improved heat recovery. Instead of heating up the fixed volume tank by recovering heat from boiling, the latter was still very often used manually to produce hot water for the variable volume tank. This leads to a reduced amount of cold water which could be heated by the STS and therefore, less operation time for the solar thermal system. Finally, the brewery staff demanded a threshold for discharging the solar heat store of minimum 40 °C for $T_{0.9}$. A further increase of system yield of six percentage points can be achieved by correcting both, the operation of heat recovery and minimum temperature for discharging, compared to solely implementing an automated discharge control (see Figure 4-9 in Section 4.3.1).

4.1.5. Component analysis

Besides the operational reasons described in the previous section, faults of the components of the system could possibly have a negative impact on the system performance. Therefore, the collector field and its piping, the heat exchangers, and the solar heat store are analyzed

in this section, in order to judge about their influence on the low performance of the STS compared to the design values.

First, the **collector field and piping** of the solar loop are investigated. In order to assess the quality of the pipe insulation, the heat loss coefficient (U-value) calculated from measured data was compared to that calculated from material properties. The latter U-value is 0.9 W/(m²K) for a thermal conductivity of 0.04 W/(mK) and 100 % insulation ($d_i = 0.04$ m; $d_{out} = 0.124$ m). To calculate a U-value from measured data, the heat transfer capacity rate (UA-value) was determined first. Therefore, operating points were selected where the pump of solar loop and charging loop were both in operation. The heat transfer capacity rate was then calculated according to Equation 3.

$$UA = \frac{\dot{m}_{solar} \cdot c_p \cdot (T_{col} - T_{SF})}{\frac{(T_{col} - T_{SF})}{2} - T_{room}} \quad (3)$$

The U-value can then be calculated by dividing the average heat transfer capacity rate by the pipe surface. A U-value of 2.8 W/(m²K) was calculated from the average measured heat transfer capacity rate of 26.8 W/K. As pipe insulation is seldom ideally installed and additional heat losses are caused by fittings, the calculated U-value is quite high, without being unrealistic.

The efficiency of the collector field was calculated from monitoring data and compared to the efficiency curve by using the collector parameters from a laboratory collector test according to (DIN EN12975-2, 2006). The temperatures (T_{CF}, T_{CR}) and volume flow (\dot{V}_C) of the charging loop are used to calculate the collector field efficiency as these sensors were calibrated before installation and the volume flow can be measured with a higher accuracy compared to the solar loop, where a water-glycol mixture is used. Thus, the calculated efficiency also incorporates the piping losses of the collector field, solar loop and the charging plate heat exchanger. Due to this fact, the collector efficiency is expected to be lower compared to the EN-tests.

To calculate the collector field efficiency, operating points were selected in which the STS was in an almost stationary state. Thus, operating points between noon and 4 pm (the collector field is orientated south-west) on cloudless days were selected, where the irradiance on the collector plane was higher than 850 W/m². In addition, operating points were only selected if the incidence angle was lower than 20°, so that effects of the incidence angle modifier (0.99 at 20°) can be neglected. Furthermore, data sets were excluded if the change of one of the temperature sensors (T_{SF}, T_{SR}) was larger than ± 0.7 K compared to the previous data set. The same was done for data sets in which the irradiance (G_t) changed more than 30 W/m². For the remaining operating points the

efficiency was calculated by dividing the power in the charging loop by the total irradiation on the collector field as shown in Equation 4.

$$\eta_{\text{col}} = \frac{\dot{m}_{\text{charge}} \cdot c_p \cdot (T_{\text{CF}} - T_{\text{CR}})}{G_T \cdot A_{\text{col}}} \quad (4)$$

The average temperature in the solar loop (T_m) is calculated as the arithmetic mean of flow (T_{SF}) and return (T_{SR}) temperature. Figure 4-6 shows the efficiency of the collector field compared to the efficiency curve of the collector for selected operating points. The calculated efficiency values are, with a few exceptions, below the efficiency curve of the collector.

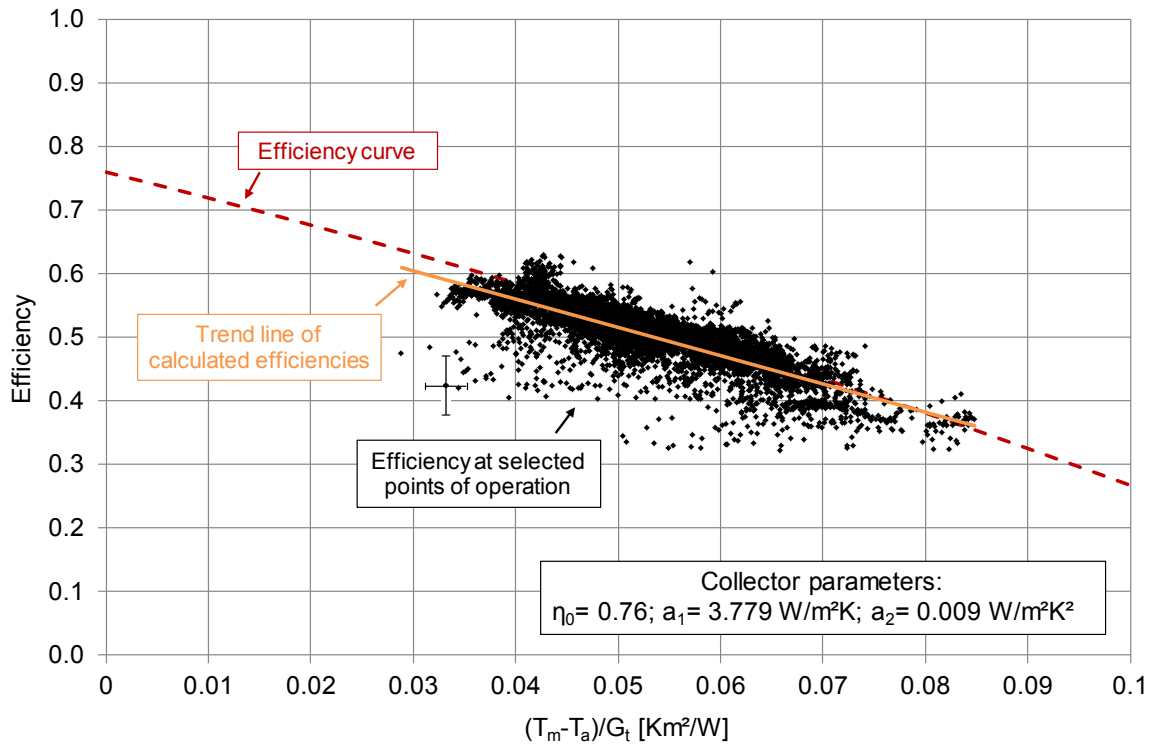


Figure 4-6: Efficiency of the collector field for selected stationary operating points compared to the efficiency curve of the collector from a collector test; the solid line shows the trend of the collector field efficiency at selected operating points; an uncertainty margin is added for a single point to demonstrate the uncertainty of measured data.

The trend line of the calculated efficiencies shows that the average of the calculated efficiencies is below the efficiency curve due to piping losses. An uncertainty margin is added for a single point to demonstrate the uncertainty of measured data. It can be concluded that the collector field at the studied brewery has a sufficiently similar performance compared to the tested collector.

The heat losses of the **solar heat store** were evaluated. Table 4-1 shows a reasonable difference between the heat quantities in the charging and discharging loop. To judge the losses of the solar heat store, at first the theoretical UA-value of the store was calculated using its geometrical properties ($d_i = 2.06$ m; $d_{out} = 2.46$ m; $h = 3$ m) and thermal conductivity (0.04 W/(mK)) of the insulation to be 6 W/K. In addition, periods were analyzed in which the store was neither charged nor discharged. In total 13 periods with durations between 24 and 336 h were analyzed and an average UA-value of 15.1 W/K with an uncertainty of ± 3.6 W/K was determined. To further investigate the rather high heat losses of the solar heat store in detail, Figure 4-7 shows the temperatures within the store, the discharge return and the room temperature for two days in August 2011. Additionally, the volume flows in charging, discharging and brewing water loop are shown.

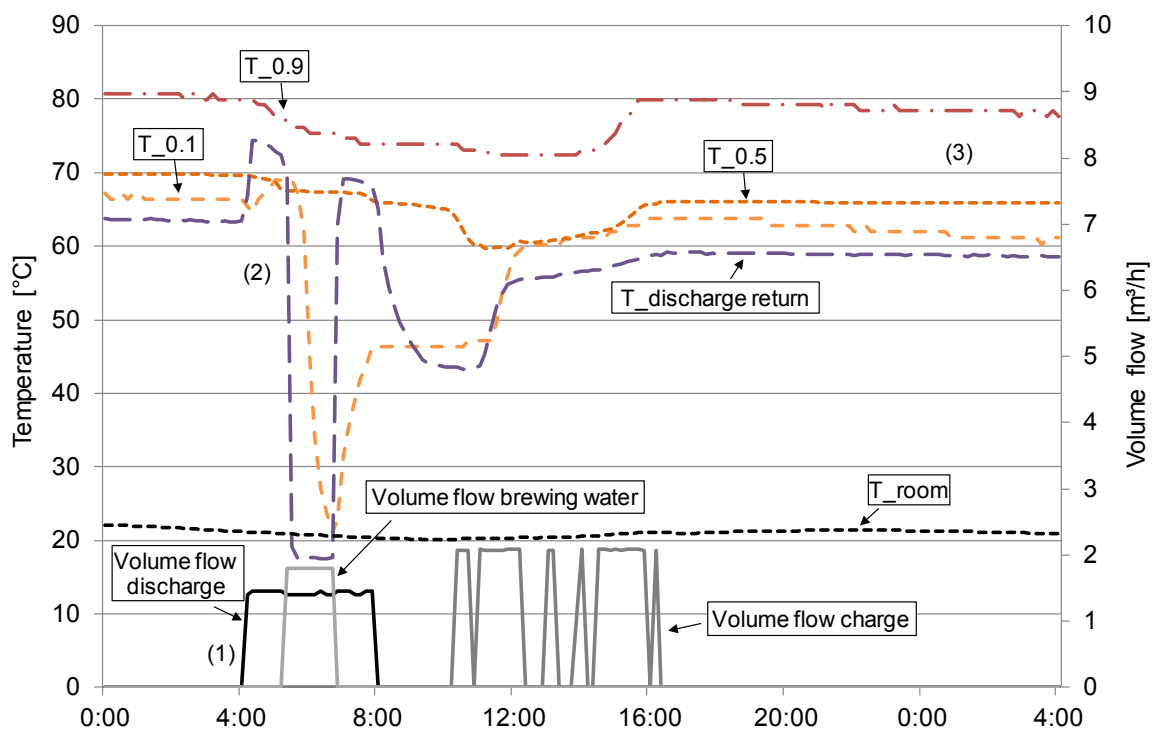


Figure 4-7: Temperatures within the store, the discharge return, the room temperature and the volume flows in charging, discharging and brewing water loop for a day in August 2011.

First of all, the manual interference in the operation of the brewing water pump is shown on the first day (1), as explained above in Section 4.1.4. The discharge of the store starts at 4:00 h, but as the brewing water pump was switched off the day before until it is switched on only at 5:00 h, the store is mixed by the discharge loop. The temperature in the discharge return is close to the one at the top of the store and the lower part is heated up (2). The brewing water pump is switched on after 1 hour and both temperatures in the discharge return and in the lowest store level drop.

After charging the store at around 16:00 h, it can be seen from the figure that both the highest and the lowest temperature (3) of the store fall faster than the temperature in the middle which remains almost constant over the next 12 hours. This is because the bottom of the store is not insulated and is placed on a metal ring on the ground. Therefore, an air gap of about 20 cm exists under the store which is only insulated on its sides. The insulation at the top of the store is not ideal either, as quarter circles are simply put on top. Additional heat losses occur through the discharge return pipe. As shown in Figure 4-7 the discharge return temperature (T_{DCR}) remains slightly under the lowest store temperature ($T_{0.1}$) after the discharge pump stops. In the following, T_{DCR} is always slightly lower than $T_{0.1}$ although it should be close to room temperature. This is because no convection barrier was installed in the discharge return close to the solar heat store. This causes a thermal convection out of the lower part of the store into the discharge loop and therefore additional heat losses through non insulated pump and fittings. The high heat losses shown in Table 4-1 can be explained by the missing insulation at the bottom of the store and the missing convection barrier. The system yield increases by 3 % if the heat losses in the simulation model (described in the next section) are reduced to a value calculated from insulation thickness and properties (see Figure 4-9 in Section 4.3.1).

Both **heat exchangers** of the system are analyzed. The heat exchanger for charging the solar heat store was designed with a UA-value of 20.2 kW/K, which corresponds to a logarithmic temperature difference of 5.7 K at a nominal heat transfer capacity of 115 kW. This leads to a specific value related to the collector field aperture area of $u_a = 130 \text{ W}/(\text{m}^2_{ap}\text{K})$ that is larger than the recommended value of $100 \text{ W}/(\text{m}^2_{ap}\text{K})$ in (VDI 6002, 2004). The heat exchanger for discharging was designed with a UA-value of 23.5 kW/K (logarithmic temperature difference of 6.5 K at a nominal heat capacity of 153 kW). The measured UA-value for this heat exchanger is lower at an average of 15.5 kW/K because the mass flow rates in operation are lower than assumed.

The logarithmic temperature difference for the charging heat exchanger was much higher than its design value of 5.7 K and reaches values up to 25 K. The UA-value is far below its design value of 20.2 kW/K at an average of 4.7 kW/K because a wrong model of the designed heat exchanger was delivered by the manufacturer. This heat exchanger was replaced with the correct model that reached its design values. Replacing the charging heat exchanger in the simulation model leads to a 6 % increase of system yield. Correcting the UA-value of the discharge heat exchanger leads to a further increase of three percentage points (see Figure 4-9 in Section 4.3.1).

4.2. Validation of simulation model

This section explains the development of the simulation model of the pilot plant at the brewery and displays the results of validation.

4.2.1. Simulation model

The simulation model of the STS was developed in TRNSYS 17 (Klein et al., 2009). The model includes all components shown in Figure 4-3 except for the variable volume tank. Table 4-2 shows an overview of the most important parameters of the simulation model.

Table 4-2: Main parameters of the simulation model; additional heat losses (UA convection losses) were added for the piping and various fittings due to pipe internal recirculation in the discharge return pipe, as described in Section 4.1.5.

Parameter	Value	Unit
General		
Weather data	Kassel, Germany	
Collector loop		
Collector aperture area - A_{ap}	155.5	m^2
Collector type	Flate plate	-
Optical efficiency - η_0	0.76	-
Heat loss coefficients - a_1	3.779	$W/(m^2_{ap}K)$
Heat loss coefficients - a_2	0.009	$W/(m^2_{ap}K^2)$
$IAM_{direct(50^\circ)}$	0.9	-
$IAM_{diffuse}$	0.9	-
Heat capacity	10.5	$kJ/(m^2_{ap}K)$
Collector loop - specific mass flow	15.5	$kg/(m^2_{ap}h)$
Charging loop - specific mass flow	12.5	$kg/(m^2_{ap}h)$
Share of glycol	35	%
Azimuth	40 SW	$^\circ$
Tilt angle	28	$^\circ$
UA - charging heat exchanger	4.7	kW/K
Collector pipe - length (flow)	41.5	m
Collector pipe - U-value piping	2.8	$W/(m^2K)$
Storage		
Volume	10	m^3
UA sides	8.9	W/K
UA top	1.4	W/K
UA bottom	5.0	W/K
UA convection losses	15.3	W/K
Discharge		
Discharge loop - specific mass flow	9.2	$kg/(m^2_{ap}h)$
Brewing water - specific mass flow	8.9	$kg/(m^2_{ap}h)$
UA - discharging heat exchanger	15.5	kW/K

A modular approach was applied to model the solar loop as well as the thermal storage. These modules were developed and tested on different field test systems by de Keizer (2012) and offer a variety of control options. The control strategy of the pilot plant could be modeled as described in Section 4.1.1. The collector is modeled with Type 832, developed by Perers (Haller et al., 2009). The model for the thermal storage is Type 340 (Drück, 2006). The parameters and input values for the model were either taken from a test report (ITW, 2009) in case of the collector or determined from the monitoring data (e.g. mass flows, UA-values of heat exchangers). The UA-value for the bottom of the store was raised due to the missing insulation. Further, additional heat losses (UA convection losses in Table 4-2) were added for the piping and various fittings due to pipe internal recirculation in the discharge return pipe, as described in Section 4.1.5. A measured load profile for the entire year 2011 was used as an input for the model in the brewing water loop to consider the manual interference of the discharge control.

4.2.2. Validation results

The validation of the simulation model was based on the comparison of simulated and measured data for the year 2011. The comparison between measured and simulated heat quantities is displayed in Table 4-3. The measured irradiation on the collector plane is an input to the simulation model. As the table shows, the heat quantities for charging the store are in very good agreement with a deviation of only 0.5 %. The simulated heat discharged from the store is slightly higher than the measured value. Nevertheless, the deviation of 2.2 % is still within the uncertainty margin of the measured heat flows of 4 %.

Table 4-3: Measured and simulated heat quantities for 2011.

Energy quantity / performance indicator	Measured	Simulated	Deviation [%]
Irradiation on collector plane [kWh/m ² _{ap}]	1167	1167	0.0
Heat charging the store [kWh/m ² _{ap}]	373	371	-0.5
Heat discharging the store [kWh/m ² _{ap}]	311	318	2.2
Night cooling: charging loop [kWh/m ² _{ap}]	8	9	11.1
Night cooling: discharging loop [kWh/m ² _{ap}]	3	1	-200.0
Charging loop utilization ratio [%]	32.0	31.8	-0.5
System utilization ratio [%]	26.6	27.2	2.2

Only a minor part of this deviation can be explained with lower heat losses by night cooling in the simulation compared to the measurement, as shown in Table 4-3. The relative deviation of night cooling in the discharging loop appears large at first sight. As the absolute heat quantities for night cooling are very small, this can be caused by one or

two additional nights of night cooling due to slightly higher simulated temperatures in the store. Figure 4-8 shows the monthly measured and simulated heat quantities for 2011. The measured collector yield is slightly higher than the simulated one except for June and July.

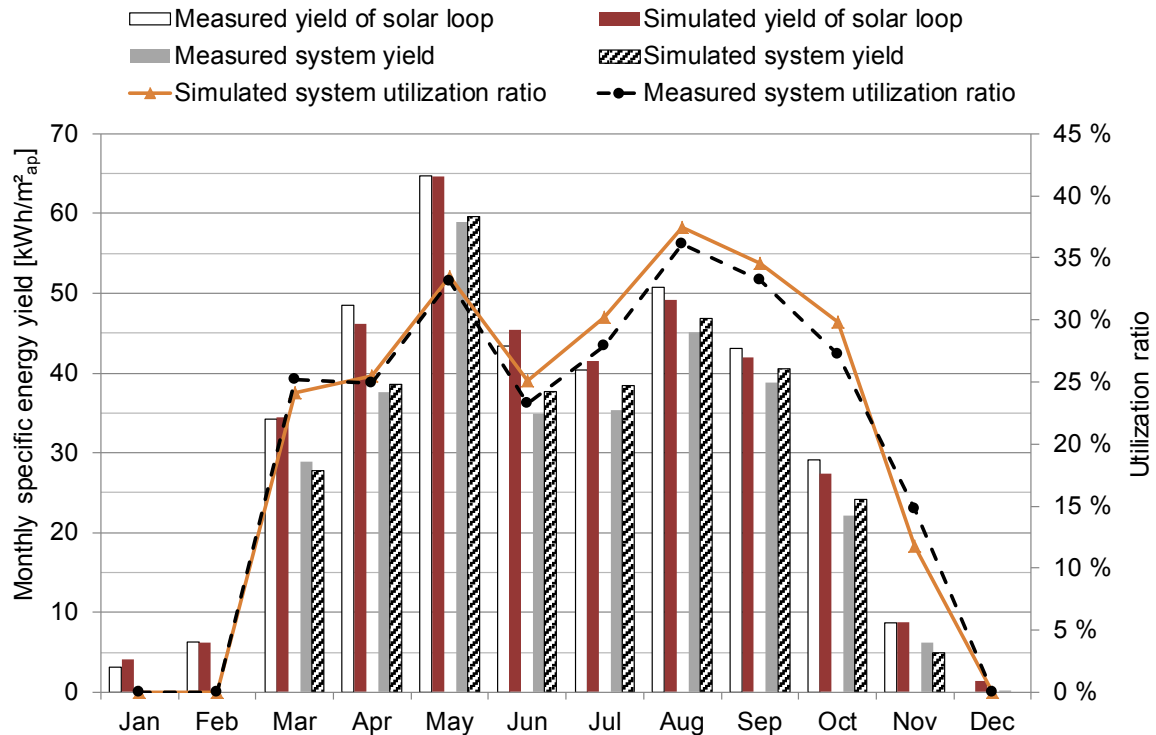


Figure 4-8: Monthly measured and simulated heat quantities for 2011; in January, February and December the discharge was turned off manually; the yield of solar loop was measured as indicated in Figure 4-3 (Q_{Charge}); the simulated yield of solar loop was calculated using the corresponding temperatures and flow rate in the simulation model.

In contrast, the measured system yield is slightly below the simulated values except for March and November, where the absolute heat quantities are quite low. These deviations indicate that the model probably still underestimates the heat losses of the store. Nevertheless, as the comparison of utilization ratios shows, the simulation results are in good agreement with the measured values.

4.3. System analysis with simulations

Within this section, the STS is analyzed by simulating the different faults which were detected within the monitoring and component analysis. Further, a global and a local sensitivity analysis are performed.

Decisions about the realization of projects and their subsequent evaluation afterwards are mainly based on an economic analysis. Therefore, the specific system yield is an important

performance indicator as it directly influences the economic feasibility of a solar process heat system in combination with the specific system cost. Besides the specific system yield, the collector loop and system utilization ratio are used as main performance indicators.

4.3.1. Identified faults and influence on system performance

All faults described in Section 4.1.4 and 4.1.5 have a negative influence on the system performance. The different faults were modeled to determine their quantitative impact. Figure 4-9 summarizes the results of the simulated faults. The first column shows the results of the validated model as a base case. To evaluate the impact of the individual faults on the system performance one fault at a time was corrected in the model. While store losses, UA-values and discharge control were corrected individually, the minimum temperature of the discharge control and the heat recovery operation were corrected after implementing the automated discharge. This was necessary as the effect of eliminating both faults can only be evaluated for an automated discharge control.

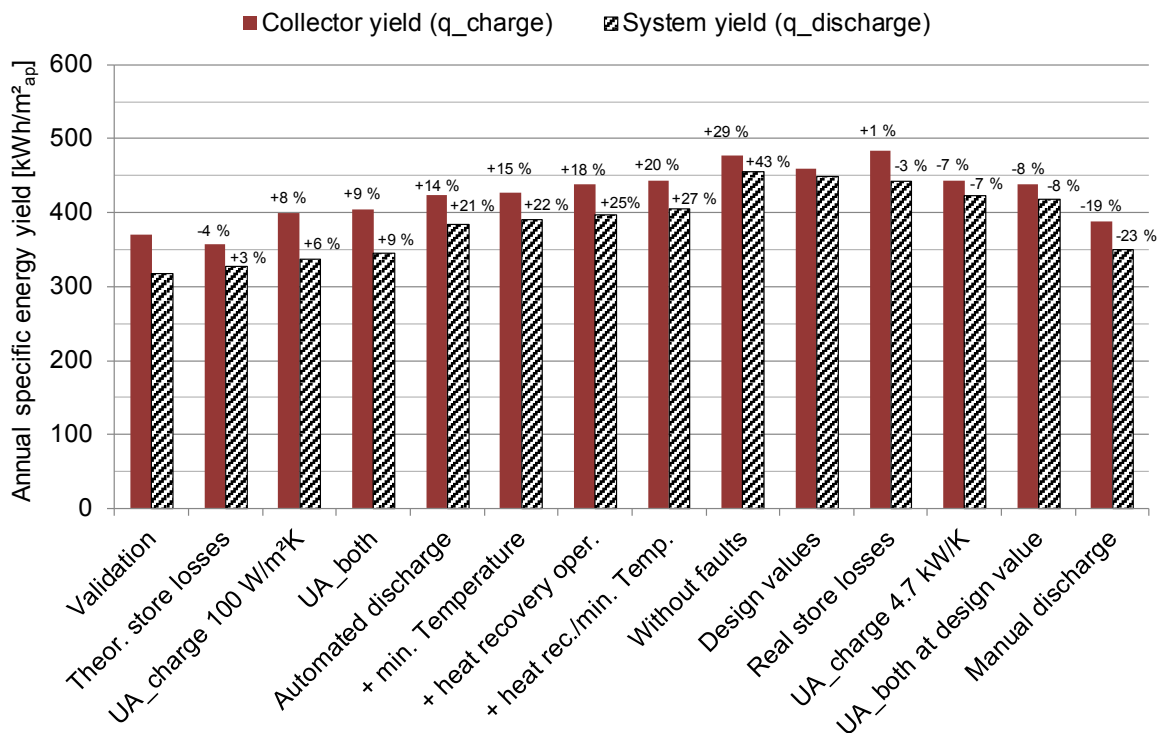


Figure 4-9: Simulated heat quantities for different faults; the first red and shaded columns show the values for the validated model; afterwards one fault at a time was corrected in the model; the increase/decrease compared to the validated model is given in percent; for “UA_both”, the UA-value for both heat exchangers was corrected; after “design values”, one fault at a time was added to the model; the increase/decrease compared to the model without faults is provided.

First, the losses of the heat store were reduced to a theoretically calculated UA-value considering a correction factor for real installation of insulation (UA-value for the whole store = 7.2 W/K). The difference between collector and system yield is reduced due to lower heat losses of the store and thus less charging, but the impact is rather small. Afterwards, the UA-value of the charging heat exchanger was changed to 100 W/(m²_{ap}K) related to the collector field aperture area as suggested in (VDI 6002, 2004), replacing the initial value from validation (Table 4-2). This change has a considerable impact of 6 % of the system yield, whereas the change of UA-value for the discharge heat exchanger to 23.5 kW/K leads only to a minor deviation of the collector and system yield. Collector and system yield rise by 14 % and 21 % respectively after implementation of an automated control for discharging. The minimum temperature for discharging and an ideal operation of heat recovery only cause a minor increase of collector and system yield. If all faults are removed from the model, the collector yield is 29 % higher and the system yield 43 % higher than for the model validated with the faulty system.

After removing all faults, single ones were implemented again to evaluate their impact on a properly running system. Increasing the heat losses of the store to the measured values, the system yield falls by 3 %. The influence of reduced UA-values of the charging heat exchanger is about twice as high. The reduced value (Table 4-2) for the discharging heat exchanger has only a very small impact. Adding the manual interference to the model has the largest impact on collector and system yield. Table 4-4 shows an overview of simulated heat quantities for the validated model and model without faults for 2011 as well as the design model.

Table 4-4: Simulated heat quantities for validated model and model without faults for 2011 as well as for the design model.

Energy quantity / performance indicator	Validated [kWh/m ² _{ap}]	Without faults [kWh/m ² _{ap}]	Design [kWh/m ² _{ap}]
Irradiation on collector plane	1167	1167	1076
Solar heat from collector	394	496	475
Heat losses solar loop piping	-23	-19	-15
Solar heat charging the store (collector yield)	371	477	460
Heat losses store	-42	-10	-12
Solar heat discharging the store (system yield)	318	455	448
Night cooling charging loop	10	12	0
Night cooling discharging loop	-0.6	-0.2	0
Solar loop utilization ratio	31.8 %	40.9 %	42.8 %
System utilization ratio	27.2 %	39.0 %	41.6 %

The system utilization ratio for the model without faults is about 12 percentage points higher than in the validated model. The average temperature of the store and therefore its heat losses decline significantly for the model without faults because the store is discharged more often. Further, the heat losses of the solar loop piping are lower than in the validated model. Both utilization ratios for the model without faults are below the design values because the irradiation in the design case was lower than in 2011. Therefore, the system performance is slightly lower than designed, although collector and system yield are higher.

4.3.2. Global sensitivity analysis

This section describes the results of a global sensitivity analysis performed for the STS with the Morris method (Saltelli, 2004). Table 4-5 shows the considered parameters for the global sensitivity analysis and their variation range.

Table 4-5: Considered parameters for the global sensitivity analysis and their variation range; parameters were varied about $\pm 20\%$ from their value of Table 4-2; in case this leads to unrealistic values (e.g. $\eta_0 = 0.91$), the other limit was extended accordingly to ensure a constant variation range for all parameters; the UA-value for the charging heat exchanger was varied from $100 \text{ W}/(\text{m}^2_{\text{ap}}\text{K})$ related to collector field aperture area (VDI 6002, 2004).

No.	Parameter	Variation range	Unit
Collector loop			
1	Optical efficiency - η_0	0.55..0.85	-
2	Heat loss coefficient - a_1	2.5..4.0	$\text{W}/(\text{m}^2\text{K})$
3	Heat loss coefficient - a_2	0.007..0.011	$\text{W}/(\text{m}^2\text{K}^2)$
4	b_0	0.15..0.22	-
5	$\text{IAM}_{\text{diffuse}}$	0.83..0.90	-
6	Collector loop - specific mass flow	12.5..18.5	$\text{kg}/(\text{m}^2_{\text{ap}}\text{h})$
7	Charging loop - specific mass flow	10..15	$\text{kg}/(\text{m}^2_{\text{ap}}\text{h})$
8	UA - charging heat exchanger	80..120	$\text{W}/(\text{m}^2_{\text{ap}}\text{K})$
9	Collector pipe - length (flow)	40..60	m
10	Collector pipe - U-value piping	2.2;3.4	$\text{W}/(\text{m}^2\text{K})$
Storage			
11	Heat loss coefficient sides	4..6*	W/K
12/13	Heat loss coefficient top/bottom	0.9..1.3*	W/K
Discharge			
14	Discharge loop - specific mass flow	7.4..11	$\text{kg}/(\text{m}^2_{\text{ap}}\text{h})$
15	Brewing water - specific mass flow	7.1..10.7	$\text{kg}/(\text{m}^2_{\text{ap}}\text{h})$
16	UA - discharging heat exchanger	12.4..18.6	kW/K

*both changed from the corrected UA-value as described in Section 4.1.5

As a first step, parameters of the simulation model described in Section 4.2.1 but no external inputs were considered for the sensitivity analysis. As a second step, the influence of the most important parameters identified in the global sensitivity analysis was compared to external inputs (temperature and load profile). Control parameters were not considered, as Kusyy et al. (2008) found that they have minor influence on the fractional energy savings, which can be assumed for system yield as well.

Figure 4-10 shows the overall influence and the non-linearity of the influence of the investigated parameters after evaluating 453 simulations according to the Morris method. The value for the overall influence is the average change of the specific system yield, if a parameter is changed from a certain point by half of its variation range, as shown in Table 4-5.

The optical efficiency of the collector is by far the most influential parameter. As its value for non-linearity is very low, its influence on the system yield is similar within the variation range. In case of a high non-linearity (e.g. charging loop mass flow) the influence of the parameter changes within the variation range.

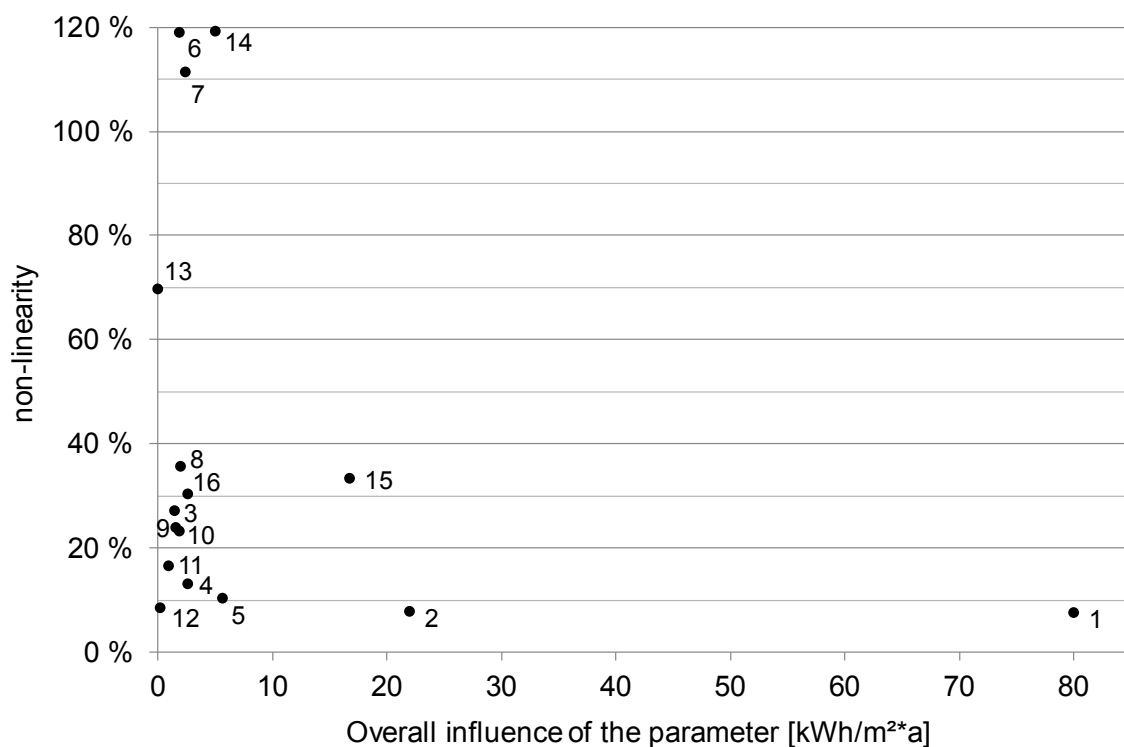


Figure 4-10: Ranking of parameters by the Morris method. The value for the overall influence is the average change of the specific system yield if a parameter is changed from a certain point by half of its variation range, shown in Table 4-5.

The heat loss coefficient (a_1) of the collector and the mass flow in the brewing water loop are two additional parameters which have a considerable influence within the varied range.

The value for non-linearity of the mass flow in the brewing water loop is higher than the ones for optical efficiency and heat loss coefficient (a_1) which means that its influence varies for different points. The overall influence of the other mass flows (6, 7, 14) is low, although their influence is highly variable.

4.3.3. Local sensitivity analysis of load and influential parameters

The brewing water return temperature (T_BWR) and the load profile are expected to be the most important influence factors for the system performance of a solar process heat system (Schmitt et al., 2012a). This section describes the results of a local sensitivity analysis performed for the most important parameters identified in the global sensitivity analysis as well as the load return temperature (T_BWR) and the load profile. The local sensitivity analysis directly shows the influence of a parameter on the system yield.

In order to investigate the influence of the load profile, different cases were developed to investigate the influence of the load profile. In all cases, 63 m³ of cold water are heated within the brewing water loop as this is the average load of a typical production week. The difference between the cases is the distribution of these 63 m³ over one week, which means that the total load is constant and only its distribution changes. Table 4-6 shows the investigated cases for sensitivity analysis of the load profile.

Table 4-6: Investigated cases for sensitivity analysis of the load profile.








No	Description	Days	Time	Profile
1	Profile with optimized heat recovery	Mon - Fri	varies	
2	Load on 5 days in the morning	Mon - Fri	4:00h - 13:00h	
3	Load on 5 days in the afternoon	Mon - Fri	14:00h - 23:00h	
4	Extended load on 3 days	Mon, Wed, Fri	4:00h - 19:00h	
5	Shorter load on 7 days	Mon - Sun	4:00h - 10:27h	
6	Extended load on 5 days with halved mass flow	Mon - Fri	4:00h - 22:00h	
7	Shorter load on 5 days with doubled mass flow	Mon - Fri	4:00h - 8:30h	

Figure 4-11 shows the results of the local sensitivity analysis for the most important parameters. The high influence of the optical efficiency, which the global sensitive analysis

showed, is also visible in the upper left of Figure 4-11. The system yield declines from 479 kWh/(m²_{ap}a) to 357 kWh/(m²_{ap}a) from the optical efficiency for a good flat plate collector of 0.84 to a lower optical efficiency of 0.6. The influence of the heat loss coefficient (a_1) and the specific mass flow in the brewing water are much smaller but in case of a badly insulated collector (e.g. 4.5 W/(m²_{ap}K)) the system yield is reduced by 5 % compared to the one used for the studied STS.

Regarding the load profile, the first case shows the weekly profile with optimized heat recovery as described in Section 4.1.1. If the load is distributed equally between Monday and Friday (Case 2) the system yield declines slightly by 4 % and further by 2 % if the load is shifted to the afternoon (Case 3). This can be explained by operation of the STS at lower efficiencies as the temperatures in the store and thus the collector field rise before the store is discharged.

An extended load on 3 non consecutive days (Case 4) leads to the same system yield (454 kWh/(m²_{ap}a)) as the base case (Case 1). This is possible because the store is charged on days without load and discharged longer on others. This means that processes with operation on more days of the week are not always preferable unless the total load is higher. The advantage of a process requiring heat on more consecutive days is the lower necessary store volume. Accordingly, the highest yield (475 kWh/(m²_{ap}a)) is achieved with a shorter load on seven days (Case 5). A longer operation (Case 6) compared to Case 2 with halved mass flow only leads to a minor increase of system yield.

A shorter operation with doubled mass flow (Case 7) decreases the system yield. The temperature of the load or process, which is in this case the brewing water return temperature (T_{BWR}) has a large impact on the system yield as Figure 4-11 shows. An increased return temperature from 20 °C to even 40 °C reduces the system yield from 475 kWh/(m²_{ap}a) to 310 kWh/(m²_{ap}a) which would lead to a system that is not economically viable.

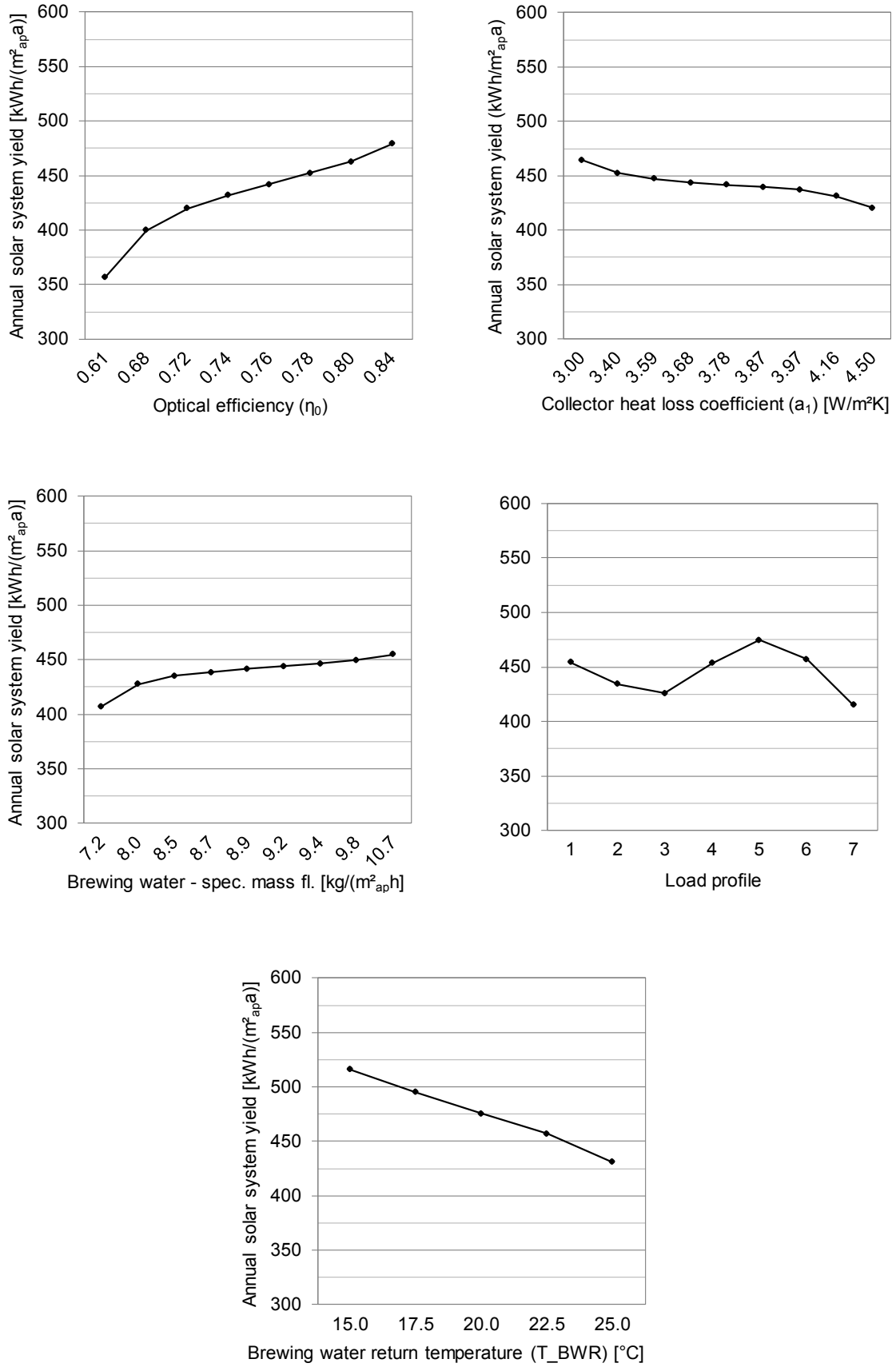


Figure 4-11: Results of local sensitivity analysis.

4.4. Conclusion

To begin with, this section describes the integration of an STS into the hot water supply of a brewery. It was shown that a large effort can be necessary to integrate solar heat into an industrial process. The analysis of the STS and its components showed that faults of single components can have a considerable impact on overall performance.

To evaluate the identified faults, a TRNSYS simulation model for a solar process heat system was developed and validated with measurements. The simulated and measured heat quantities for 2011 are in good agreement. The analysis of several faults detected in the system showed that the amount of available load has the highest impact on system performance. In case of the studied system, the load was reduced by manual interference in the discharge control, leading to a substantially lower system yield than expected. The correct estimation of available load is crucial to predict the performance of an STS before installation. Further faults which have a considerable impact are a reduced UA-value of the charging heat exchanger due to wrong design or malfunction and increased heat losses of the store. If all faults are corrected, the design values can be reached. Therefore, monitoring and failure detection of solar process heat systems is especially important as many faults can occur and reduce the system yield considerably.

Finally, a global and local sensitivity analysis showed that the most important factors for system yield are the choice of a suitable and well-functioning collector the process temperature and to certain extent the load profile. Further investigation regarding the influence of the load profile is therefore necessary as considerable effort is associated with its determination in the design phase of a solar process heat system. As the collector efficiency is very important for the overall system performance, a methodology for choosing a suitable collector for a certain process heat application is necessary.

5. Preliminary design of low-temperature solar process heat systems

Within this section important solar process heat applications are identified, an approach for pre-dimensioning of collector field and heat store is presented and typical utilization ratios of selected low-temperature process heat applications are determined in order to facilitate the estimation of a system yield.

Design guidelines have been developed for solar process heat systems with a constant load (Gordon and Rabl, 1982), open processes (Collares-Pereira et al., 1984), a certain region e.g. the United States (Kutscher et al., 1982) systems for a specific brewery and dairy (Benz et al., 1998) or concentrating systems (Kulkarni et al., 2008). Aidonis et al. (2004) found within a comprehensive simulations study that the available load utilization (heat demand per m² of collector area) has the biggest influence on the system performance. Aidonis et al. (2005a) and Hess and Oliva (2011) followed an approach of nomograms for design of solar process heat systems but provided nomograms for specific applications, process temperatures and locations only. VDI 6002 (2004) presents an approach for dimensioning for large (>20m²_{ap}) STS for DHW preparation. The publication describes dimensioning of the collector field for a summer day with good irradiation and further provides design guidelines for heat store and additional components.

So far, no approach exists for simple and fast (hence cost effective) pre-design of solar process heat systems without simulations and for various process heat applications, locations and collector types. This is especially important for a fast feasibility assessment in the initial phase of system design. Within this thesis the focus is on process heat applications below 100 °C and water-based solar process heat systems. Steam generation and air systems are not investigated. The objectives of this section are to identify important process heat applications below 100 °C and to develop an approach for pre-dimensioning of the collector field and heat store for low-temperature solar process heat systems. Furthermore, annual utilization ratios are determined for different applications, locations, and collector types.

In order to achieve these objectives, suitable sectors and processes (displayed in Figure 3-6 in Section 3.4) are analyzed to identify and describe important low-temperature process heat applications. For the collector field, the approach of dimensioning for a “good” summer day (VDI 6002, 2004) is transferred from DHW to process heat applications. This approach leads to an economically favorable system size as an extensive energy excess in summer is prevented. The load is the main difference for the design phase of a solar thermal system for process heat generation compared to systems for domestic applications.

Both, the temperatures of the consumers and the load profile differ completely compared to DHW or space heating loads. Therefore, this section also investigates the influence of the load profile, process temperature and other boundary conditions e.g. location or collector types on the collector field dimensioning. The heat store is dimensioned in accordance to the weekly load profile instead of the daily profile in case of a DHW system and typical annual utilization ratios of selected low-temperature process heat applications are determined to facilitate the estimation of a system yield.

Section 5.1 explains the integration principles and identifies and describes major applications of solar process heat systems. Parts of Section 5.1 were published in (Lauterbach et al., 2011a) and (Schmitt et al., 2011). Section 5.2 describes the configuration of the simulation model used to derive the design values and Section 5.3 illustrates the selected locations for the simulations study. Further, Section 5.4 presents the considered load profiles, Section 5.5 explains the dimensioning of the collector field and Section 5.6 illustrates the dimensioning of heat store. Section 5.7 shows the results of simulations to determine the system yield of selected process heat applications. Finally, Section 5.8 provides the conclusion.

5.1. Integration and applications of solar process heat systems

In general, the integration of an STS on supply level can be distinguished from the integration on process level. Figure 5-1 illustrates the distinction between supply and process level and the integration of solar heat in the return of a hot water circuit.

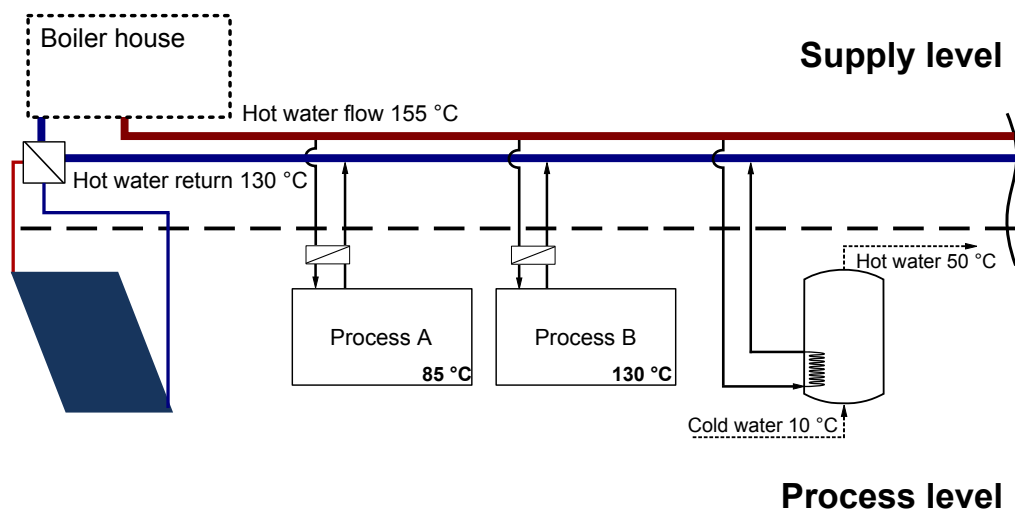


Figure 5-1: Distinction between supply and process level and integration of solar heat in the return of a hot water circuit.

In this example, all processes are heated by a pressurized hot water circuit with a flow temperature of 155 °C. Regarding the integration of solar thermal systems on supply level, it can be distinguished between (pressurized) hot water systems and steam circuits. A pressurized hot water system consists mainly of a boiler that heats the return of the water circuit. This circuit is usually closed and no water leaves the system. A solar thermal system can be integrated to increase the return temperature right before the boiler by a serial connection, as shown in Figure 5-1.

Several possibilities exist for integrating a solar thermal system on supply level in case heat is distributed by steam system. The first possibility is the parallel integration of a solar thermal system to generate and feed-in steam. Secondly, the feed water temperature can be increased. The feed water can be heated from approx. 100 °C up to 150 °C after degasification, depending on the steam pressure that is produced within the boiler. However, the preheating of boiler feed water should usually be realized by an economizer that uses waste heat from the exhaust gas. The third possibility is the preheating of make-up water before it enters the degasification if a sufficient amount of make-up water is needed but no possibilities for heat recovery exist. A larger variety than on supply level exists for the integration of STS on process level. Solar heat can be used directly for one or more processes at temperatures below the return temperature of the heat distribution network. Therefore, the supply of solar heat on process level generally comes along with lower temperatures compared to the integration on supply level. Figure 5-2 shows three exemplary processes that are fed by a hot water circuit.

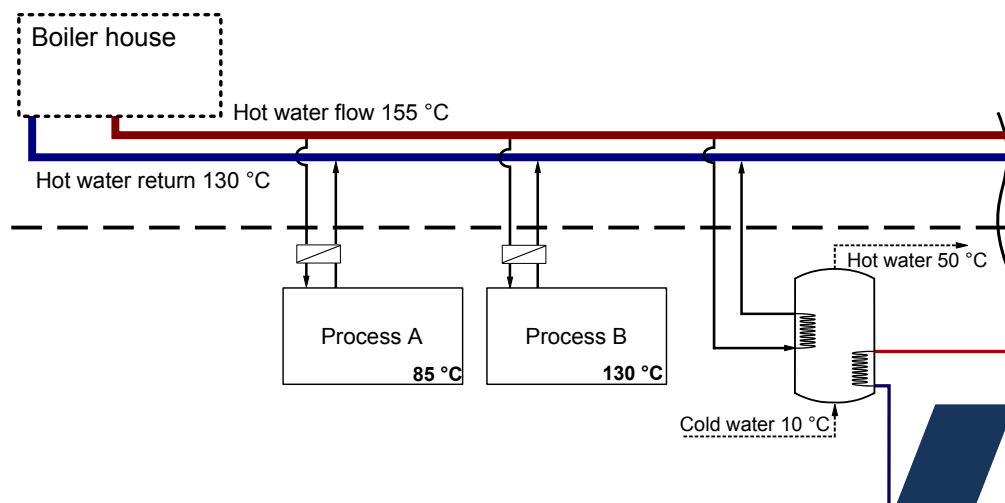


Figure 5-2: Integration on process level.

(Schmitt et al., 2011) described further details regarding the integration of STS in industrial processes. The most promising possibilities for integration of solar heat both on supply and on process level need to be identified in order to justify the system configurations for the simulation study within this section. The analysis of industrial

sectors shows that many similar processes exist across several sectors which seem to be promising for the integration of solar heat. Additionally, similar processes can be categorized into typical applications for solar process heat across industrial sectors. The processes displayed in Figure 3-6 in Section 3.4 were identified as promising for the integration of solar heat in this thesis and various other studies (Aidonis et al., 2005a; Müller et al., 2004; Schweiger et al., 2001) as they all take place at low or medium temperatures. Many of these processes can be categorized in the following three major applications:

- **Heating of fluid streams:** This application includes processes where a cold (or preheated) fluid stream has to be heated up to a certain temperature. These processes can be found in almost all industrial sectors, e.g. washing and cleaning. Further, preheating of make-up or boiler feed water and heating of a hot water circuit on supply level belong to this application.
- **Heating of baths/vessels/stores:** These processes have in common that a bath, vessel or store filled with a liquid has to be heated to a certain temperature and/or kept at this temperature during production hours. These processes can be found in almost all industrial sectors as well. Examples are blanching, pasteurizing, degreasing and surface treatment.
- **Thermal separation processes:** This application includes drying with convective and contact dryers covering the majority of drying installations as well as evaporators that are used for distillation and rectification besides general evaporation processes (Schmitt, 2014).

The results of previous studies and working groups were analyzed to verify the importance of the industrial processes displayed in Figure 3-6 in Section 3.4 and of the classification of solar process heat applications. Various STS built in industrial companies in the past were analyzed within “Task 33/IV - Solar Heat for Industrial Processes” of the International Energy Agency’s Solar Heating and Cooling Programme. The selected processes for the integration of the STS were documented. 36 (51 %) of 71 installed STS were used to provide hot water, heat up make-up water or washing processes, which refer to the application “heating of fluid streams”. 14 % of the analyzed systems were integrated in processes of the application “heating of baths/vessels”, 6 % for drying processes and 29 % for other processes which do not belong to the industrial sector (most of them being car washing facilities) (Vannoni et al., 2006). Puente Salve (2011) performed a short analysis of 90 industrial companies identifying suitable processes for the integration of solar heat. The processes cleaning/washing, preheating of make-up water and preheating in general which can be assigned to the application “heating of fluid streams” represented 40 % of the identified processes. The application “heating of baths/vessels” had a major share of 35 %.

The way of heating a certain process was used as the main criterion to select the system configuration for the following investigation. For the application “heating of fluid streams” the most common configuration for the discharge of the solar thermal system or the heating of the process is the use of a plate heat exchanger. In many cases, the heating of a bath, vessel or store can be realized with an external heat exchanger as shown in Figure 5-3 (right).

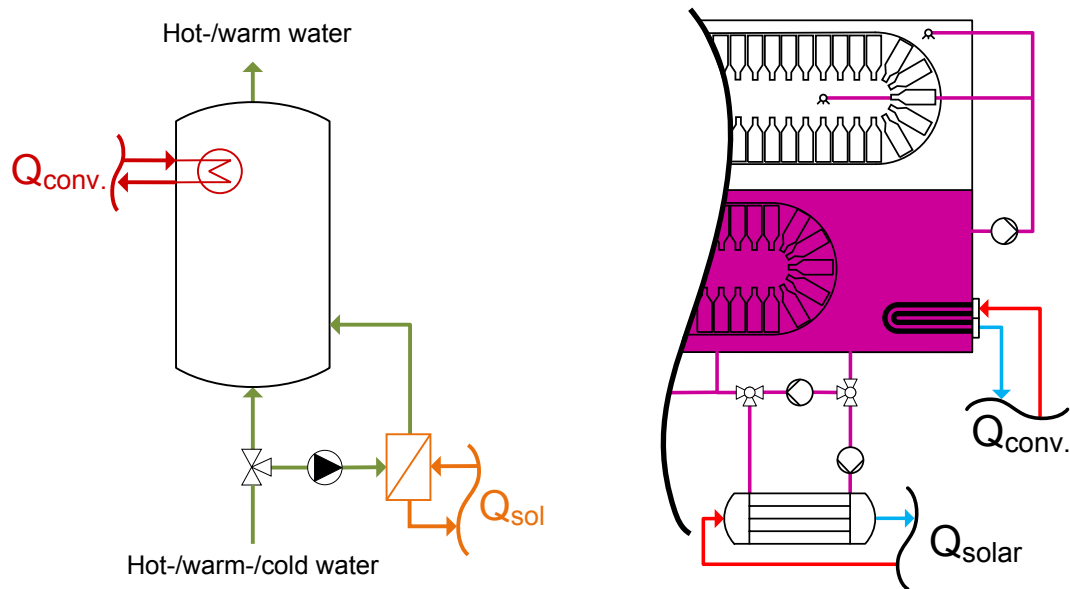


Figure 5-3: Heating of a cold water stream with a plate heat exchanger (left) and heating of a bottle washing machine with an external tube bundle heat exchanger (Schmitt, 2014).

The figure shows an application of heating a cold water stream with a plate heat exchanger (left) and the heating of a bottle washing machine with an external tube bundle heat exchanger. The installation of an external heat exchanger is necessary in many cases because no space for internal heat exchangers is available in industrial baths or vessels. The heating with an external heat exchanger is very often the best choice as retrofitting of existing installations will be most common for solar process heat applications. The use of a plate heat exchanger is not possible in some cases because the used fluid is contaminated with particles. A tube bundle heat exchanger can instead be used for the heating of a process as shown in Figure 5-3. Schmitt (2014) investigates the integration of solar thermal systems in industry in detail.

The main difference resulting from the use of a tube bundle or internal heat exchanger compared to a flat plate heat exchanger is a higher temperature difference for the heating of a specific process. This difference is considered within the simulations by different temperature levels as describes in Section 5.5.1.

5.2. System configuration, parameters and control

STS will mostly be used in existing plants and processes in industry. A conventional heating of the process is usually already installed in these cases and therefore not combined with the STS. Due to this fact, the back-up heating was not modeled in the investigated system shown in Figure 5-4. This configuration was chosen as in many cases existing processes can be supplied with solar heat by an additional external heat exchanger, as described above (Schmitt, 2014).

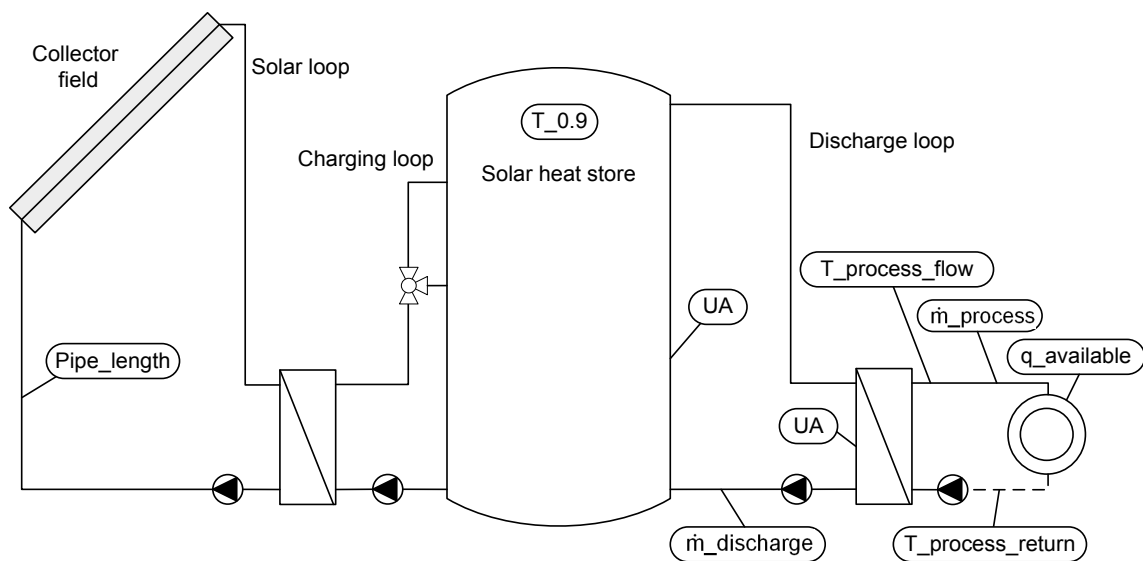


Figure 5-4: System configuration for “heating of a fluid stream” or “heating of a bath/vessel/storage” with external heat exchangers.

In order to model different solar process heat applications several changes are necessary compared to the simulation model described in Section 4.2.1. A different approach is necessary for the discharge of the solar heat store in order to achieve results which are independent from the system size. The parameters or boundary conditions which were changed compared to the simulation model described in Section 4.2.1 are shown in Figure 5-4. Further, a different way of charging the heat store at two levels was implemented.

The length of piping for the solar loop was set to $0.25 \text{ m}/(\text{m}^2_{\text{ap}})$ for one way. Half of the piping is assumed to be outside. 100 % insulation is assumed for indoor pipes and 150 % insulation for outdoor pipes. A correction factor of two for the heat losses is assumed to account for real installations. Additionally, the UA-value for the store is calculated depending on its size. For example, the UA-value is 8 W/K for a 10 m^3 heat store. A specific heat store volume of $50 \text{ l}/\text{m}^2_{\text{ap}}$ is mentioned as an adequate value for many cases in literature (Aidonis et al., 2005b; Hess and Oliva, 2011; VDI 6002, 2004). The volume of the solar heat store is adjusted depending on the difference between the process return

temperature and the maximum temperature, as the available capacity of the store depends on the difference between these two temperatures. Assuming $T_{\text{process_return}} = 12 \text{ }^\circ\text{C}$, $T_{0.9_max} = 95 \text{ }^\circ\text{C}$ and a specific volume of $50 \text{ l/m}^2_{\text{ap}}$ the available storage capacity of the heat store is:

$$q_{\text{store}} = v_{\text{store}} \cdot c_p \cdot \rho_{\text{Water}} \cdot (T_{0.9_max} - T_{\text{process_return}}) = 4.8 \frac{\text{kWh}}{\text{m}^2_{\text{ap}}} \quad (5)$$

Regarding the process load, specific demand values are used in the following sections to achieve results which are independent from system size. The specific available load defined as the maximum available specific energy demand for $1 \text{ m}^2_{\text{ap}}$, is used in the following sections to decouple the results from the solar thermal system size and absolute amount of load. The available daily load is defined as:

$$q_{\text{available}} = \frac{m_{\text{available}}}{1 \text{ m}^2_{\text{ap}}} \cdot \frac{1}{\text{d}} \cdot c_p \cdot (T_{\text{process_flow_max}} - T_{\text{process_return}}) \quad (6)$$

Typical values for the available load are in the range of 1 to 10 kWh/(m²_{ap}d) (Aidonis et al., 2004; Hess and Oliva, 2011; VDI 6002, 2004). $m_{\text{available}}$ can be calculated for a certain available load e.g. $q_{\text{available}} = 4 \text{ kWh}/(\text{m}^2_{\text{ap}}\text{d})$ and for a certain temperature range of a process e.g. 12 to 60 °C :

$$m_{\text{available}} = \frac{q_{\text{available}}}{c_p \cdot (T_{\text{process_flow_max}} - T_{\text{process_return}})} = \frac{4 \text{ kWh}/(\text{m}^2_{\text{ap}}\text{d})}{4,18 \frac{\text{kJ}}{\text{kgK}} \cdot (60 - 12)\text{K}} = 71,8 \frac{\text{kg}}{(\text{m}^2_{\text{ap}} \text{d})} \quad (7)$$

A daily profile is then used for the hourly distribution of the load as shown in Figure 5-6.

The UA-value for the discharge heat exchanger is determined depending on the daily profile. A UA-value corresponding to a logarithmic temperature difference of 5 K at maximum mass flow was assumed for profiles without major peaks. For profiles with high peaks, the UA-value was set to a value for which a logarithmic temperature difference below 5 K can be reached for 90 % of the day.

The maximum discharge mass flow of the STS is calculated depending on the daily profile and set to the maximum hourly mass flow in the process. The mass flow of the process loop is provided as an input and the discharge mass flow of the discharge loop is calculated to reach $T_{\text{process_flow_max}}$ using Type 805 (Heimrath and Haller, 2007).

5.3. Selected locations

The location of a foreseen STS plays a major role for its design. Therefore, four representative locations were selected for the following investigation to cover a wide range of climatic conditions (Copenhagen and Madrid adopted from Henning, 2004):

- Copenhagen (Denmark) for a moderate, northern European climate,
- Wuerzburg (Germany) for a warm, central European climate,
- Toulouse (France) for a moderate southern European climate,
- Madrid (Spain) for a Mediterranean, continental climate.

Table 5-1 shows annual global horizontal and tilted irradiation as well as the number of days with more than 7 kWh/(m²d) and the average daily irradiation for those days on a tilted surface (tilt angle = latitude - 15°) for the selected locations. These “good” summer days are used for the collector field design in the following.

Table 5-1: Meteorological data for the selected locations, irradiation for July days on a tilted surface (tilt angle = latitude - 15°).

Location	Latitude	Global irradiation [kWh/(m ² a)]	H _t [kWh/(m ² a)]	July days > 7 kWh/(m ² d) [-]	H _{t,day_avg} [kWh/(m ² d)]
Copenhagen	55.7	988	1191	9	7.61
Wuerzburg	49.8	1094	1264	11	7.54
Toulouse	43.6	1351	1552	14	7.81
Madrid	40.5	1660	1887	20	7.76

Figure 5-5 shows the monthly averages of ambient air temperature and global horizontal irradiation for each of the selected locations from (Meteotest, 2009).

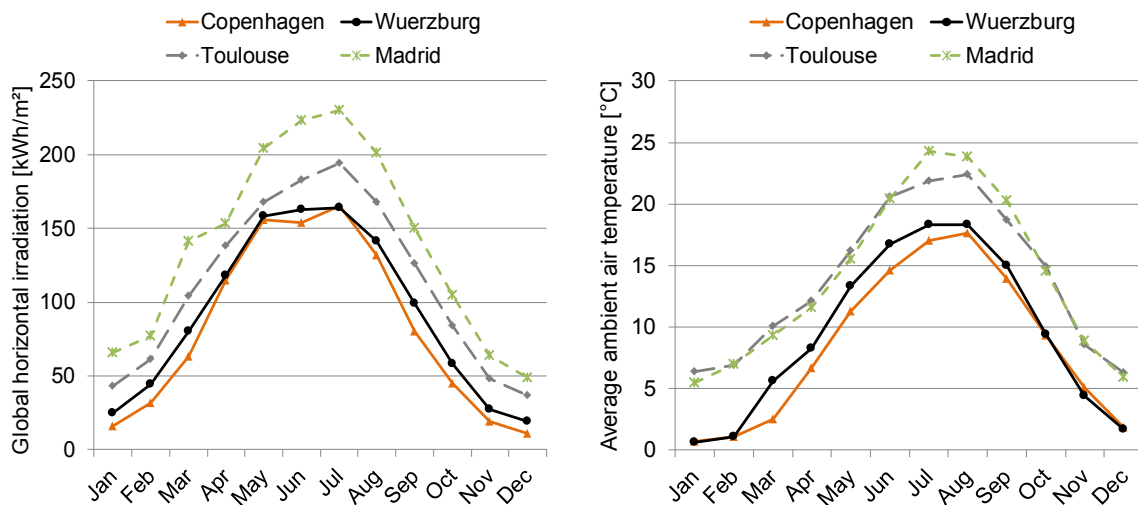


Figure 5-5: Average monthly global horizontal irradiation (left) and average monthly ambient air temperatures for the selected locations.

5.4. Load profiles

The load profile and load temperatures are the main differences of process heat applications for STS compared to domestic ones. This section introduces the daily, weekly and annual load profiles which were considered for the following investigation.

For the analysis of the influence of **daily load profile** the following were selected:

- **Daytime** is a typical profile for operation between 8:00 and 18:00 h on a weekday. This profile (originally named G1) was selected from representative load profiles developed by the German association of electricity industries (Verband der Elektrizitätswirtschaft, VDEW) for the estimation of electrical energy consumption of smaller commercial enterprises. This is because it can be assumed that the profiles of electrical and thermal energy consumption behave similar during operation hours. The profile is considered for the following investigation. The profile was taken from (Westnetz GmbH, 2013) and is described in (Bastian, 2012; Kalab, without year).
- **Constant** is a typical profile for a commercial enterprise with constant load during day, week and year which is also a representative load profile (originally named G3) developed by the German VDEW. It was also taken from (Westnetz GmbH, 2013) and is described in (Bastian, 2012; Kalab, without year).
- **Cleaning** describes a load profile for an enterprise in the food sector working in two shifts. Heat is used for continuous cleaning of containers and at the end of the working day for cleaning of production facilities (Hess and Oliva, 2011).
- **Heating bath/vessel** is a typical profile for this application with a high demand for the start-up at night and a lower demand until noon. The profile was measured within a case study at a brewery.
- **Heating bath all day** is a similar profile derived from "heating bath/vessel" but with a more steady heat demand during a working day.
- **Heating bath daytime** was also derived from "heating bath/vessel" but has a heat demand with lower peaks and is during daytime only.
- **Variable hot water** shows a profile for preparation of hot water, measured within a case study in a company producing non-alcoholic beverages.
- **Periodical hot water** shows a profile for the preparation of make-up water for a steam boiler (Hess and Oliva, 2011).

- **Steady hot water** shows a profile for the preparation of hot water similar to Figure 4-5 which was measured within a case study at a brewery.

Figure 5-6 shows an overview of the selected load profiles. With these profiles, a certain available load can be distributed over a day.

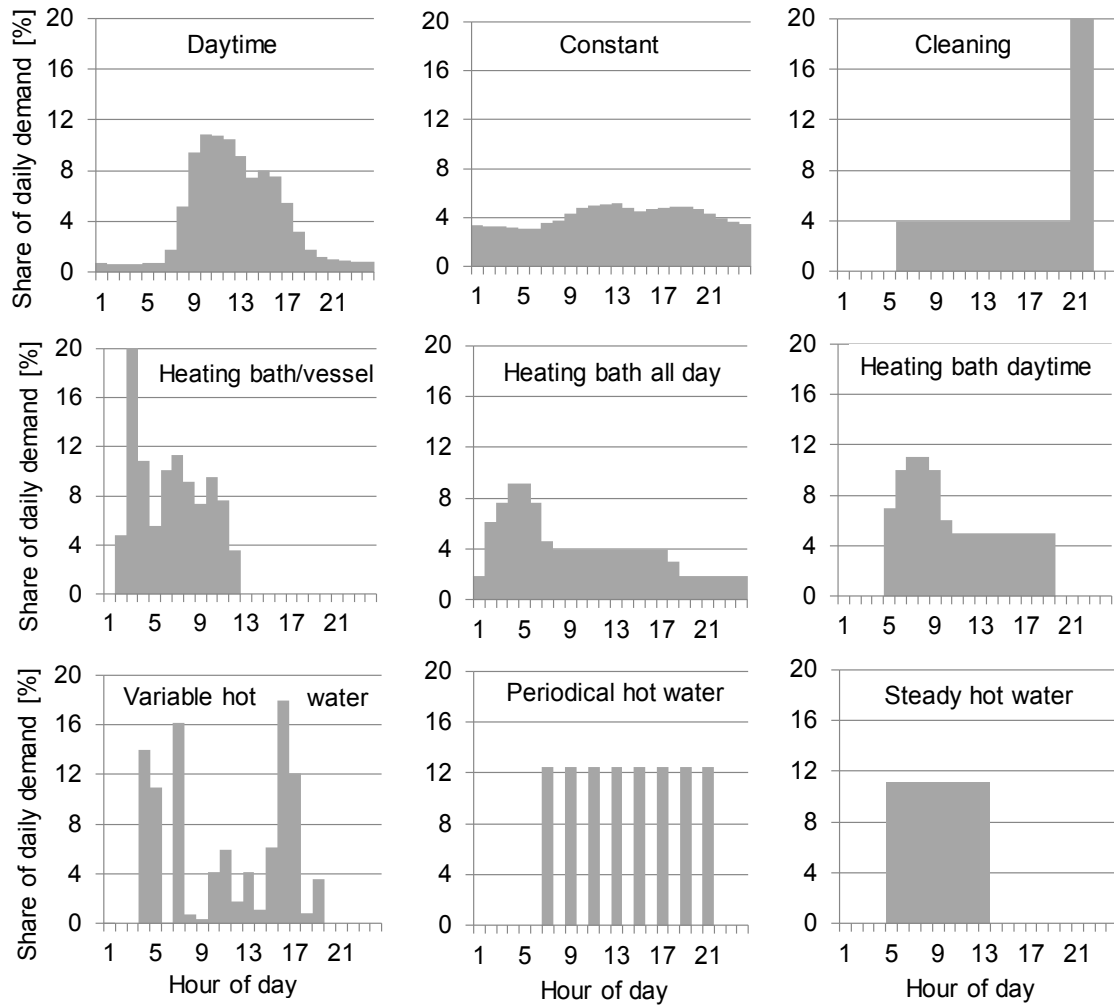


Figure 5-6: Overview of the selected daily load profiles; values can be found in Annex B.

The **weekly profile** is important for the dimensioning of the collector field and especially the heat store. Further, the achievable annual system yield is influenced by the weekly profile as well. Following weekly load profiles for industrial processes were considered (see Figure 5-7):

- **Constant week** (originally named G3) is a representative weekly load profile developed by the German VDEW (Westnetz GmbH, 2013) for a company with a constant heat demand.
- **6 days** considers the fact that some industries also work on Saturdays.
- **G1** is another representative weekly load profile (Westnetz GmbH, 2013) for a company without production on weekends.
- **5 days peak** is a weekly load profile with a common peak on the first day of the production week due to the heating up of production facilities.
- **4 days** and **4 days row** were considered to evaluate the feasibility of process heat applications with three days without production within a week

Weekly profiles Constant week and 5 days peak were considered for simulations regarding dimensioning of collector field, heat store, and for determination of typical annual system yield because they represent a typical production schedule of industrial companies. The difference to G1 is insignificant and the necessary store volume for 6 days is expected to be between the considered profiles. Furthermore, information is given in Section 5.7.1 for estimating the reduction of system yield for profiles with only 4 days of heat demand.

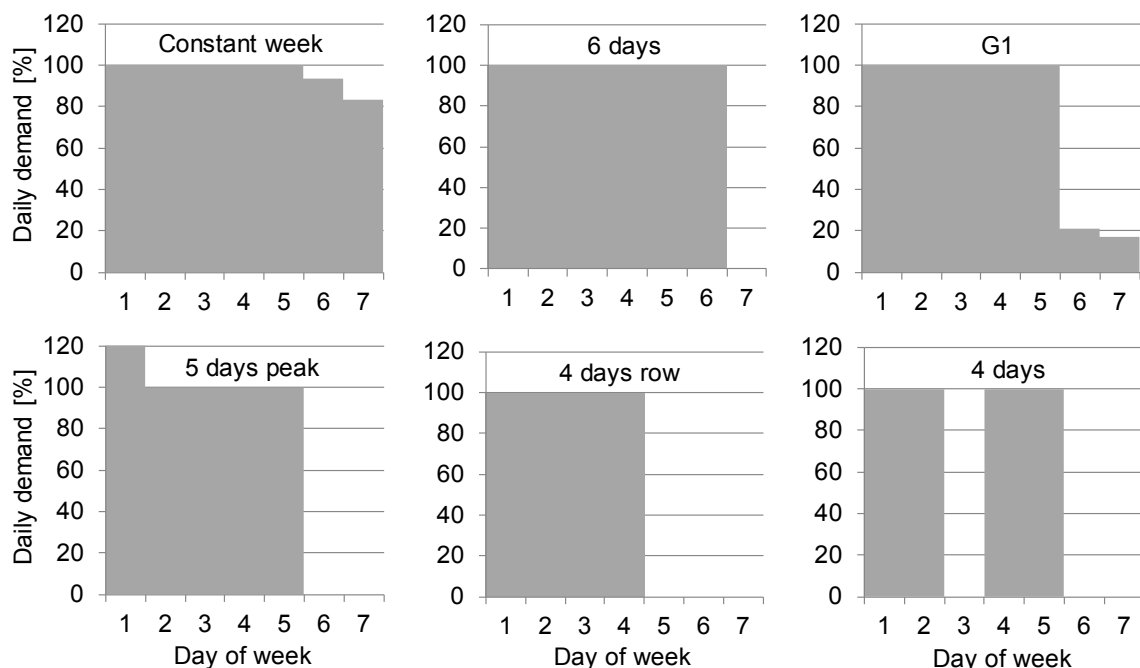


Figure 5-7: Overview of weekly load profiles; values can be found in Annex B.

The **annual load** profile is important for the determination of typical annual system yields for different process heat applications. Following profiles were considered:

- A **Constant** annual profile (upper left) is taken as reference for the following investigation.
- **Summer peak** shows a profile with a higher heat demand in summer than the rest of the year, which is the case e.g. in the beverages sector. A peak for two and four months was considered in Section 5.7.1.
- **Space heating** (originally named G1) is a representative profile by German VDEW taken from (Westnetz GmbH, 2013) and shows a typical heat demand for industries with a space heating demand in winter.
- The **Summer only** profile was selected to show the influence of an absent load during winter which can occur if an STS is out of operation due to a freezing protection of the discharge/ distribution loop.
- **Summer break** shows a profile with typical production holidays (two and four weeks considered) during summer.
- **Variable peak** shows a load profile determined for a process during a case study in a beverage industry company.

Figure 5-8 shows an overview of the annual load profiles considered for the simulations.

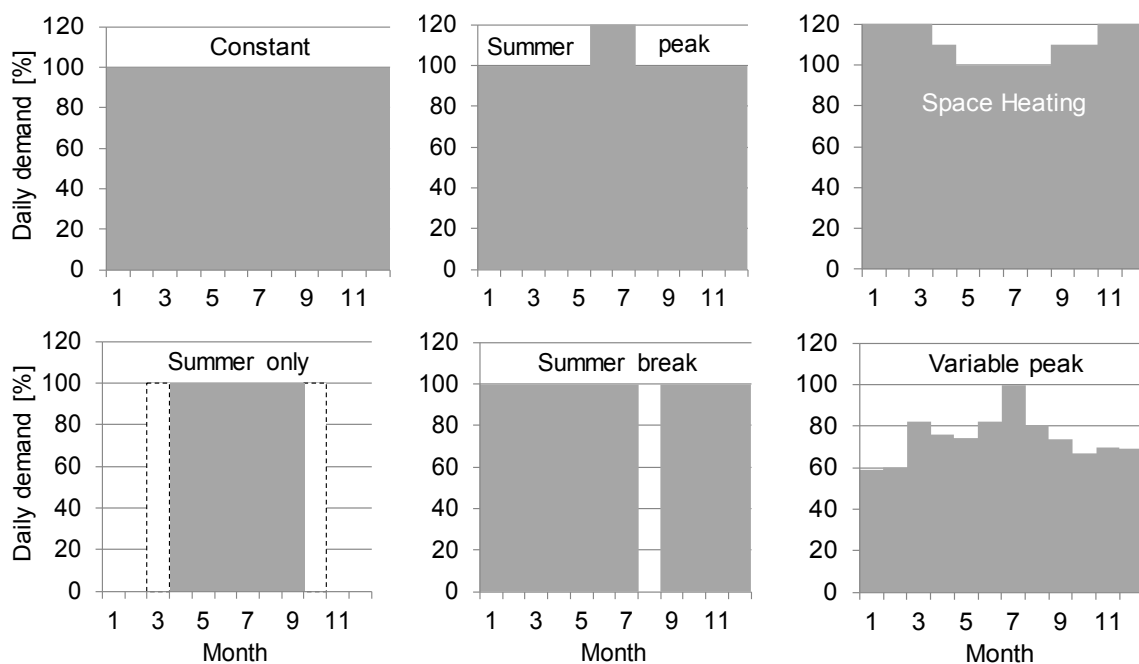


Figure 5-8: Overview of different annual load profiles considered for the simulations; values can be found in Annex B.

5.5. Dimensioning of collector field

The approach of VDI 6002 (2004) of dimensioning the collector field for summer days with good irradiation shall be transferred to process heat applications. Summer days are defined as days with a global horizontal irradiation of more than 7 kWh/(m²d). This design approach avoids that gained energy exceeds demand on many days and therefore leads to the most economical STS. The achievable solar fractions for solar process heat are low in many cases as the available roof area is a constraint at many industrial sites. This is because the ratio of consumed energy in relation to available roof and land area (energy consumption density) is much higher than for domestic applications as e.g. shown in (Müller et al., 2013).

A major advantage of this approach is the comparability of typical summer days for various locations. The difference between locations is mainly the number of such days and their chronological occurrence during the year. Further, the daily load profile influences the daily system yield not as strongly as the annual load profile influences the annual system yield which is used for dimensioning on an annual basis. Finally, a typical daily energy demand can be determined much easier in an industrial company than an annual distribution or even detailed load profiles. In order to determine the collector field size for which little excess energy is produced, a design point has to be identified for which the solar fraction on a typical summer day is just below 100 %. The solar fraction for such a day is defined as:

$$f_{\text{sol_day_avg}} = \frac{q_{\text{sol_day_avg}}}{q_{\text{available}}} \quad (8)$$

The daily system yield is determined by the simulation of an average “good” summer day as defined in Table 5-1 for a certain location. The average daily system yield $q_{\text{sol_day_avg}}$ is defined as the resulting yield for such a day. The utilization ratio of an average “good” summer day is another important value for the design of the collector field. It is defined as:

$$\bar{\eta}_{\text{sys_day_avg}} = \frac{q_{\text{sol_day_avg}}}{H_{\text{t_day_avg}}} \quad (9)$$

$H_{\text{t_day_avg}}$ is the daily irradiation of the defined day. Figure 5-9 shows an example of a daily and annual utilization ratio and a solar fraction for two different temperature levels supplied by an advanced flat plate collector as described in Section 5.5.2, a daily profile Daytime as described in Section 5.4, and for the location Wuerzburg. As the figure shows, $f_{\text{sol_day_avg}}$ just below 100 % is reached at different values for the available load (1) and (2) for both temperature levels. This value q_{design} , which is defined as the available load at a

daily solar fraction just below 100 % on an average “good” summer day (see Table 5-1), is used as the design value for the collector field.

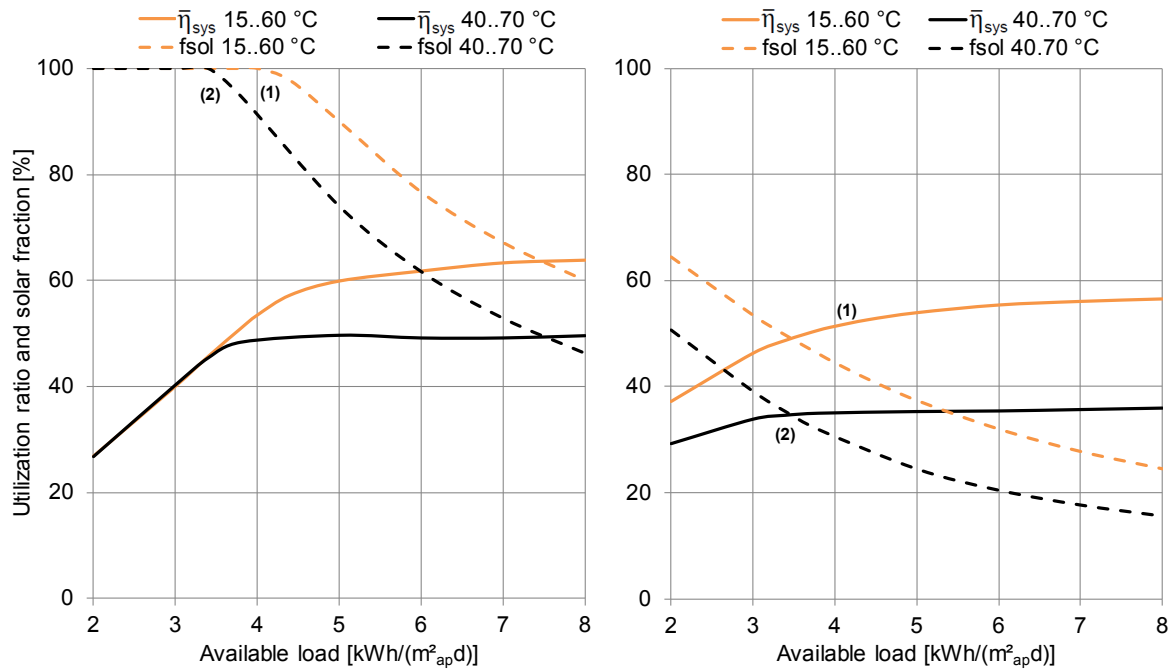


Figure 5-9: Utilization ratio for good summer days (left) and annual utilization ratio (right) for 15..60 °C and 40..70 °C, FPC_advanced, daily profile Daytime, weekly profile 7 days, annual profile Constant, location Wuerzburg.

As shown in the figure, the values for q_{design} are 4.2 kWh/(m²_{ap}d) for temperatures of 15 to 60 °C, and 3.6 kWh/(m²_{ap}d) for temperatures of 40 to 70 °C. This means that one m² of collector aperture area (in this case an advanced flat plate collector) should be installed for 4.2/ 3.6 kWh/d of process load. The values for q_{design} were determined by the variation of the available load in steps of 0.2 kWh/(m²_{ap}d) using TRNEDIT (Klein et al., 2009).

The collector area can be calculated as follows if the typical process load for one or more selected suitable processes or integration points were e.g. 1 MWh/d for a process with temperatures 40..70 °C:

$$A_{\text{ap}} = \frac{Q_{\text{process, day}}}{q_{\text{design}}} = \frac{1 \text{ MWh/d}}{3.6 \text{ kWh/(m}^2_{\text{ap}}\text{d)}} = 278 \text{ m}^2_{\text{ap}} \quad (10)$$

As shown in Figure 5-9 (right) the annual utilization ratio at an available load of 4.2/ 3.6 kWh/(m²_{ap}d) corresponds to a range on the curve where the utilization ratio is not significantly increased by selecting higher values for the available load. This means that the value for q_{design} is a lower limit for economic design. A higher value and therefore smaller STS does not influence the economic feasibility negatively unless the systems cost

rise due to higher specific costs for smaller systems. Reducing the available load leads to a less economical design. In cases with a very high system yield (favorable location, low process temperature) this can be feasible and should be investigated in detailed design through simulations.

The choice of a typical daily process load influences the design considerably. Usually, a typical production day in July or August should be selected to avoid a frequent stagnation of the STS. It might be a better choice to dimension the collector field for a typical day in autumn or spring for industries or processes with a low demand during these periods because quite a few days with high irradiation can occur. It can be necessary to design the collector field small enough to be able to build a system without heat store to achieve sufficient yields for applications with high process temperatures. These are especially favorable for higher process temperatures as the heat losses can be reduced considerably by designing a system without store. Further, high process temperatures lead to very high specific heat store volumes as the available temperature decreases with rising temperatures.

Within the following sections, different influencing factors for the collector field size are introduced and analyzed to judge about their impact on the dimensioning and the necessary accuracy for their determination. These influence factors are process temperature, collector type, orientation and slope, load profile, and store volume.

5.5.1. Influence of process temperature

The temperature level of an industrial process obviously has a strong influence on the design of the overall STS and the dimensioning of the collector field as its efficiency depends strongly on the provided temperature. Various temperature levels have to be considered although the investigation within this thesis focuses on process temperatures below 100 °C. Besides the heating of cold water, higher process return temperatures often occur due to the preheating through heat recovery, for hot water networks and the heating of baths/vessels/stores within the production. Figure 3-6 (Section 3.4) shows the temperature levels of a large number of promising processes for the integration of solar heat that were identified within several potential studies. As the figure shows, processes for the integration of solar heat can be found at various temperatures below 100 °C. Figure 5-10 (left) shows the temperature level of 71 existing STS in industry (Vannoni et al., 2006). A share of 20 % of the STS supplies heat at temperatures below 40 °C or between 40..60 °C and 40 % between 60..100 °C. Processes higher than 100 °C have a share of 21 % in total (Vannoni et al., 2006). The temperature level of suitable processes for the integration of solar heat of 90 industrial companies is shown in Figure 5-10 (right) (Puente Salve, 2011). Processes at temperatures below 30 °C have a very small share of 5 %. Many processes are in the range of 30..60 °C and over 75 °C and 20 % are between these levels.

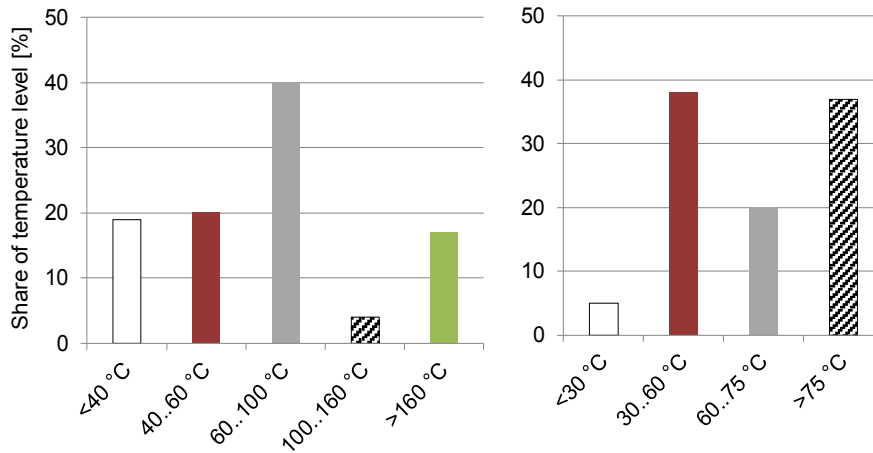


Figure 5-10: Temperature level of processes supplied by existing STS (left) (Vannoni et al., 2006) and temperature level of promising processes/applications identified in (Puente Salve, 2011); own figure based on these references.

Several other publications show the temperature level of the supported processes of existing STS in industry. Examples for the applications “heating of fluid streams” especially preheating of cold water to $60\text{ }^\circ\text{C}$ or $80\text{ }^\circ\text{C}$ can be found in (Anthrakidis et al., 2013; O.Ö. Energiesparverband, 2011a). In other cases, a preheated stream (e.g. by heat recovery) is heated further by an STS (e.g. make-up water from 20 to $90\text{ }^\circ\text{C}$ (Eisenmann et al., 2011)) or a hot water network return could be heated from temperatures of about $60..70\text{ }^\circ\text{C}$ (Anthrakidis et al., 2010; Müller et al., 2011).

Various bath or process temperatures are possible for the applications “heating of baths/vessels/store” and “thermal separation processes”. Temperatures can be as low as $30\text{ }^\circ\text{C}$ for degreasing of metal parts and as high as $90\text{ }^\circ\text{C}$ e.g. for blanching in the food industry (Anthrakidis et al., 2010). Table 5-2 shows the selected temperature levels for the investigation within this thesis which is based on a review of existing solar process heat systems and an analysis of suitable processes.

Table 5-2: Investigated temperature levels for collector field dimensioning.

Temperature [$^\circ\text{C}$]	
Return	Flow (max.)
15	60/80
30	60/80
40	70/90
50	80
60	90
70	90
80	95

Figure 5-11 shows the influence of process temperatures on the utilization ratio and q_{design} exemplarily for different return and flow temperatures. As the left figure illustrates, a slightly higher return temperature obviously reduces the utilization ratio for all available loads. In case of the same return temperature (15 °C) and different flow temperatures (60 and 80 °C) q_{design} is lower for a lower flow temperature because the collector efficiency is higher.

For large available loads the difference in utilization ratio declines as the STS just increases the return temperature. The utilization ratio is constantly lower for higher temperatures for an equal temperature difference (right) between flow and return whereas q_{design} declines. For a large temperature difference, an increased available load leads to lower system temperatures as the return temperature is less increased. Therefore, the utilization ratio increases considerably with an increasing available load for large temperature differences (left).

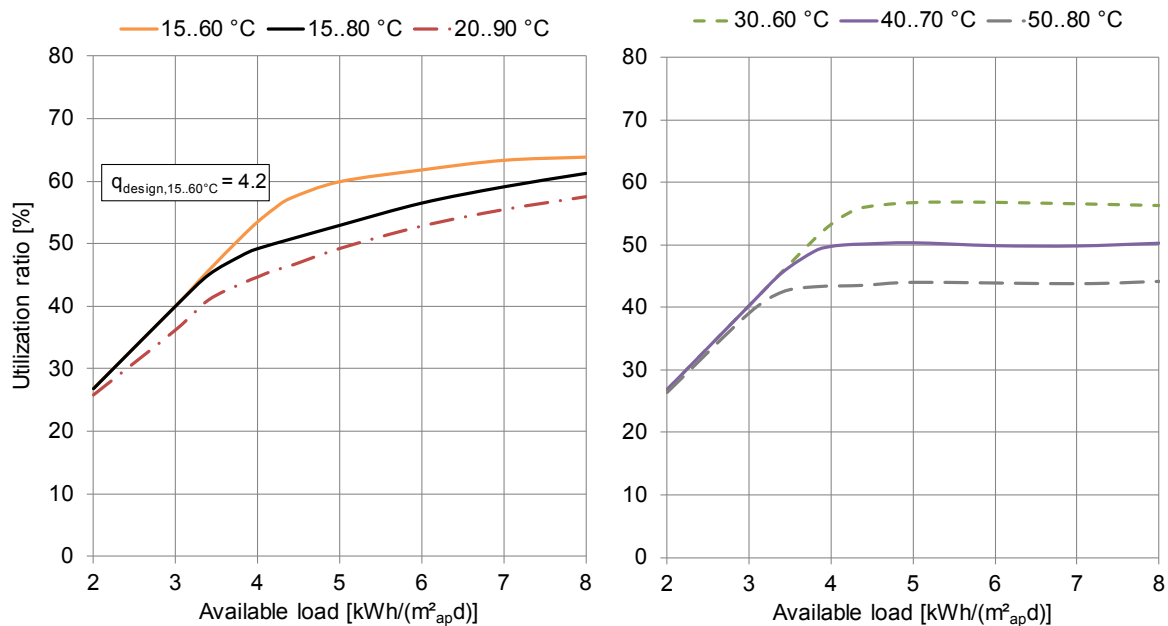


Figure 5-11: Utilization ratio for good summer days for different flow and return temperatures (left) and constant temperature difference with varying return and flow temperatures (right) for FPC_advanced, daily profile Daytime, location Wuerzburg.

5.5.2. Influence of collector type

Different collector types can be used for process heat applications and their various temperature levels. Only non-concentrating collectors were considered as the investigation in this thesis focuses on temperatures below 100 °C. Following collector types were used for the simulations:

- Flat-plate collector (FPC)
- Double-covered flat-plate collector (FPC-DG)
- Evacuated tube collector (ETC)
- Evacuated tube collector with compound parabolic concentrator (CPC)

Table 5-3 shows the considered collectors, their optical efficiency (η_0) and linear (a_1) as well as quadratic (a_2) heat loss coefficients. These values were selected for each collector type after an extensive market research in (ESTIF, 2013). A representative standard, advanced and high performance collectors were selected for the four different collector types to cover the variety of collectors on the market. Figure 5-12 shows the corresponding efficiency curves for the “advanced” collectors. As shown in the figure, at low temperatures, the efficiency of FPC, FPC-DG and ETC is significantly higher than for CPC. At medium temperatures the efficiency of all collector types is very similar. For high temperatures, the efficiency of FPCs drops significantly whereas ETCs are still reasonably efficient.

Table 5-3: Collector parameters for each collector type used in the simulations; FPC_DG_high performance is actually not double covered but a vacuum FPC.

Collector type	η_0 [-]	a_1 [W/(m ² K)]	a_2 [W/(m ² K ²)]	Source
FPC_standard	0.795	3.342	0.0160	(TÜV Rheinland, 2012)
FPC_advanced	0.831	3.520	0.0167	(ISFH, 2012)
FPC_high performance	0.841	3.016	0.0140	(SP, 2009)
FPC_DG_standard	0.811	2.710	0.0100	(AIT, 2011)
FPC_DG_advanced	0.804	2.564	0.0050	(TÜV Rheinland, 2011)
FPC_DG_high performance	0.759	0.508	0.0070	(ITW, 2012b)
ETC_standard	0.745	2.007	0.0050	(ITW, 2011)
ETC_advanced	0.751	1.240	0.0060	(ISFH, 2008)
ETC_high performance	0.804	1.360	0.0022	(SPF, 2011)
CPC_standard	0.718	0.974	0.0050	(ITW, 2012d)
CPC_advanced	0.644	0.749	0.0050	(ITW, 2012c)
CPC_high performance	0.688	0.583	0.0030	(ITW, 2012a)

Overall, considering the efficiency curves for the selected collector types can give a hint but is not sufficient for the choice of an appropriate collector type for a certain temperature level or solar process heat application.

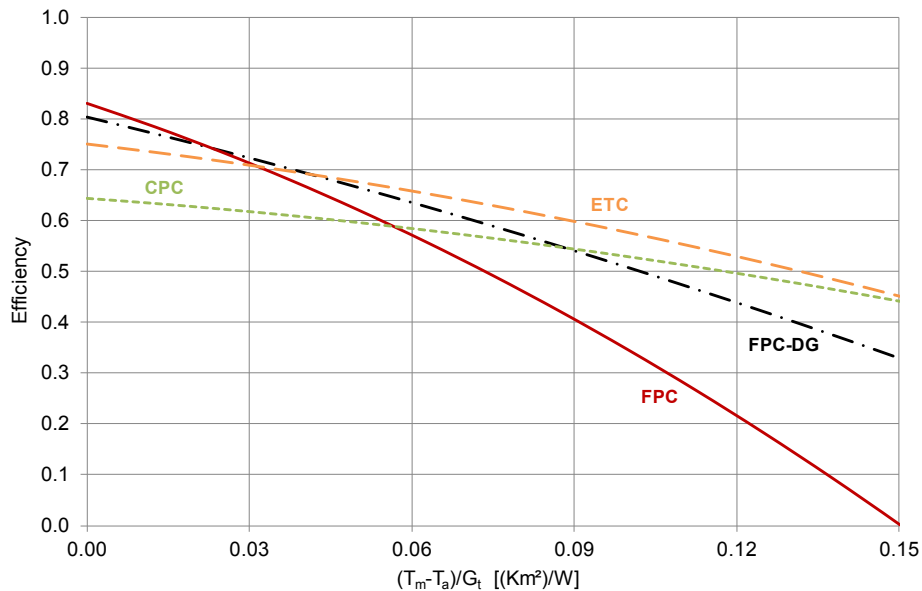


Figure 5-12: Efficiency curves for advanced collectors based on aperture area.

For this choice, it is necessary to consider annual system yields as well as costs for the different collector types. Figure 5-13 shows a comparison of different collectors at two temperature levels in order to assess the influence of the collector types listed above.

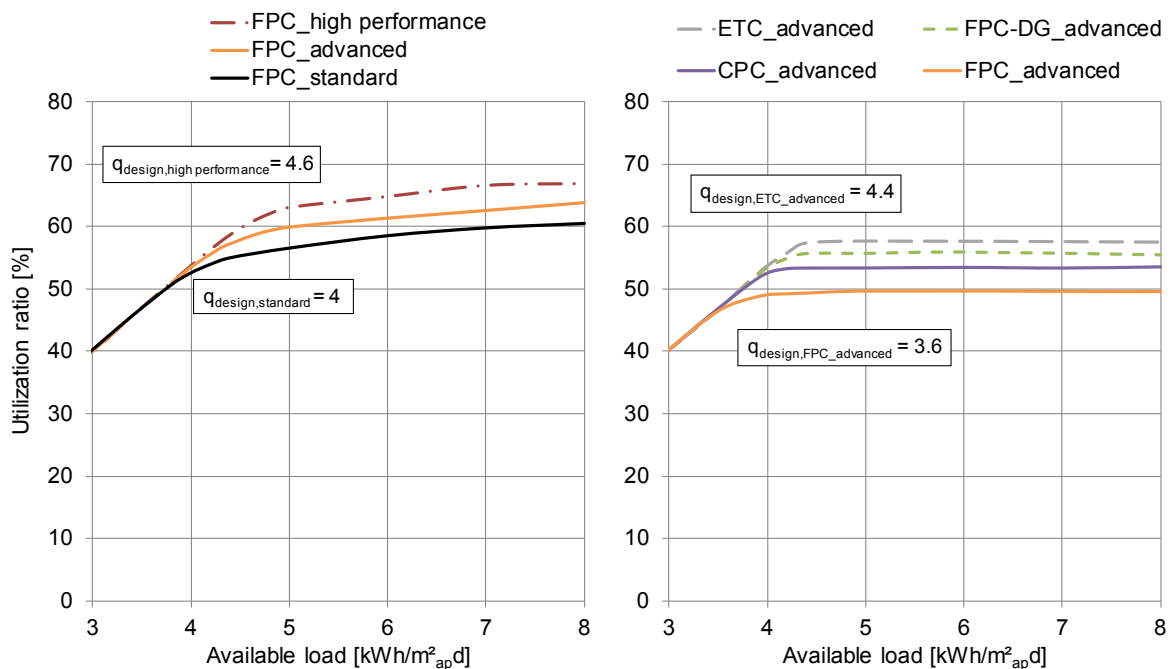


Figure 5-13: Utilization ratio for good summer days for 15..60 °C (left) and 40..70 °C for different collector types, daily profile Daytime, and location Wuerzburg.

The left figure shows the utilization ratio for different FPC for heating of cold water from 15..60 °C. For lower values of the available load, the utilization ratio is identical as it is limited by the energy demand. The available load at which the solar fraction is just below 100 % (q_{design}) differs for the three collectors. For FPC_standard q_{design} is 4 kWh/(m²_{apd}) and slightly higher for FPC_advanced (4.2 kWh/(m²_{apd})). FPC_high performance can cover the load almost completely at an energy demand of 4.6 kWh/(m²_{apd}). For higher values of q_{design} the difference of the utilization for the three collectors is almost constant.

The comparison between four different collector types for process temperatures of 40..70 °C shows that q_{design} and the utilization is generally lower and the STS could be larger if the economics are acceptable. It is clear that the choice of collector type and collector model is important for the dimensioning the collector field. In order to limit the complexity for preliminary design, the advanced versions of all collector types were considered to determine the design values in Section 5.5.5. q_{design} has to be slightly reduced/increased for standard and high performance collectors. Table 5-4 shows q_{design} for the two selected temperature levels for all considered collectors. As expected, collectors with a higher efficiency lead to smaller collector fields. The lower utilization for less efficient collectors could partly be compensated by their (usually) lower cost. A slight increase or reduction (0.2 to 0.4 kWh/(m²_{apd})) compared to an advanced version has to be considered for standard or high performance collectors as the deviation between the different versions of a collector type shows.

Table 5-4: Influence of collector type on q_{design} for 15..60 °C and 40..70 for daily profile Daytime and location Wuerzburg.

Collector type	15..60 °C		40..70 °C	
	q_{design} [kWh/(m ² _{apd})]	$\bar{\eta}_{\text{sys_day_avg}}$ [%]	q_{design} [kWh/(m ² _{apd})]	$\bar{\eta}_{\text{sys_day_avg}}$ [%]
FPC_standard	4.0	53	3.4	44
FPC_advanced	4.2	56	3.6	47
FPC_high performance	4.6	61	4.0	53
FPC_DG_standard	4.6	61	4.2	54
FPC_DG_advanced	4.6	61	4.2	55
FPC_DG_high performance	5.0	65	4.6	60
ETC_standard	4.6	61	4.4	57
ETC_advanced	4.6	60	4.4	57
ETC_high performance	5.0	66	4.6	61
CPC_standard	4.4	58	4.2	54
CPC_advanced	4.2	55	4.0	53
CPC_high performance	4.6	60	4.4	57

In case of CPC, the CPC_standard is more efficient than the CPC_advanced for the shown temperatures due to its higher optical efficiency (see Table 5-3). The choice of considering the two collectors as standard and advanced can be justified because CPCs are especially suitable and used for higher temperatures.

5.5.3. Influence of orientation and slope

Orientation and slope of an STS should be considered for the dimensioning of the collector field as both influence the annual system yield. q_{design} is displayed for two process temperatures and various orientations and slopes in Table 5-5. As the table shows, the orientation plays a minor role for a system with heat store as the yield on such days is not significantly reduced for the considered deviation from a southward orientation. It is clear that the slope changes the total daily system yield and therefore q_{design} . Lower slopes (unless close to horizontal) lead to smaller systems and vice versa. As in industry STS will mostly be installed with a slope and orientation close to the optimum (especially for flat roofs) both were not considered for the design values in Section 5.5.5. Nevertheless, it is especially important to consider the slope if it is far from the values considered here. Obviously, the orientation becomes influential for systems without heat store.

Table 5-5: Influence of orientation and slope on q_{design} for 15..60 °C and 40..70 °C, daily profile Daytime, FPC_advanced and location Wuerzburg; positive values for west orientation.

Orientation / slope	15..60 °C		40..70 °C	
	q_{design} [kWh/(m ² _{apd})]	$\bar{\eta}_{\text{sys_day_avg}}$ [%]	q_{design} [kWh/(m ² _{apd})]	$\bar{\eta}_{\text{sys_day_avg}}$ [%]
0 ° / 35 °	4.2	56	3.6	47
0 ° / 20 °	4.4	58	3.8	49
0 ° / 50 °	4.2	55	3.2	43
15 ° / 35 °	4.2	56	3.6	47
30 ° / 35 °	4.2	56	3.6	47
45 ° / 35 °	4.2	56	3.6	47
-15 ° / 35 °	4.2	56	3.6	47
-30 ° / 35 °	4.2	56	3.6	47
-45 ° / 35 °	4.2	56	3.6	47

5.5.4. Influence of load profile and store volume

This section analyzes the influence of load profile and store volume on the dimensioning of the collector field. Table 5-6 shows q_{design} for two process temperatures and all considered daily load profiles for an average summer day in Wuerzburg with a specific irradiation of 7.46 kWh/(m²d). A specific heat store volume of 5 kWh/m²_{ap} was used.

As the table shows, the influence of the daily load profile is quite limited for systems with heat store. Only profiles with very high peaks outside daylight hours have a lower utilization and therefore reduced q_{design} . Profiles without major peaks and heat demand mostly during daytime hours lead to similar results for the utilization ratio and q_{design} as Daytime. Therefore, Daytime, Heating bath/vessel and Constant, being a nearly constant daily profile, are considered in the following sections for the dimensioning of the heat store and the determination of the system yield.

In order to consider a weekly profile for the dimensioning of collector field, Figure 5-14 shows annual utilization ratios for process temperatures 15..60 °C and 40..70 °C, a heat store capacity of 5 kWh/m²_{ap}, daily profile Daytime and different weekly profiles as described in Section 5.4.

Table 5-6: Influence of daily load profile on q_{design} for 15..60 °C and 40..70 °C, heat store capacity of 5 kWh/m²_{ap}, daily profile Daytime and different weekly profiles.

Daily profile	15..60 °C		40..70 °C	
	q_{design} [kWh/m ² _{ap} d]	$\bar{\eta}_{\text{sys_day_avg}}$ [%]	q_{design} [kWh/m ² _{ap} d]	$\bar{\eta}_{\text{sys_day_avg}}$ [%]
Daytime	4.2	56	3.6	47
Constant	4.0	52	3.6	47
Cleaning	3.8	49	3.6	45
Heating bath/vessel	3.8	49	3.4	45
Heating bath all day	3.8	50	3.6	47
Heating bath daytime	4.2	56	3.6	47
Variable hot water	4.2	55	3.6	46
Periodical hot water	4.4	57	3.6	47
Steady hot water	4.0	52	3.6	47

It is clear that profiles with a heat demand on less than 7 days lead to lower annual utilizations than profiles with a constant heat demand. A simple increase of the heat store capacity alone does lead to much higher annual utilization ratios as shown in Section 5.6. The size of the collector field needs to be reduced to reach a higher available load in order to increase the annual utilization. As a rule of thumb compared q_{design} can be increased by

at least 1 kWh/(m²_{ap}d) for a 6 day profile and at least another 1 kWh/(m²_{ap}d) for a 5 day profile in comparison with a 7 day profile.

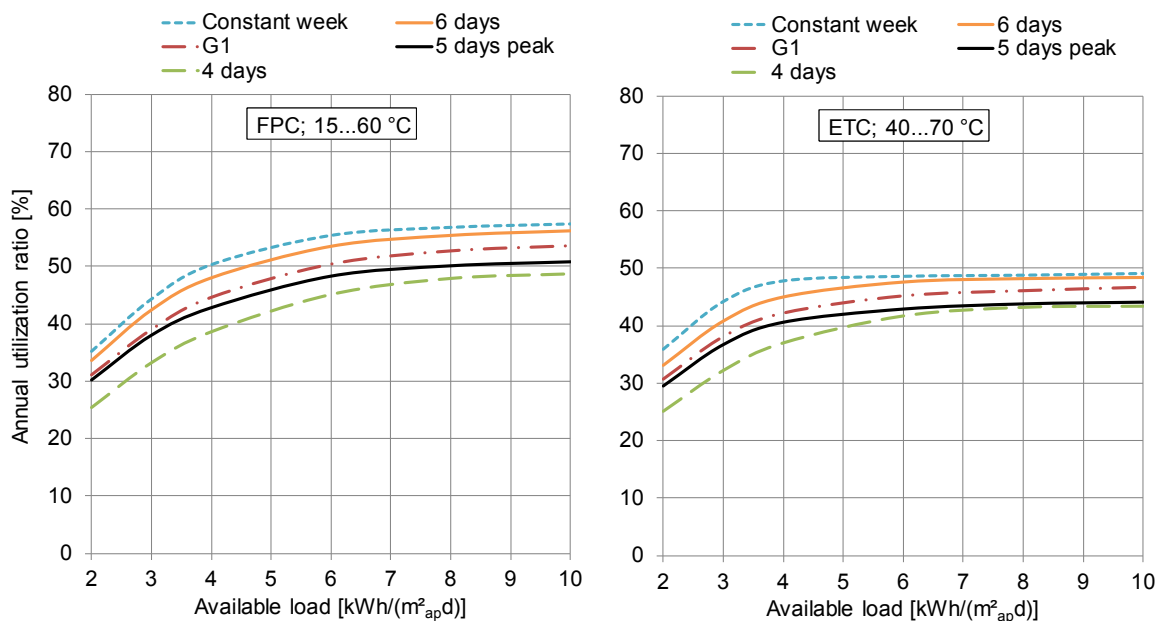


Figure 5-14: Annual utilization ratio for different weekly profiles; as shown in Figure 5-7, specific heat store volume of 5 kWh/m²_{ap}, “G1” is a weekly profile with full heat demand on 5 days and little demand on weekends.

As shown in Figure 5-14, increasing q_{design} e.g. from 4 kWh/(m²_{ap}d) for a 7 day profile to 5 kWh/(m²_{ap}d) for 6 days and 6 kWh/(m²_{ap}d) for 5 days, leads to similar utilization ratios for the same heat store volume. In addition, it shall be considered to increase the specific heat store capacity as shown in Section 5.6.

The heat store capacity can of course influence the utilization ratio and q_{design} . Figure 5-15 illustrates this influence for the three selected daily load profiles. For Daytime, the influence of heat store capacity is very limited as heat demand exists mainly during day time. The utilization is almost the same for specific heat store capacities of 3, 5, and 7 kWh/m²_{ap} and for less than 1 kWh/m²_{ap}.

For Heating bath/vessel, the utilization ratio and q_{design} are very low for a heat store capacity of 3 kWh/m²_{ap}. A specific capacity of 7 kWh/m²_{ap} leads to a considerable increase both for the utilization ratio and q_{design} except for the Daytime profile. A difference in utilization ratio and q_{design} exists for specific heat store capacity below 5 kWh/m²_{ap} for low available loads and a daily load profile Constant. An increase to 7 kWh/m²_{ap} does not have any influence. The difference in utilization ratio and q_{design} decreases for an increased available load (which means low solar fractions). The heat store volume has no influence

and STS can be designed without store for very large values of $q_{\text{available}}$ not only for the Constant profile but also for the Daytime one.

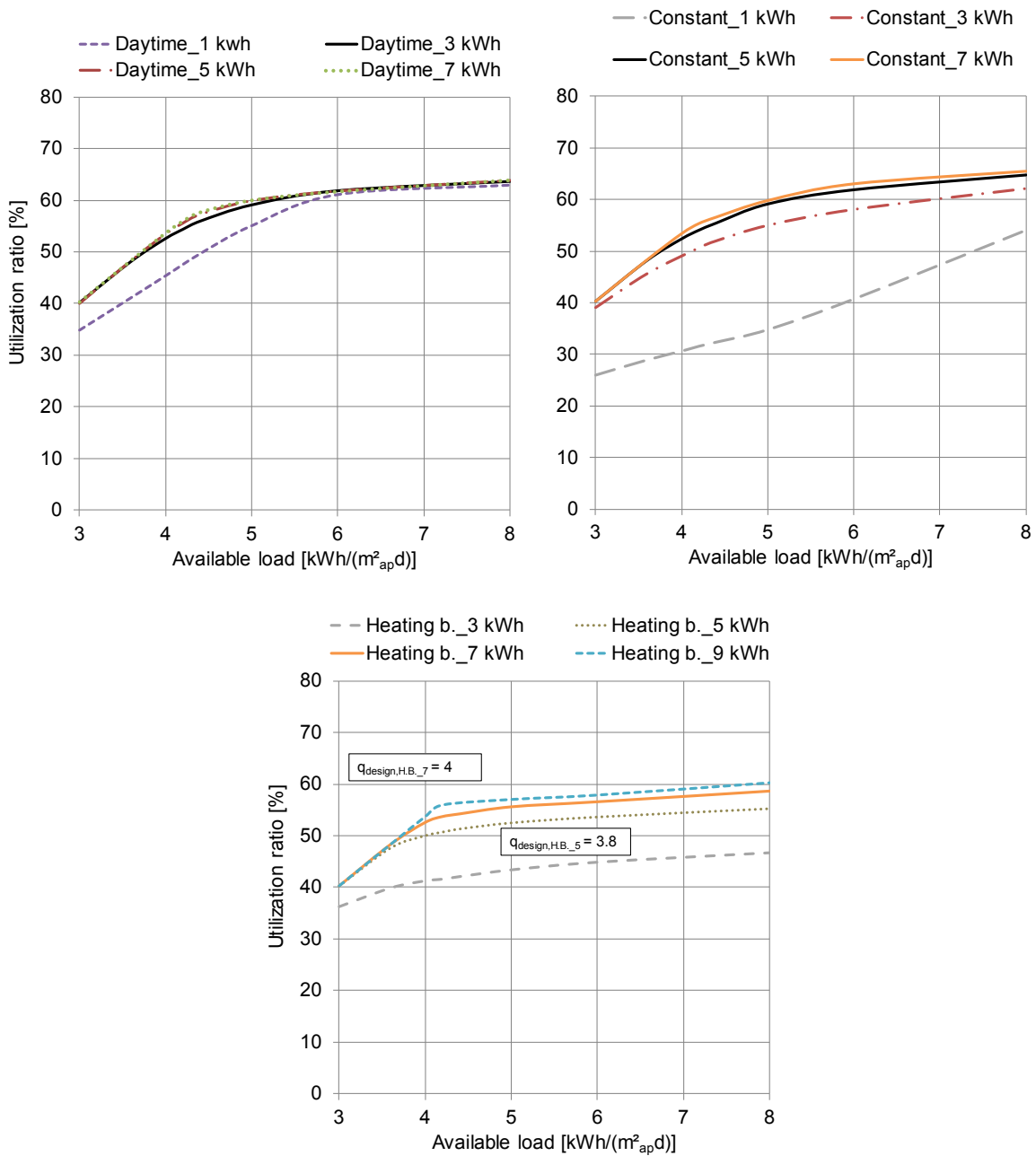


Figure 5-15: Utilization ratio for good summer days for 15..60 °C, different storage volumes and profiles, FPC_advanced, and location Wuerzburg; daily profile Heating bath/vessel abbreviated “Heating b.”.

5.5.5. Simulated design values

This section illustrates the results of system simulations to obtain design values (q_{design}) for several process heat applications. Several temperature levels, load profiles, collectors and locations were selected based on the described investigation regarding influence factors within the previous sections.

Figure 5-16 shows the simulated design values for different temperature levels, collectors, daily load profiles and the locations Wuerzburg and Madrid. As the figure shows, the simulated values for q_{design} (the specific heat demand per m^2_{apd} for which the solar fraction on a good summer day is just below 100 %) are in the range of 2.0 and 5.0 $\text{kWh}/(\text{m}^2_{\text{apd}})$. As expected, q_{design} declines with rising temperatures because the system efficiency is worse at higher temperatures. If the approach described above is followed, the collector field size can be higher for higher process temperatures. As shown in the figure, the dependency on temperature is of course higher for collectors with higher heat loss coefficients like FPC and FPC-DG. For example q_{design} varies between 4.2 and 2.2 $\text{kWh}/(\text{m}^2_{\text{apd}})$ for FPC and profile Daytime from 15..60 °C to 80..95 °C for Wuerzburg and 4.8 and 2.6 $\text{kWh}/(\text{m}^2_{\text{apd}})$ for Madrid. For the CPC the bandwidth is 4.2 to 3.6 $\text{kWh}/(\text{m}^2_{\text{apd}})$ for Wuerzburg and 4.4 to 4.0 $\text{kWh}/(\text{m}^2_{\text{apd}})$ for Madrid.

Regarding the difference for the selected locations, the variation for Daytime is between 3.4 to 4.2 $\text{kWh}/(\text{m}^2_{\text{apd}})$ for Wuerzburg and Madrid for 15..80 °C and an FPC. The difference is just 0.4 $\text{kWh}/(\text{m}^2_{\text{apd}})$ between Wuerzburg and Madrid for several temperature/collector type combinations. The slightly higher variation for FPC at 15..80 °C can be explained with higher temperatures and irradiation on good summer days in Madrid compared to Wuerzburg. In general, only minor deviations exist between the locations Copenhagen and Wurzburg and between Toulouse and Madrid. Concerning the differences between the daily load profiles, the simulated design values show that the daily load profile only has a small influence on q_{design} (simulated with heat store capacity of 5 $\text{kWh}/\text{m}^2_{\text{ap}}$ for daily profiles Daytime and Constant and 7 $\text{kWh}/\text{m}^2_{\text{ap}}$ for Heating of bath). The small difference between locations and load profiles (which is mostly only 0.2 $\text{kWh}/(\text{m}^2_{\text{apd}})$) does not represent a real difference but is due to the approach for determining q_{design} as $q_{\text{available}}$ was varied for the simulations in steps of 0.2 $\text{kWh}/(\text{m}^2_{\text{apd}})$.

The average daily irradiation on “good” summer days for the selected locations is between 7.54 $\text{kWh}/\text{m}^2_{\text{ap}}$ for the Wuerzburg and 7.81 $\text{kWh}/\text{m}^2_{\text{ap}}$ for Toulouse. A comparison of the simulated design values with the sum of daily irradiation shows that the system utilization ratio can reach 56 % for low temperatures (15..60 °C and an FPC) and still 45 % for ETC and 80..95 °C on such days for location Wuerzburg at an available load equivalent to q_{design} . The values for Figure 5-16 and for locations Copenhagen and Toulouse can be found in Annex C.

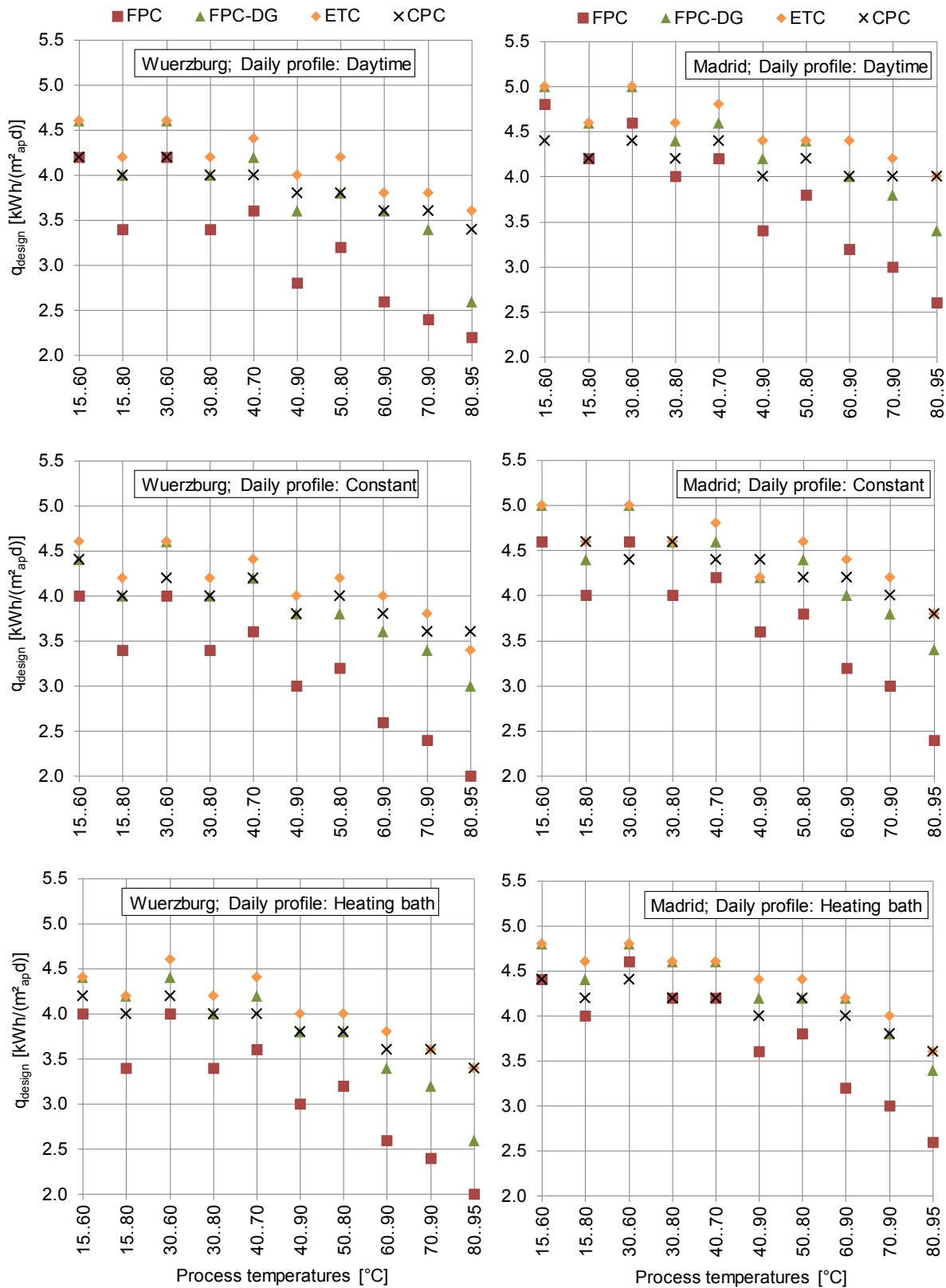


Figure 5-16: Simulated design values of q_{design} for different temperature levels, daily load profiles, locations Wuerzburg and Madrid, and collector types “advanced”, specific heat store capacity of 5 kWh/m^2_{ap} for Daytime and Constant and 7 kWh/m^2_{ap} for Heating bath; for detailed results see Annex C.

Figure 5-17 shows the annual utilization ratio for different process temperatures and daily profiles for Wuerzburg (above) and Madrid (below) in order to evaluate the design approach on an annual basis.

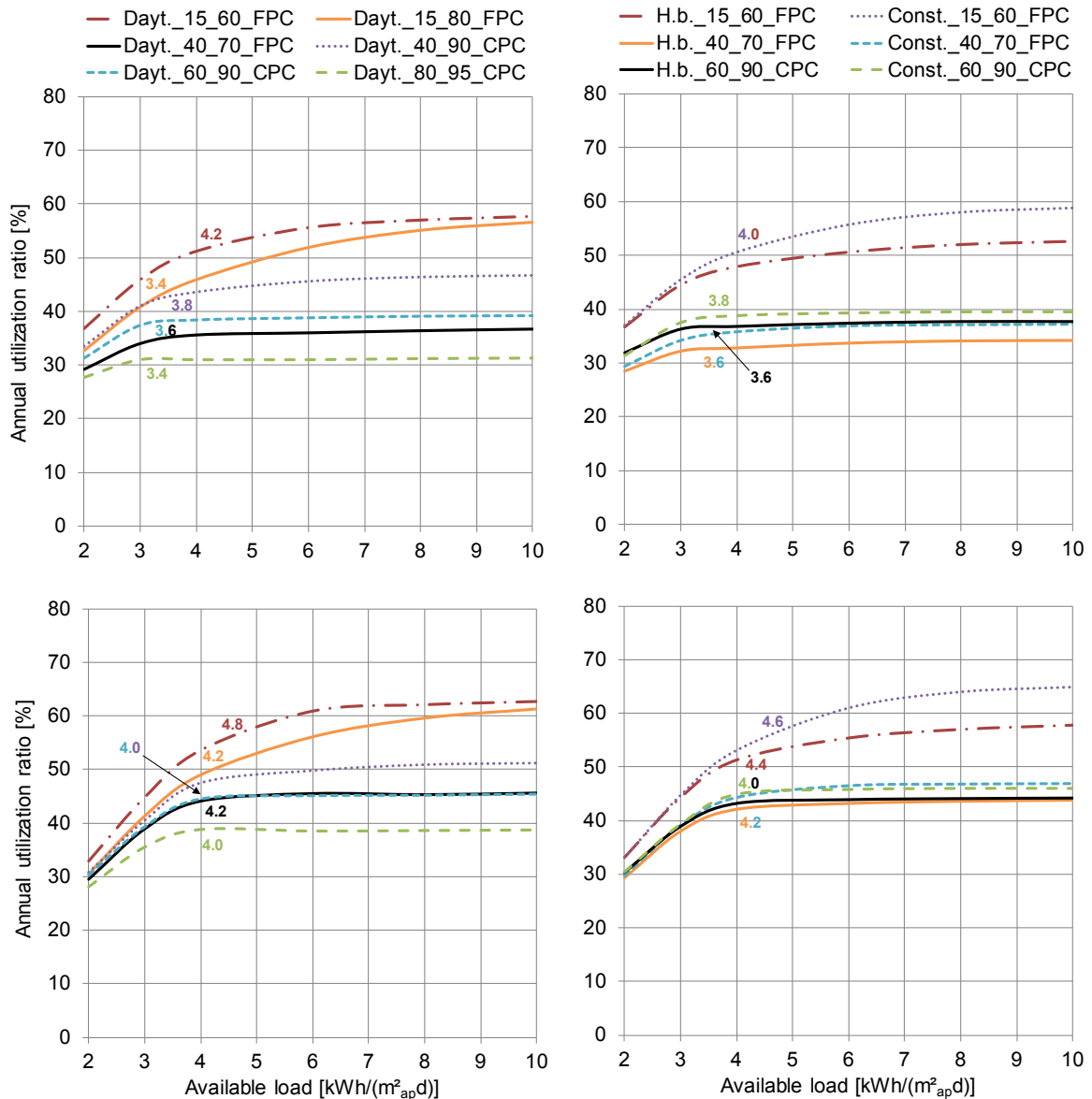


Figure 5-17: Annual utilization ratio for different temperatures, daily profile Daytime (left) and Constant as well as Heating bath (both right), weekly profile Constant week, specific heat store capacity of 5 kWh/m^2_{ap} for daily profile Daytime and Constant and 7 kWh/m^2_{ap} for daily profile Heating bath, and location Wuerzburg (above) and Madrid (below); the numbers in the figures show q_{design} .

The simulated design values of Figure 5-16 are displayed in the figure. As shown, q_{design} represents a range on the utilization curve for which the slope increases strongly if $q_{available}$ was decreased and the slope remains rather low for an increased $q_{available}$. Therefore, q_{design} represents a lower limit for the dimensioning of the collector field to avoid STS with low

efficiency. Further, the figure shows that for larger temperature differences and rather low temperatures, an increased $q_{\text{available}}$ leads to substantially higher utilization ratios. An increase of $q_{\text{available}}$ does not increase the annual utilization substantially for processes with a low available temperature difference.

Figure 5-18 illustrates the annual utilization ratio for different processes with a high temperature difference between flow and return. An increased $q_{\text{available}}$ leads to a substantially increased utilization ratio for almost all shown process/collector type combinations in contrast to some of the utilization ratio curves in Figure 5-17.

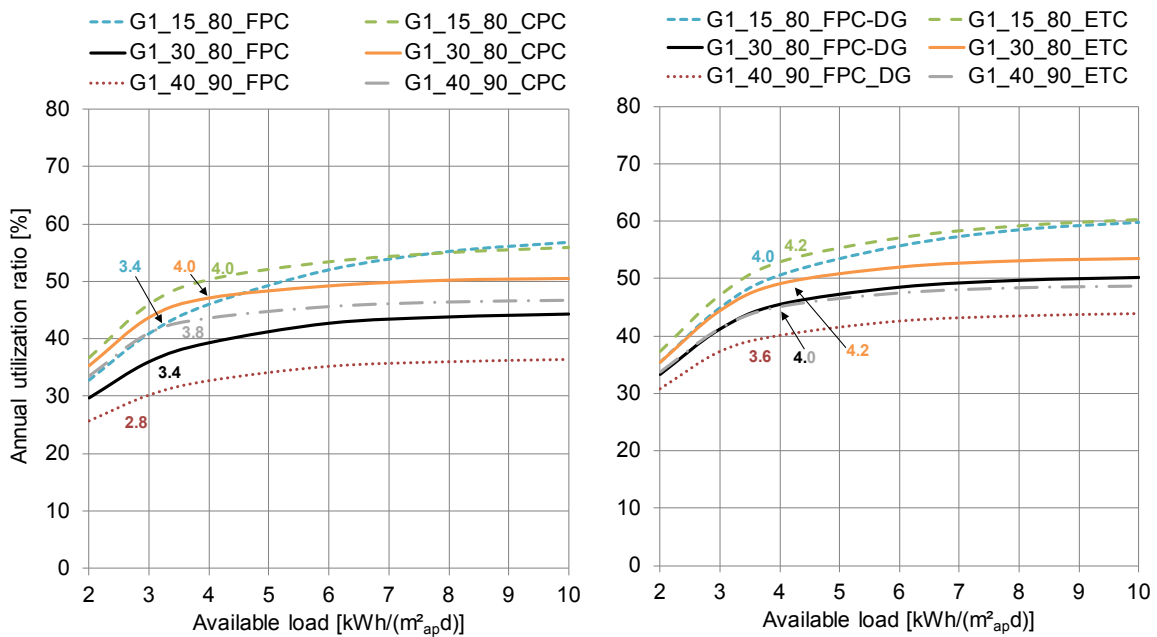


Figure 5-18: Annual utilization ratio for different temperatures with high difference between return and flow, different collector types, daily profile Daytime, weekly profile Constant week, specific heat store capacity of $5 \text{ kWh/m}^2_{\text{ap}}$, and location Wuerzburg.

Only for CPC, the curves are rather flat due to its low heat losses and low optical efficiency. In general, the utilization ratio can be increased considerably by raising $q_{\text{available}}$ for higher available temperature differences between flow and return in combination with a high optical efficiency. This is because an increased $q_{\text{available}}$ means that the return temperature is increased less by the STS and thus the temperatures in the system and in the collectors decline. For higher temperature differences this effect is obviously higher than for small ones of e.g. 30 K. This fact has to be considered when using the described design approach by increasing the design values shown in Figure 5-16 slightly (e.g. to a minimum of $4 \text{ kWh}/(\text{m}^2_{\text{ap}}\text{d})$ for higher available temperature differences.

The weekly load profile has an influence on the dimensioning of the collector field as mentioned in the previous section. Figure 5-19 shows the annual utilization ratio for

different temperatures, daily profile Daytime, weekly profile 5 days peak, specific heat store capacity of $5 \text{ kWh/m}^2_{\text{ap}}$, and location Wuerzburg (left) and Madrid (right). The heat store capacity should obviously be increased as described in the following section. Nevertheless, simply increasing the heat store volume is not sufficient for collector field dimensioning if load is available on less than 7 days a week. The collector field size needs to be reduced in order to increase the specific system yield substantially.

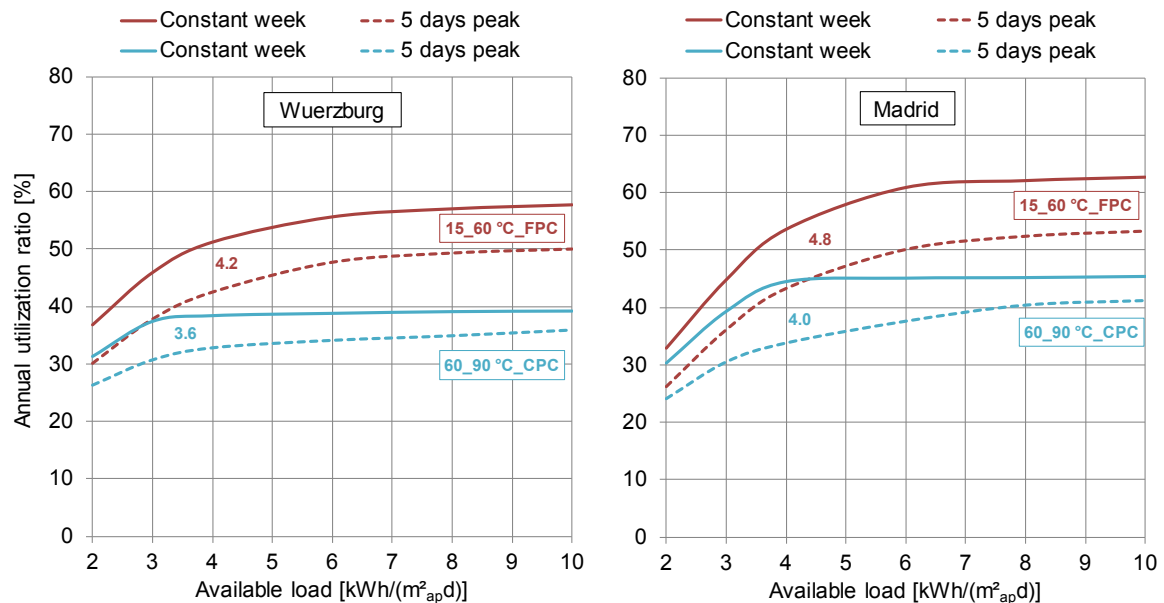


Figure 5-19: Annual utilization ratio for different temperatures, daily profile Daytime, weekly profile Constant and 5 days peak, specific heat store capacity of $5 \text{ kWh/m}^2_{\text{ap}}$, and location Wuerzburg (left) and Madrid (right).

As shown in the figure, the inclination of the utilization curve is higher for a weekly profile 5 days peak than for Constant week. In general, the annual utilization ratio is substantially lower due to fewer days with heat demand. An increase of $q_{\text{available}}$ and therefore smaller collector field sizes can compensate for the lower utilization to a certain extent. As a rule of thumb $q_{\text{available}}$ should be increased by at least $1 \text{ kWh}/(\text{m}^2_{\text{ap}}\text{d})$ per day of the week without heat demand. E.g. for $15..60 \text{ }^\circ\text{C}$ this would lead to an increased q_{design} of $6.2 \text{ kWh}/(\text{m}^2_{\text{ap}}\text{d})$ for Wuerzburg and $6.8 \text{ kWh}/(\text{m}^2_{\text{ap}}\text{d})$ for Madrid leading to an increase of the utilization ratio of five percentage points and about four percentage points respectively. It is necessary to evaluate its suitability on an annual basis considering the system yield and costs if q_{design} is much lower for a collector type at a certain temperature range.

5.6. Dimensioning of heat store

This section considers both the daily and weekly load profile to determine specific store volumes for preliminary design. Weekly profiles Constant week and 5 days peak were considered for the simulations within this section as the difference to G1 (weekly profile with full heat demand on 5 days and little demand on weekends) and 7 days is insignificant and the necessary store volume for 6 days is expected to range between the considered profiles. As mentioned in Section 5.2, the available capacity of the store depends on the process return temperature and the maximum temperature in the store. Table 5-7 shows the specific store volume in l/m^2_{ap} for different specific store capacities depending on the process return temperature. A maximum store temperature of $110\text{ }^\circ\text{C}$ was assumed for processes with maximum flow temperatures of 90 and $95\text{ }^\circ\text{C}$. Especially for high temperatures, large store volumes are necessary for store capacities of 7 or $9\text{ kWh}/m^2_{ap}$ although the maximum temperature of $110\text{ }^\circ\text{C}$ reduces the necessary store volume.

Table 5-7: Specific store volumes for different temperature levels; ^{*1}For these return temperatures a flow temperature of $90/95\text{ }^\circ\text{C}$ is considered in the simulations. Therefore, a maximum store temperature of $110\text{ }^\circ\text{C}$ was assumed; ^{*2} the specific store volume was calculated for a maximum store temperature of $95/110\text{ }^\circ\text{C}$.

Specific store capacity [kWh/(m ² _{ap} d)]	Specific store volume [l/m^2_{ap}] for return temperature [$^\circ\text{C}$]						
	15	30	40 ^{*2}	50	60 ^{*1}	70 ^{*1}	80 ^{*1}
1.0	11	13	16/12	19	17	21	29
3.0	32	40	47/37	57	52	64	86
5.0	54	66	78/61	96	86	107	143
7.0	75	93	109/86	134	120	150	201
9.0	97	119	141/111	172	155	193	258

A specific heat store volume of $50\text{ l}/m^2_{ap}$ is suggested for large STS for DHW preparation in (VDI 6002, 2004). Hess and Oliva (2011) also mention a specific heat store volume of $50\text{ l}/m^2_{ap}$ as a suitable starting point for system design. A wider range of heat store volumes has to be considered for process heat applications as the variety of both weekly (as shown in Figure 5-7) and daily load profiles is larger in industry than in domestic applications. A specific heat store capacity of $5\text{ kWh}/m^2_{ap}$ ($54\text{ l}/m^2_{ap}$) is taken as a reference within this section as suggested in (Hess and Oliva, 2011; VDI 6002, 2004). This specific heat store capacity was reduced to a minimum of $1\text{ kWh}/m^2_{ap}$ and increased to a maximum of $9\text{ kWh}/m^2_{ap}$ for different combinations of weekly and daily load profiles, as well as, process temperatures, collectors, locations and values for the available load. The choice of the available load or the size of the collector field obviously influences the dimensioning of

the heat store. This is because for large collector fields (small $q_{\text{available}}$) a higher specific heat store capacity is suitable compared to small collector fields (large $q_{\text{available}}$). As shown in Section 5.5.5, q_{design} is in the range of 2..5 kWh/m²_{ap} (with suitable values for many process temperatures in the range of 4 kWh/m²_{ap}). Therefore, Figure 5-20 shows the change of the annual system yield for different specific heat store capacities, daily and weekly load profiles, location Wuerzburg (above) and Madrid (below) and FPC_advanced exemplarily for process temperatures 15..60 °C and $q_{\text{available}} = 4 \text{ kWh/m}^2_{\text{ap}}$.

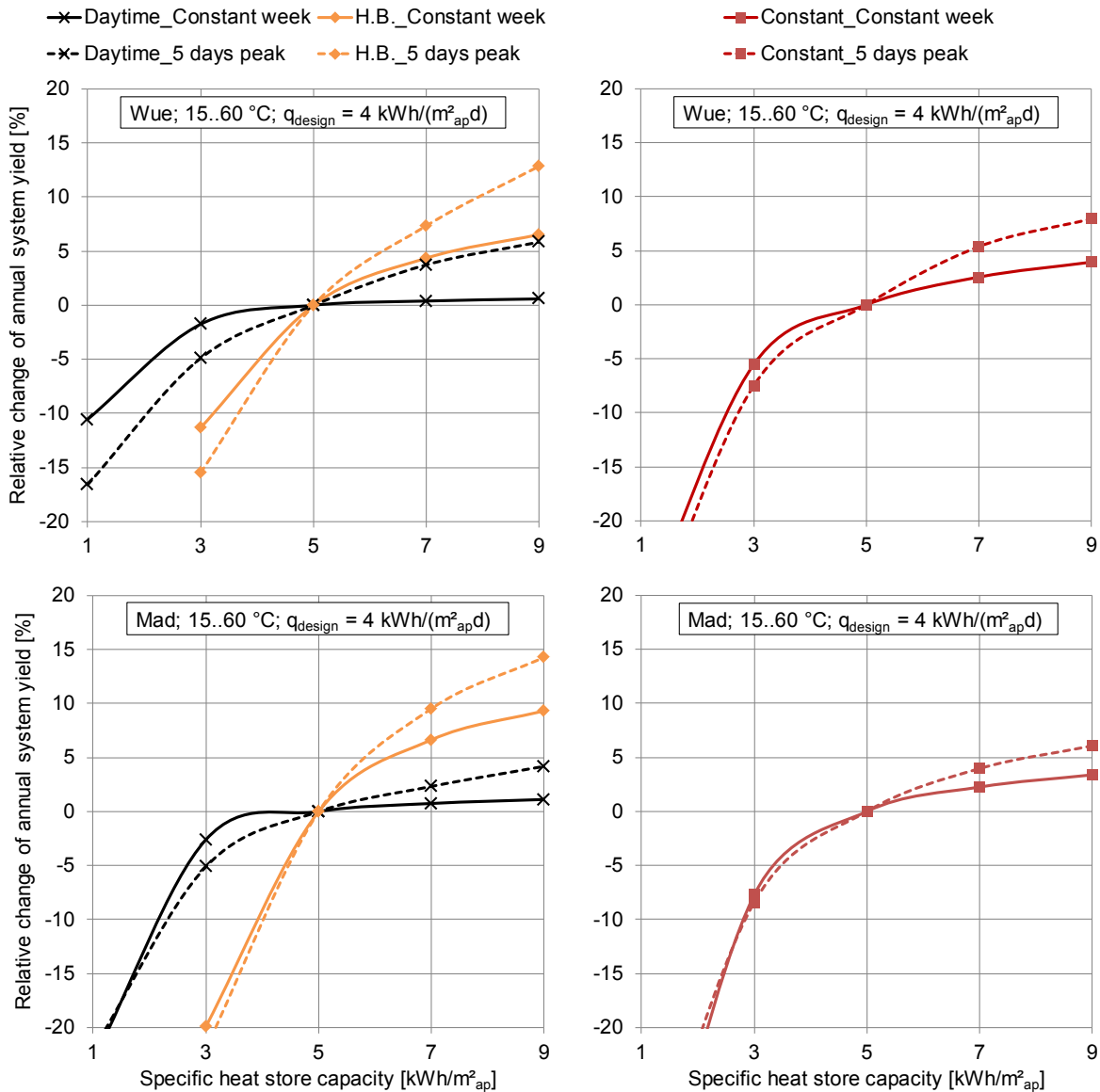


Figure 5-20: Change of annual system yield for different specific heat store capacities, daily and weekly load profiles, location Wuerzburg (above) and Madrid (below) and FPC_advanced.

As shown in the upper left figure, an increase of the specific heat store capacity larger than 5 kWh/m²_{ap} does not lead to a considerable increase of the annual system yield for the daily profile Daytime and an almost constant weekly profile (Constant week). Further, a

decrease to 3 kWh/m²_{ap} only leads to a decrease of 2 %. The decrease to 3 kWh/m²_{ap} already leads to a change of the annual system yield of approximately 5 % for the same daily load profile but heat demand on only 5 days a week. An increased specific heat store capacity larger than 5 kWh/m²_{ap} leads to a stronger but not to a major increase of the annual system yield.

For the daily profile Heating bath/vessel, a decreased store capacity reduces the annual system yield considerably and an increase also leads (especially for weekly profile 5 days peak) to a major increase of the system yield. For the daily profile Constant, Figure 5-20 shows similar results as specific heat store capacities larger than 5 kWh/m²_{ap} lead to a considerable change of the system yield for a 5 day production week only. It is important to consider the location of a planned STS and its influence on the dimensioning of the heat store for preliminary design. Figure 5-20 (lower figure) shows that the results for the location Madrid differ slightly from the ones for Wuerzburg. This can also be derived from the detailed results in Annex D. For the daily profile Heating bath/vessel, the annual system yield is more sensitive to a change of the heat store capacity.

In general, the results for Madrid are similar to the ones for Wuerzburg and would not lead to a different choice of heat store capacity at least not for preliminary design. The cost of additional heat store volume has to be considered in order to calculate its economic impact for detailed design. This is not the scope of the preliminary design consideration presented here. For a quick assessment within preliminary design, Figure 5-20 shows that, depending on the weekly profile, a specific heat store capacity of 3.5 kWh/m²_{ap} is suitable for the daily profile Daytime. For the daily profile Constant, a specific heat store capacity of 5.7 kWh/m²_{ap} is suitable, depending on the weekly profile. For the daily profile Heating bath/vessel, the heat store capacity needs to be enlarged to 7 kWh/m²_{ap} whereas even 9 kWh/m²_{ap} could be necessary for only 5 production days. Detailed results for different process temperatures, available loads and collector types can be found in Annex D. These show that the influence of specific heat store capacity differs only very little for the other considered collector types so the presented results can also be used for other non-concentrating collectors.

The process temperatures have an impact on the influence of the heat store volume as exemplarily shown in Figure 5-21 (change in kWh/m²_{ap} instead of %). As shown in the figure, a change of specific heat store capacity from 5 kWh/m²_{ap} for process temperatures 40..70 °C (right) leads to a smaller change compared to process temperatures 15..60 °C (left). This can be explained by higher (additional) heat losses for higher process temperatures.

The heat store capacity can be reduced at higher process temperatures (return temperature >40 °C) to 5 kWh/m²_{ap} for the daily profile Heating of bath and 3 kWh/m²_{ap} for the daily

profile Constant for a constant weekly load (Constant week) as Figure 5-21, Figure 5-22, Figure 5-23 as well as the results in Annex D show. A specific heat store capacity of $7 \text{ kWh/m}^2_{\text{ap}}$ is sufficient for higher temperatures (return temperature $>40 \text{ }^\circ\text{C}$) for 5 days of process load (5 days peak) and the daily profile Heating of bath. The specific heat store capacity can be reduced to $3 \text{ kWh/m}^2_{\text{ap}}$ for the daily profile Constant and Daytime.

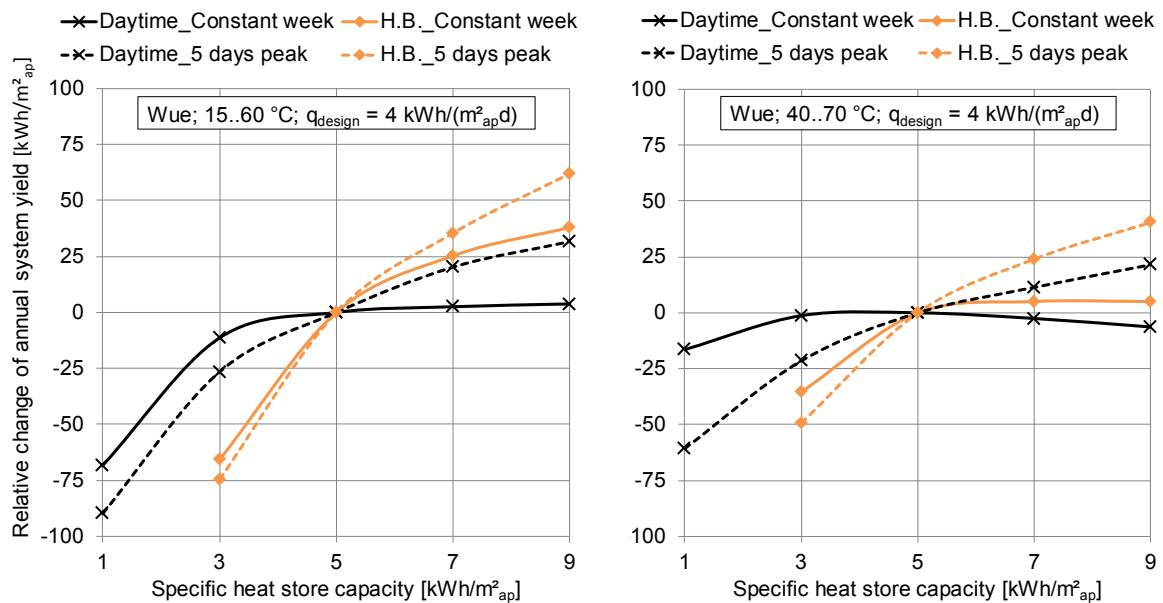


Figure 5-21: Change of annual system yield for different process temperatures, specific heat store capacities, daily and weekly load profiles, location Wuerzburg, and FPC_advanced.

The size of the collector field or available load obviously influences the dimensioning of the heat store as mentioned above. Therefore, Figure 5-22 shows the annual utilization ratio for different specific heat store capacities, process temperatures $15..60 \text{ }^\circ\text{C}$, the daily profiles Daytime and Heating bath (both left) as well as Constant (right), the weekly profile Constant week (above) and 5 days peak (below) at the location Wuerzburg over the available load.

First of all, the results shown in the figure support the above mentioned values for heat store capacity for preliminary design. For the weekly profile Constant week (upper figure) the figure shows that for the daily profile Daytime (left) the annual utilization ratio is not increased for specific heat store capacities larger than $3 \text{ kWh/m}^2_{\text{ap}}$. The same is true for the daily profile Constant (right) and a specific heat store capacity of $5 \text{ kWh/m}^2_{\text{ap}}$. Further, the figure shows that the specific heat store capacity can be reduced to $1 \text{ kWh/(m}^2_{\text{ap}}\text{d)}$ for a constant weekly process load for $q_{\text{available}} > 6 \text{ kWh/(m}^2_{\text{ap}}\text{d)}$ and the daily profile Daytime and $q_{\text{available}} > 10 \text{ kWh/(m}^2_{\text{ap}}\text{d)}$ and daily profile Constant. STS with such small collector fields might be designed without any (or a very small) heat store without leading to a reduction of the annual system yield. Further advantages of such systems are slightly lower

system temperatures (as only one heat exchanger is necessary) and reduced cost due to less indispensable components. The design of a system without (or a very small) heat store needs more detailed information on the load profile which is normally not available for preliminary design. Therefore, such systems should be designed based on system simulations using detailed load profiles.

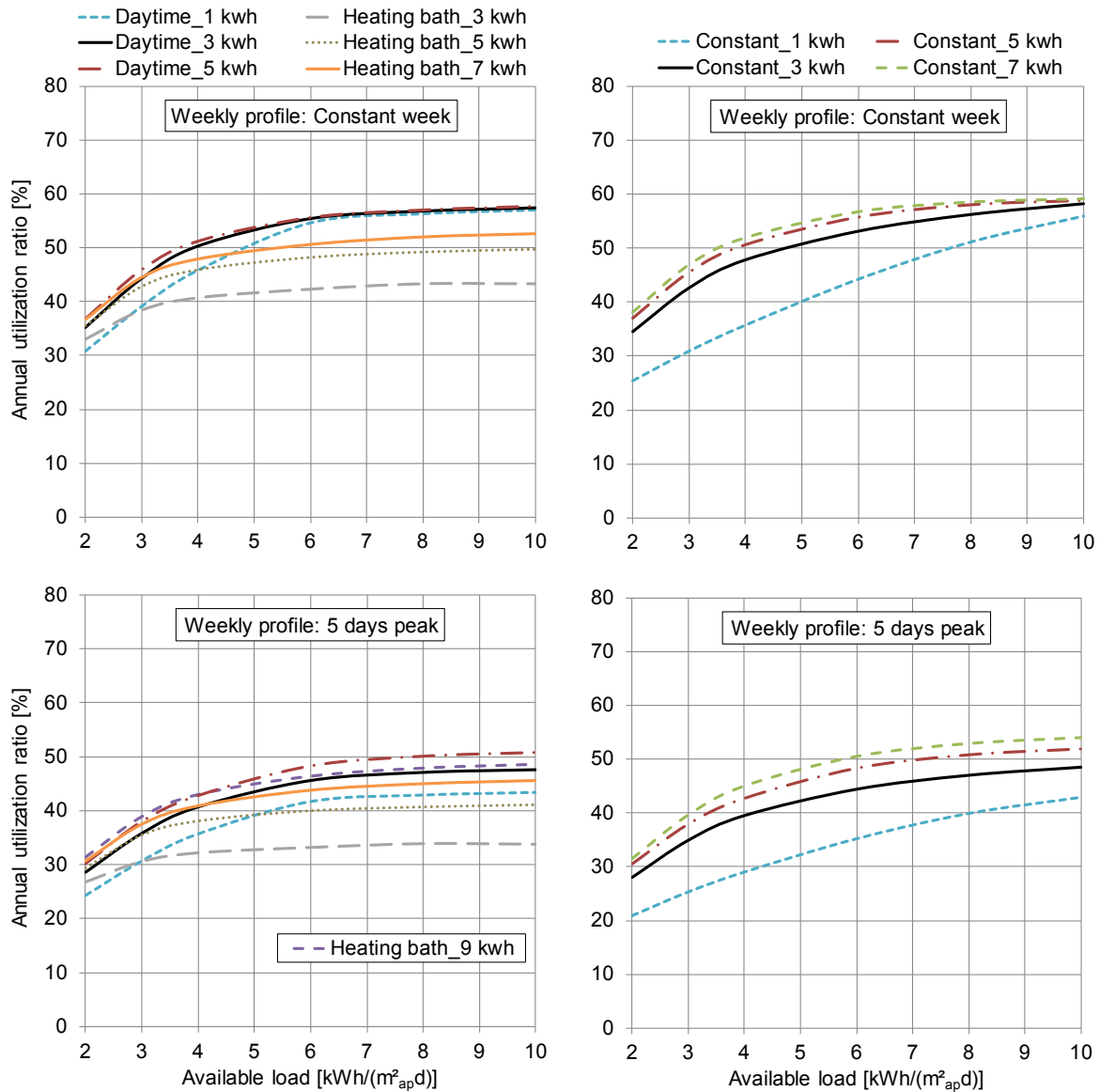


Figure 5-22: Annual utilization ratio for different specific heat store capacities, process temperatures 15..60 °C, daily profiles Daytime and Heating bath (both left) as well as Constant (right), weekly profile Constant week (above) and 5 days peak (below), FPC_advanced at location Wuerzburg.

As expected, a reduction of the specific heat store capacity to 1 kWh/m²_{ap} or even systems designed without heat store are not advisable for a 5 day weekly load profile (see Figure

5-22). The values of $5 \text{ kWh/m}^2_{\text{ap}}$ for Daytime and Constant and $7 \text{ kWh/m}^2_{\text{ap}}$ for Heating of bath are suitable across all shown values for $q_{\text{available}}$ for such processes. As mentioned above, the specific heat store capacity can be reduced for higher process temperatures without considerably decreasing the annual utilization ratio. Figure 5-23 shows the annual utilization ratio for different specific heat store capacities, process temperatures $60..90 \text{ }^\circ\text{C}$, the daily profiles Daytime and Heating bath (both left) as well as Constant (right), the weekly profile Constant week (above) and 5 days peak (below) at the location Madrid.

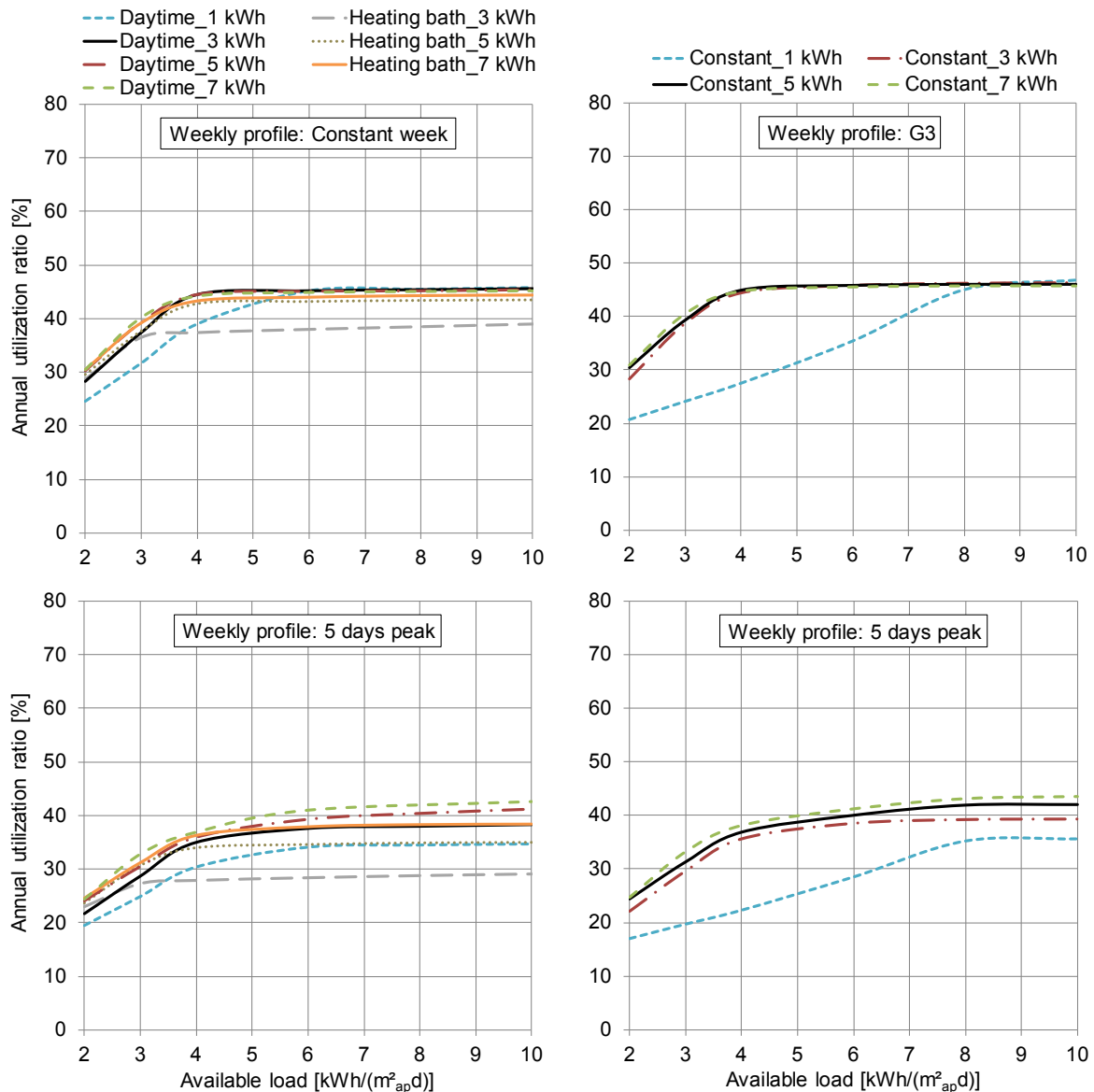


Figure 5-23: Annual utilization ratio for different specific heat store capacities, process temperatures $60..90 \text{ }^\circ\text{C}$, daily profiles Daytime and Heating bath (both left) as well as Constant (right), weekly profile Constant week (above) and 5 days peak (below), CPC_advanced at location Madrid.

First, the figure also shows that the heat store can be dimensioned small for a constant weekly load (upper figure) and an available load $>6 \text{ kWh}/(\text{m}^2_{\text{ap}}\text{d})$ for the daily profile

Daytime and $>8 \text{ kWh}/(\text{m}^2_{\text{ap}}\text{d})$ for the daily profile Constant. Further, the figure shows that for the daily profile Heating bath/vessel and a constant weekly load (upper left) the specific heat store capacity can be reduced to $5 \text{ kWh}/\text{m}^2_{\text{ap}}$ and to $3 \text{ kWh}/\text{m}^2_{\text{ap}}$ for the daily profile Constant (upper right). This is also true for the weekly profile 5 days peak and the daily profile Constant (lower right).

5.7. Utilization and yield for selected process heat applications

This section presents results regarding the influence of annual, weekly and daily load profiles on the system yield. Furthermore, annual utilization ratios and specific energy yields for selected applications in industry were determined. This shall help to estimate a system yield for a specific project and generally assess the feasibility of low-temperature solar process heat systems at different locations, for different process temperature levels and collector types.

5.7.1. Influence of load profile

The determination of a load profile for a specific industrial plant or process is often difficult and needs a lot of effort. Therefore, the influence of daily, weekly and annual load profiles is assessed within this section to provide a foundation for a basic feasibility assessment of a certain application in industry. The results help to assess the necessary accuracy of the determined load profile per year, the impact of periods without load during certain times of the year and minimum working days with load per week.

Regarding the annual load profile, Constant is taken as the reference. Further, a profile with a summer peak of two and four month was considered in the simulations. Space heating examines a typical heat demand for industries with a space heating demand in winter. The Summer only profile was selected to show the influence of an absent load during winter which can occur if an STS is out of operation. Summer break is a profile with typical production holidays (two and four weeks are considered) during summer. Finally, Variable peak is a load profile determined for a process during a case study in a beverage industry company.

Simulations were carried out for different available loads, process temperatures $15..60 \text{ }^\circ\text{C}$ (for $40..70 \text{ }^\circ\text{C}$ see Annex E), the daily profile Daytime, the weekly profile Constant week and locations Wuerzburg and Madrid. Figure 5-24 shows the change of the annual system yield for different annual load profiles for process temperatures $15..60 \text{ }^\circ\text{C}$. As the figure shows, an operation of an STS for only six or eight months leads to a considerable yield reduction as expected. The impact is even larger for the location Madrid. The impact is less for higher process temperatures especially for central European climates because higher

temperatures are seldom reached during the winter months. The considered summer break leads to a reduction of yield of a little more than 10 % (four weeks) and just over 5 % (2 weeks). The measured profile (Variable peak) leads to a reduction of approximately 5 to 10 % depending on the maximum daily available load and the location.

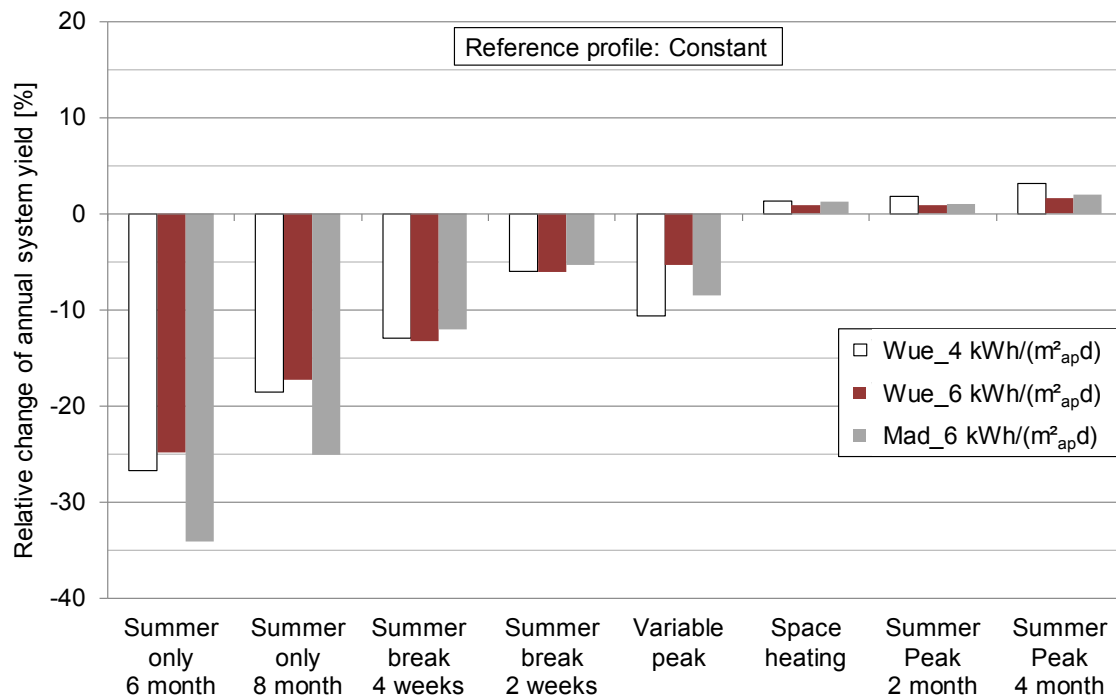


Figure 5-24: Change of annual system yield for different annual load profiles, different available loads, process temperatures 15..60 °C, daily profile Daytime, weekly profile Constant week, specific heat store capacity of 3 kWh/m²_{ap}, FPC_{advanced} and locations Wuerzburg and Madrid. For process temperatures 40..70 °C and ETC see Annex E.

The profiles Space heating and Summer peak (two and four months) only lead to a minor increase in yield. The increase is larger for the lower value of the available load (6 kWh/(m²_{apd})) as for $q_{\text{available}} = 6 \text{ kWh}/(\text{m}^2_{\text{apd}})$ a sufficient load is available anyway.

Figure 5-25 shows the annual utilization ratio for different annual load profiles, process temperatures 15..60 °C and 40..70 °C, FPC_{advanced} and ETC_{advanced} for Wuerzburg. As the figure shows, the influence of the annual load profile is similar across different values of the available load or system sizes respectively. For Summer peak the influence is slightly larger at low $q_{\text{available}}$ as an additional load cannot be utilized by the STS. As the figure further shows, the reduction of an annual utilization ratio declines with a rising $q_{\text{available}}$ for Variable peak for the same reason as described above for Summer peak.

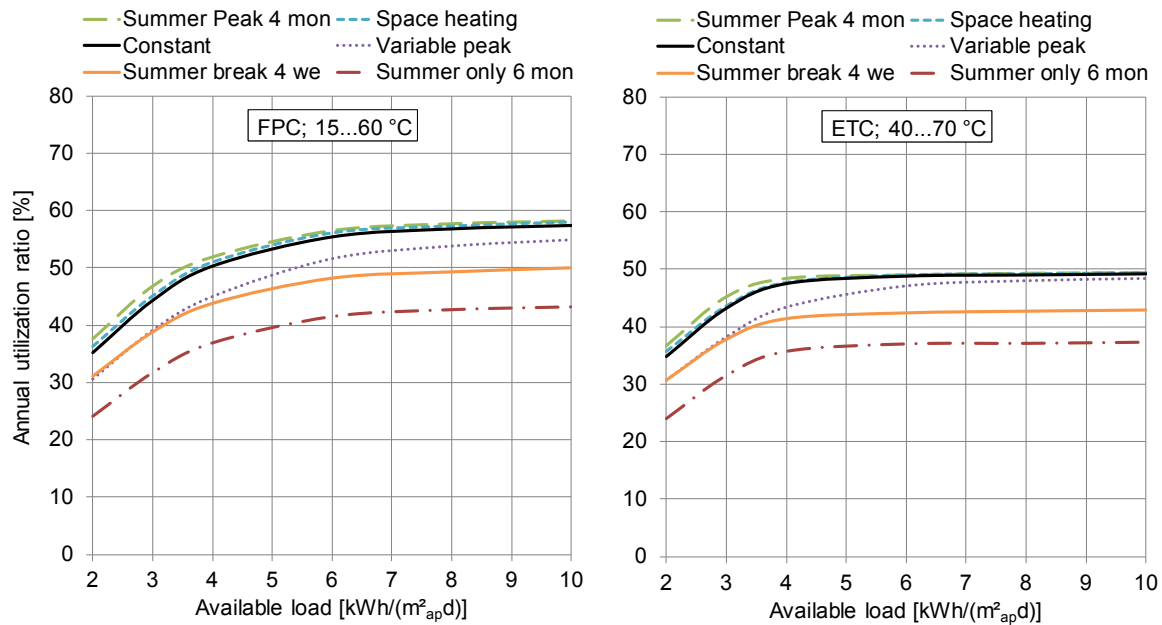


Figure 5-25: Annual utilization ratio for different annual load profiles, process temperatures 15..60 °C and 40..70 °C, specific heat store capacity of 5 kWh/m²_{ap}, FPC_advanced and ETC_advanced for Wuerzburg.

In addition, the influence of the weekly load profile is of importance for preliminary design, as well, as production hours for industrial companies often differ in the course of a week. Some publications (Aidonis et al., 2005a; Hess and Oliva, 2011) recommend that load should be available at least 5 days a week. Therefore, two profiles with load on only four days were taken into account. The profile 5 days peak is taken as reference.

Figure 5-26 shows the change of the annual system yield for different weekly load profiles, different available loads, process temperatures 15..60 °C, FPC_advanced and the locations Wuerzburg and Madrid. As the figure shows, a load on only four days a week obviously reduces the annual system yield. The reduction is not as high that an STS would generally not be feasible in case of such a profile depending on the available load on days with heat demand. Single days without heat demand can be compensated with the heat store. As the figure shows, the decrease of the system yield can partly be compensated by a higher heat store capacity. Nevertheless, it has to be mentioned that the achievable yield for a weekly profile with five days of heat demand is already considerably lower than for a constant heat demand of seven days per week. The general feasibility of an application with only four days of heat demand has to be evaluated on the basis of actual costs and estimated yields.

With respect to the influence of the daily load profile, Figure 5-27 shows the change of the annual system yield for different daily load profiles as shown in Figure 5-6.

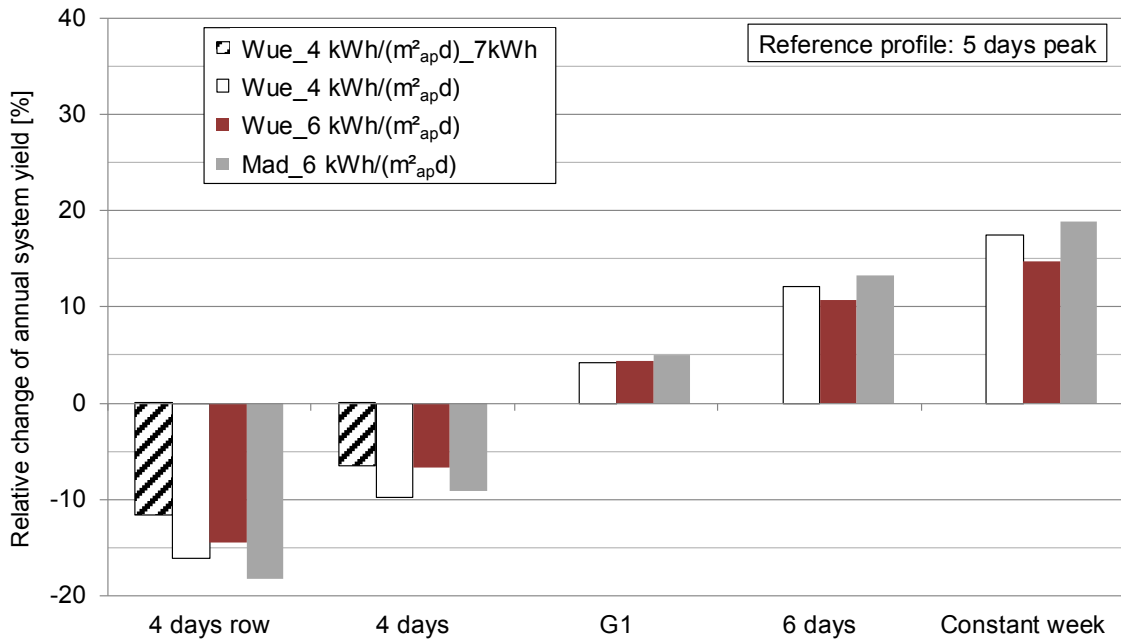


Figure 5-26: Change of annual system yield for different weekly load profiles, different available loads, process temperatures 15..60 °C, specific heat store capacity of 5 kWh/m²_{ap}, FPC_advanced and locations Wuerzburg and Madrid, for profiles with only 4 days of heat demand a fourth bar with specific heat store capacity of 7 kWh/m²_{ap} is shown, “G1” is a weekly profile with full heat demand on 5 days and little demand on weekends; for process temperatures 40..70 °C and ETC see Annex E.

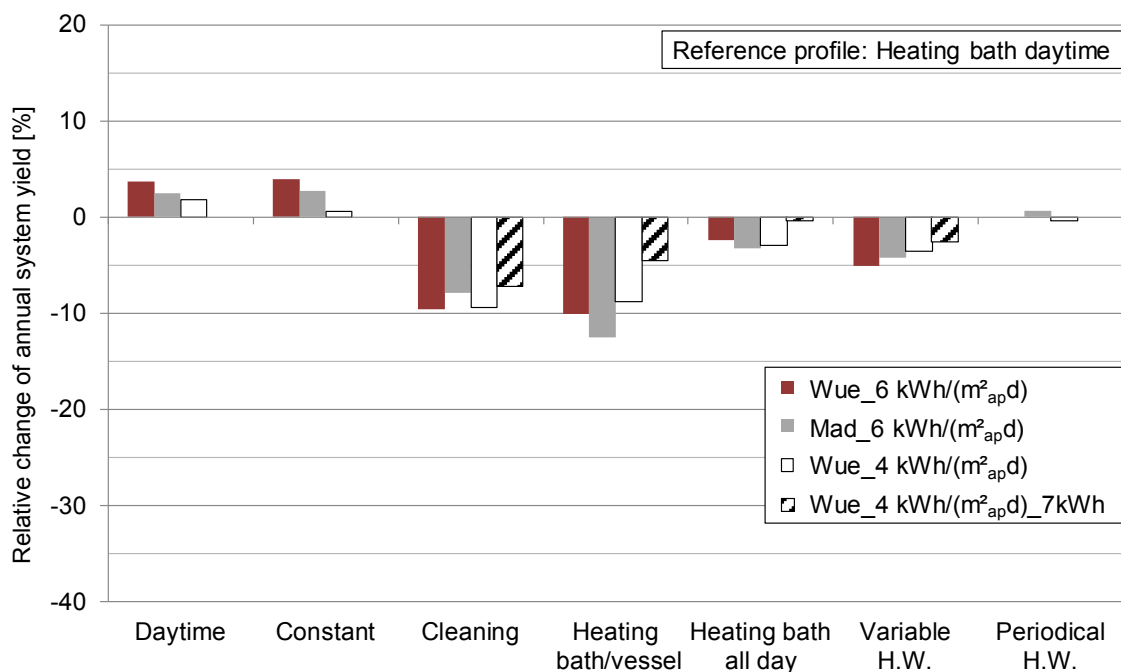


Figure 5-27: Change of annual system yield for different daily load profiles, different available loads, process temperatures 15..60 °C, constant weekly and annual profile, FPC_advanced, specific heat store capacity of 5 kWh/m²_{ap}, for profiles with peaks a fourth bar with specific heat store capacity of 7 kWh/m²_{ap} is shown, locations Wuerzburg and Madrid.

As the figure shows, the influence of the daily load profile on the annual system yield is much lower than for the annual and weekly load profiles. The yield is slightly increased for a heat demand almost exclusively during daylight hours (Daytime) and nearly constant profile (Constant). Profiles with major peaks (Cleaning, Heating bath, Heating bath all day, Variable hot water) reduce the annual system yield. This reduction can of course be mitigated by an increase of the heat store capacity as suggested in Section 5.6. The profile Periodical hot water shows no change of the annual system yield.

5.7.2. Utilization and yield

The annual system yield is the most important value for assessing the economic feasibility of an STS beside the system costs. Estimating this yield is an important step during the preliminary design and feasibility assessment prior to the decision for or against the installation of an STS and a detailed design. The annual system yield is influenced by many factors such as temperature level, load profile, collector, and location.

Figure 5-28 shows the annual utilization ratio (upper figures) and system yield (lower figures) for different locations, process temperatures, and collector types, daily profile Daytime, weekly profile Constant week and annual profile Constant. As shown in the figure, the utilization ratio differs only in the range of six percentage points for 15..60 °C and nine percentage points for 60..90 °C for the different location. Further, the figure shows that the annual system yield (lower figure) differs much stronger due to the different annual irradiation of the locations. Therefore, it seems reasonable to provide utilization ratios for different process temperatures, collector types, profiles and locations for practical use. These can be found in Annex E.

The system yield for various locations can be estimated by using the utilization ratio for one of the four considered locations with a similar climate or by estimating a utilization ratio for a location which is located between two of the locations used in this thesis. Figure 5-29 shows the annual utilization ratio for different locations, process temperatures and collector types. Detailed values for further locations and other daily as well as weekly load profiles can be found in Annex E. As shown, the utilization ratios for both locations are quite similar whereas the yields differ significantly.

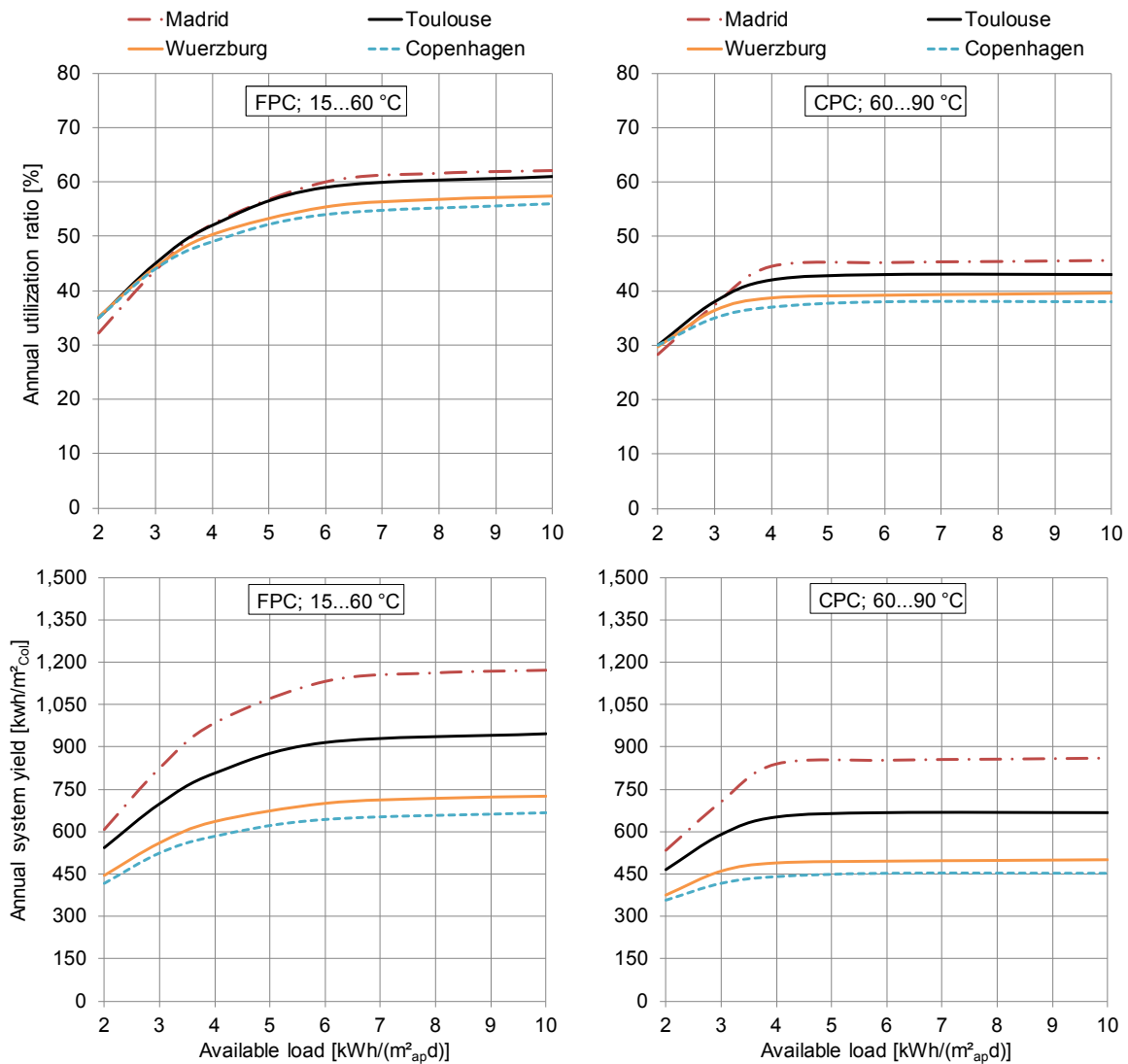


Figure 5-28: Annual utilization ratio (above) and system yield (below) for different locations, process temperatures and collector types, daily profile Daytime, weekly profile Constant week, and annual profile Constant.

In the following, the simulated yields shall be compared to values found in literature to verify the results determined with the simulation model described in Section 5.2. VDI 6002 (2004) shows the annual system utilization ratio for an STS with flat plate collectors and a typical daily load profile of a multi-family house and a constant weekly and annual load. The return/ flow temperatures are 12 and 60 °C. The utilization ratio is about 52 % for an available load of 4 kWh/(m²_{apd}) and 59 % for an available load of 8 kWh/(m²_{apd}). This is in good agreement with the results presented in Figure 5-28 (upper left figure) as the load profiles are very similar and the utilization ratios in (VDI 6002, 2004) are slightly higher due to a lower return temperature.

Hess and Oliva (2011) present the system yield for an application with process temperatures of 15..60°C, a specific heat store volume of 50 l/m², a standard FPC and considering a constant load profile at the location Wuerzburg. The annual system yield for

this application is $700 \text{ kWh}/(\text{m}^2_{\text{ap}}\text{a})$ for an available load of $10 \text{ kWh}/(\text{m}^2_{\text{ap}}\text{d})$ which is very close to the value for Wuerzburg and a FPC in Figure 5-29 (upper left).

Heinzen et al. (2011) performed simulations for a process heat application with a constant load profile, a large available load ($>10 \text{ kWh}/(\text{m}^2_{\text{ap}}\text{d})$) and a return temperature of $26 \text{ }^\circ\text{C}$. The results show an annual system yield of $550 \text{ kWh}/(\text{m}^2_{\text{ap}}\text{a})$ for FPC in central Germany which is similar to the results for $30..80 \text{ }^\circ\text{C}$ in Wuerzburg as shown in Figure 5-29.

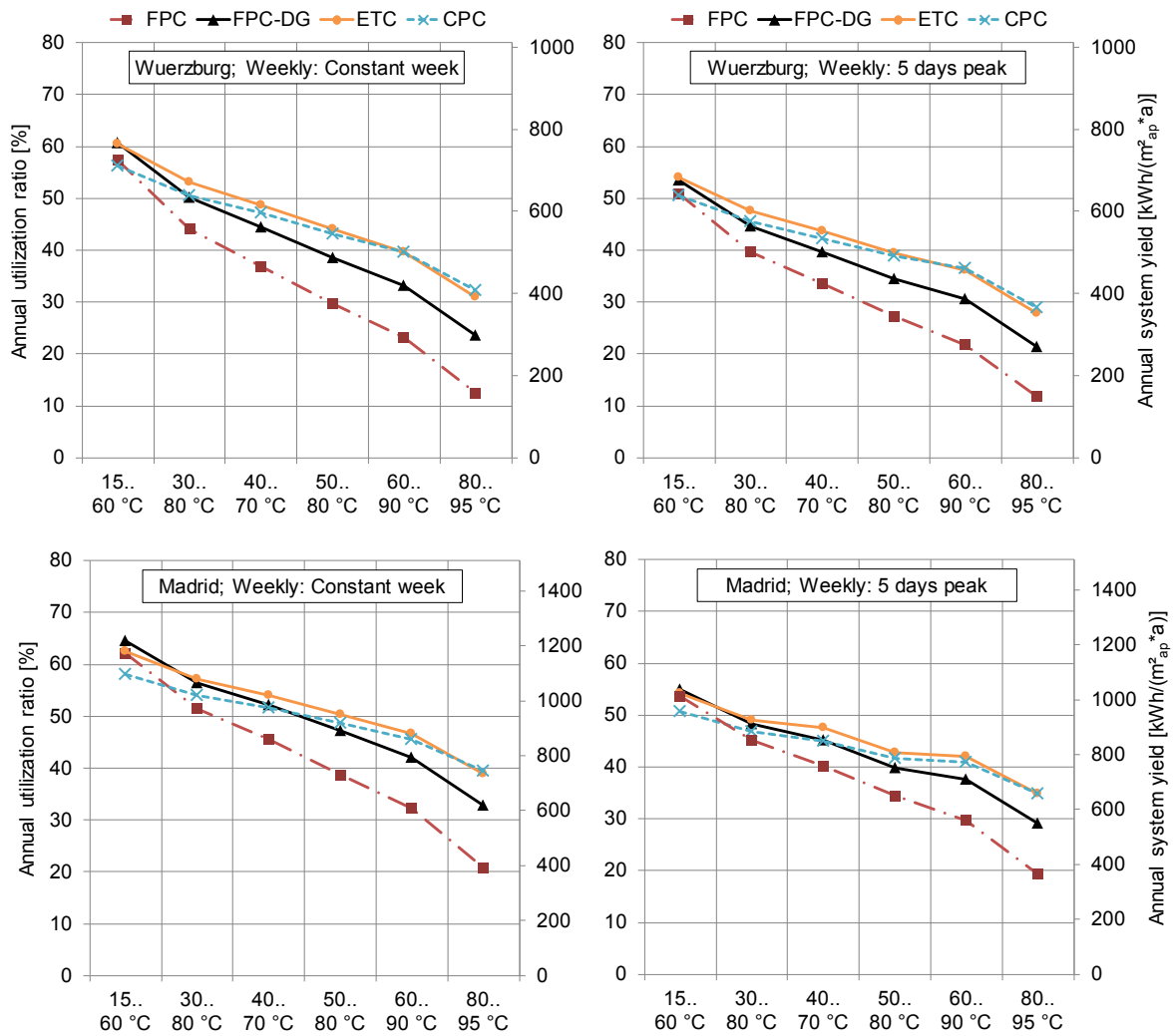


Figure 5-29: Annual utilization ratio for different process temperatures and collector types advanced, $q_{\text{available}} = 10 \text{ kWh}/(\text{m}^2_{\text{ap}}\text{d})$, daily profile Daytime and locations Wuerzburg and Madrid; detailed values for further locations and daily as well as weekly load profiles can be found in Annex E.

O.Ö. Energiesparverband (2011b) mentions an STS heating industrial baths at process temperatures $65..80 \text{ }^\circ\text{C}$ with a CPC Collector without a heat store in central Germany. The annual system yield for this application is $430 \text{ kWh}/(\text{m}^2_{\text{gross}}\text{a})$ or approximately $470 \text{ kWh}/(\text{m}^2_{\text{ap}}\text{a})$. Thus, the value is very close to the result for CPC at $60..90 \text{ }^\circ\text{C}$ in

Wuerzburg shown in Figure 5-29 (upper left). The comparison with literature shows that the results presented in this thesis are in good agreement with selected results of similar studies although the boundary conditions are not completely identical.

5.8. Summary and conclusion

At first, the analysis of industrial processes shows that similar applications for solar process heat exist across several sectors. Therefore, industrial processes can be categorized in typical applications for solar process heat. A simulation model was developed for this configuration using a concept of specific available load to decouple the simulation results from an absolute system size. With this model it was possible to obtain results for dimensioning of collector field and heat store as well as annual utilization ratios for relevant low-temperatures applications.

The results regarding preliminary design of the collector field show that process temperatures, as well as, collector type have the highest influence on the dimensioning. Daily load profile and specific heat store capacity have an influence which is, however, minor compared to the temperature and collector type. The investigation regarding the dimensioning of the heat store shows that the influence of changing the heat store capacity declines with rising temperatures.

Simple design values could be developed for the pre-dimensioning of collector field and rules of thumb for pre-dimensioning of heat store. The results are suitable for preliminary design during a fast feasibility assessment and do not replace detailed dimensioning in a later stage of the system design (most likely by simulations). The obtained values for dimensioning can be used in a step by step procedure. First, one or several solar process heat applications are identified within an industrial company (see Schmitt, 2014). Afterwards, it is necessary to analyze temperature levels and a typical daily heat demand for these applications.

With this data, the collector field can be pre-dimensioned using the values in Figure 5-16 (and Annex C). Especially for higher available temperature differences one should consider to increase the design values shown in Figure 5-16 slightly (e.g. to a minimum of $4 \text{ kWh}/(\text{m}^2_{\text{apd}})$) as this leads to higher utilization ratios.

Next, the heat store can be designed using rules of thumb as described in Section 5.6 and more precisely using the annual utilization ratios provided in Annex D. These annual utilization ratios can be used in an economic analysis to evaluate the additional system yield for an increased store volume. For this evaluation it is necessary to consider costs from heat store manufacturers.

Finally, the results shown in Figure 5-29 and especially the detailed results in Annex E can be used to estimate an annual system yield. The annual system yield can then be used to calculate solar heat generation cost and an internal rate of return or payback time within an economic analysis.

The presented results regarding the influence of the annual load profile show that in a preliminary design phase, the exact determination of a load profile is of minor importance. Load characteristics like summer breaks or months without operation should be easy to obtain from company contacts or production data. The results show that the daily load profile has a much smaller influence on the annual system yield compared to the weekly and annual profile if the approach of an available daily load is followed. This is because the daily profile in this case is only used to distribute a certain available load throughout the day. The amount of load is the same for all daily profiles, whereas the amount of load per week or year varies with a changing weekly or annual profile.

The investigation regarding the influence of load profiles (Figure 5-25, Figure 5-26, and Annex E) can be used to estimate the change of the annual system yield with changing weekly and annual load profile.

6. Summary and conclusion

6.1. Summary and implications of the results

This thesis contributes to the research on potential, system performance and possible fault as well as preliminary design of low-temperature solar process heat systems.

The first main objective of this thesis was to determine the temperature distribution of the industrial heat demand, the potential and suitable industrial sectors and processes for solar process heat in Germany. The second major objective was to identify possible faults of low-temperature solar thermal systems in industry, to quantify their impact on the performance and to identify the most important impact factors on the overall system performance. The third objective was to identify important process heat applications below 100 °C, to develop an approach for pre-dimensioning of STS for such applications, and to determine typical annual system yields of these systems to be considered for an economic feasibility assessment.

Related to the first research objective, the analysis showed that the industrial sector is very promising for the use of solar thermal technology since it accounts for a large share of the total final energy consumption (e.g. 27 % in Germany in 2010) and predominantly uses the consumed energy as thermal energy (74 % in Germany in 2010). The analysis of the temperature distribution of the industrial heat demand showed that the most important temperature ranges for the application of solar process heat in Germany are below 100 °C and between 100 and 200 °C. 21 % of the industrial heat demand is in the temperature range below 100 °C for process heat, space heating and hot water. This is very promising for the application of solar heat as the efficiency of solar thermal systems declines with rising temperatures. An additional 8 % are in the temperature range of 100 to 200 °C. The share of the industrial heat demand in the temperature range of 200 to 300 °C is considerably smaller. The sectors of Chemicals and Food and beverages have by far the highest shares of the heat demand below 300 °C. The majority of the heat demand in Germany is needed at temperatures above 500 °C with a share of 65 %, of which 78 % is used in Basic metals and Non-metallic mineral products.

The theoretical potential of solar heat for industrial processes in Germany was determined by adding the sum of process heat below 300 °C and the demand for space heating and hot water for all industrial sectors, except Basic metals and Non-metallic mineral products. These sectors were not considered as they have by far the highest waste heat potential. This leads to a theoretical potential of 134 TWh per year. In order to calculate the technical potential, further restrictions were taken into account. As shown in literature (Müller et al.,

2004; Schweiger et al., 2001), the heat demand in many industrial enterprises can easily be reduced by heat recovery measures and heat integration of several processes. Additionally, a lack of available space for installation of solar thermal systems reduces the potential. As in (Müller et al., 2004) it is assumed that a share of 60 % of the theoretical potential cannot be used because of mentioned restrictions. Further, an average solar fraction of 30 % was assumed in this study to determine the technical potential. Applying the figures for efficiency measures, restricted roof area and average solar fraction to the theoretical potential of 134 TWh per year, the technical potential for solar heat in industry in Germany can be estimated at 16 TWh per year or 3.4 % of the total industrial heat demand. The technical potential for Austria (Müller et al., 2004), Italy (Vannoni et al., 2008), the Netherlands (van de Pol et al., 2001), Portugal and Spain (Schweiger et al., 2001) ranges between 3 and 4.5 % of the industrial heat demand in the particular region. The absolute number of 16 TWh per year represents by far the highest potential of solar heat for industrial processes in European countries. Solar thermal collectors with about 25 GW_{th} (35 million m²) would be necessary to develop the technical potential assuming an average annual solar system yield of 450 kWh/(m²a). For the EU25, in total about 110 GW_{th} (155 million m²) would be necessary. This represents a substantial market for solar thermal systems.

Eleven industrial sectors were identified to be most promising for the use of solar heat. These are Chemicals, Food and beverages, Motor vehicles, Paper, Fabricated metal, Machinery and equipment, Rubber and plastic, Electrical equipment, Textiles, Printing, and Wood. Some of the selected sectors certainly offer a wide range of possibilities for the use of solar heat, whereas the restrictions of energy efficiency might reduce the theoretical potential substantially in other sectors. The sectors of Chemicals and Food and beverages have the highest potential for the use of solar heat. In Chemicals, the possibilities for the use of waste heat have to be investigated in more detail since a large amount of heat is consumed at temperatures above 500 °C. Considering its big share of the industrial heat demand at low temperatures, the results of prior studies and the variety of suitable processes, the sector of Food and beverages has the highest short-term potential for the use of solar thermal energy in the industrial sector.

The presented results facilitate the prioritized application of solar thermal energy in industrial sectors and processes for Germany and other countries.

With respect to the second research objective, an example of a low-temperature solar process heat system integrated in the hot water supply of a brewery showed that a high effort may be necessary to integrate solar heat into an industrial process. This is especially the case if heat recovery and energy efficiency measures are considered. The values for charging loop (collector) and system utilization ratio as well as specific collector and system yield show that the system performance is below the expectations as the predicted

utilization ratios are not reached in any month of first monitoring period. Further, the difference between both ratios and thus the losses of piping and heat store are higher than predicted in the design.

The analysis of the STS and its components showed that faults of single components can have a considerable impact on the system performance. In case of the studied system, the malfunction of a heat exchanger and extensive heat losses of the store reduced the system yield. These faults were already described in other publications (Karagiorgas et al., 2001; Kutscher and Davenport, 1980). Further, the performance of the system was reduced by a manual interference in the discharge control, by a minimum discharge temperature and by a reduced load due to wrong operation of heat recovery.

To evaluate the identified faults, a TRNSYS simulation model for a solar process heat system was developed and validated with measurements. The simulated and measured heat quantities for 2011 are in good agreement. The analysis of several faults detected in the system showed that the amount of the available load has the highest impact on the system performance. In case of the studied system, the load was reduced by manual interference in the discharge control, and an unfavorable operation of heat recovery leading to a substantially lower system yield than expected. Further faults which have a considerable impact are a reduced UA-value of the charging heat exchanger due to wrong design or malfunction and increased heat losses of the store. If all faults are corrected, the design values can be reached. Therefore, monitoring and failure detection of solar process heat systems are especially important as many faults can occur and reduce the system yield considerably. Finally, a global and local sensitivity analysis showed that the most important factors for system yield are the choice of a suitable and well-functioning collector and the load (amount, temperature, and profile).

The findings make a contribution to research on the performance of solar process heat systems as until now, no detailed analysis of a realized solar thermal system in industry was available which is based on measurements and simulations with a validated model. Furthermore, the most important impact factors on the performance of such a system are identified and quantified in this thesis.

Related to the third research objective, the analysis of industrial processes showed that similar applications for solar process heat exist across several sectors. Therefore, industrial processes were categorized, which facilitates the identification of typical applications for solar process heat. The three major applications are “heating of fluid streams”, “heating of baths/vessels” and “thermal separation processes”. Further possibilities to integrate solar heat exist in the heat supply level of an industrial company.

For pre-dimensioning of the collector field, an approach of dimensioning for a good summer day (VDI 6002, 2004) was transferred from DHW to process heat applications. Therefore, a value q_{design} in kWh/(m²_{ap}d) which is defined as the specific available load at a daily solar fraction just below 100 % on an average “good” summer day is used as design value for the collector field. This means that one m² of collector aperture area should be installed for the selected q_{design} . This design approach avoids that gained energy exceeds demand on many days and therefore leads to an economical STS. Another advantage of this approach is the comparability of typical summer days for various locations. Further, the daily load profile influences the daily system yield not as strong as the annual load profile influences the annual system yield which is used for dimensioning on an annual basis. Finally, it is much easier to determine a typical daily energy demand in an industrial company than an annual distribution or even detailed load profiles.

The load is the main difference for the design phase of a solar thermal system for process heat generation compared to systems for domestic applications. Both, the temperature of the consumers and the load profile, differ completely compared to DHW or space heating loads. Therefore, the influence of a load profile, process temperature and other boundary conditions e.g. location and collector types on the collector field dimensioning was investigated. The results show that process temperatures as well as collector type have the highest influence on dimensioning. Daily load profile and specific heat store capacity have an influence which is only minor compared to temperature and collector type.

The simulated values for q_{design} , the specific heat demand per m²_{ap} for which the solar fraction on a good summer day is just below 100 %, are in the range of 2.0 and 5.0 kWh/(m²_{ap}d). As expected, q_{design} declines with rising temperatures because system efficiency is worse at higher temperatures. This means that the collector field size is higher with higher temperatures if the approach described above is followed. In general, only minor deviations for q_{design} exist between the selected locations Copenhagen and Wuerzburg and between Toulouse and Madrid.

Simple rules of thumb could be developed for the pre-dimensioning of collector field as well as heat store for a fast feasibility assessment. The investigation regarding dimensioning of heat store shows that the influence of changing heat store capacity declines with rising temperatures.

The presented results regarding the influence of the annual load profile show that in a preliminary design phase, the exact determination of the load profile is not necessary. Load characteristics like summer breaks or months without operation should be easy to obtain from company contacts or production data. The results show that the daily load profile has a much smaller influence on the annual system yield compared to the weekly and annual

profile if the approach of available daily load is followed. This is because the daily profile is in this case only used to distribute a certain available load throughout a day.

6.2. Limitations and suggestions for future research

Further investigation beyond the ones addressed in this thesis is necessary in the field of solar heat for industrial processes.

The analysis of the industrial heat demand in Section 3 is based on limited literature. As the temperature distribution of the industrial heat demand is of high importance not only for application of solar thermal systems but also e.g. CHP and heat pumps, a broad bottom-up analysis of industrial companies in promising sectors could contribute to a target-orientated utilization of renewable heating technologies in industry. However, the analysis shows the importance of process temperatures below 100 °C and between 100 and 200 °C. Future collector developments should focus on cost reduction for standard collectors used below 100 °C and development of cost effective process heat collectors up to 200 °C. Steam production on supply level of an industrial enterprise is a promising application for solar process heat as the effort for integration can be reduced compared to integration on process level. As almost all steam networks are operated at pressures corresponding to temperatures lower than 200 °C, this temperature range should be a major focus for future developments. As a high share of low temperature heat demand is for space heating, the combination of solar thermal systems CHP and heat pumps needs to be investigated. With respect to the determination of the technical potential, an investigation considering sector specific figures for heat recovery potential and lack of roof space could improve the presented results. Further, the heat recovery potential should be determined for each sector depending on temperatures of heat sources and sinks.

The identification of faults in Section 4 is based on one monitored STS, limited literature and system simulations. The experience of a large number of systems is necessary to generalize the results of this study and to provide a broad basis for prevention of faults in solar process heat systems. In order to improve the performance of future systems, additional investigation regarding adapted control strategies is advisable which consider process temperatures, and which are automatically adaptive regarding the load profile and able to consider the weather of coming days to maximize system yield. Finally, research on detailed design of solar process heat systems and their components (e.g. optimal isolation thickness depending on process temperature) is suggested.

Many variables influence the design of solar process heat systems as Section 5 of this thesis indicates. Therefore, an approach for dimensioning without simulations is always limited to certain selected boundary conditions as already shown in existing literature

(Aidonis et al., 2005a; Hess and Oliva, 2011). It would be valuable to develop new or to adapt existing simulation tools based on limited input parameters for important values as e.g. shown in this thesis. Additional investigation is further necessary for other solar process heat applications, not covered in this thesis as well as applications at higher process temperatures on supply level. A methodology for choosing a collector type for a certain temperature is necessary to enable planners and customers to choose the right type for a process heat application. For detailed dimensioning, in contrast to preliminarily design the use of detailed load profiles can be advantageous to modify dimensioning of certain components and to develop a control strategy. The effort to determine such detailed load profiles is often very high and several heat flow measurements may be necessary. In order to assess the necessary accuracy of such profiles, further investigation is necessary.

Finally, comprehensive information on typical system cost should be imposed. This could be utilized to determine typical solar heat generation cost for different process heat applications in combination with typical annual system yields as presented in this thesis. Additionally, cost functions could be used for the design by cost optimization.

Nomenclature

Abbreviations

ALU	Available load utilization
ap	aperture area (of collector)
CHP	Combined heat and power
Const.	Constant
CPC	Compound parabolic concentrator
Dayt.	Daytime
DHW	Domestic hot water
ETC	Evacuated tube collector
FPC	Flat plate collector
H.B.	Heating bath/vessel
HW	Hot water
IAM	Incident angle modifier
IEA	International Energy Agency
NACE	Statistical classification of economic activities
SH	Space heating
SHC	Solar heating and cooling programme
SHIP	Solar heat for industrial processes
STS	Solar thermal system
TRNSYS	Transient system simulation program
VDEW	Verband der Elektrizitätswirtschaft e.V. (German association of electricity industries)

Symbols

a_1	First order heat loss coefficient	$W/(m^2K)$
a_2	Second order heat loss coefficient	$W/(m^2K^2)$
b_0	Constant for calculation of IAM	-
c_p	Specific heat capacity	$kJ/(kgK)$
d_i	Inner diameter	m
d_{out}	Outer diameter	m

η_0	Zero loss coefficient	-
$\bar{\eta}_{\text{charge}}$	Charging loop utilization ratio	%
$\bar{\eta}_{\text{sys}}$	System utilization ratio	%
$\bar{\eta}_{\text{sys_day_avg}}$	Utilization ratio on an average “good” summer day	%
$f_{\text{sol_day_avg}}$	Solar fraction on an average “good” summer day	%
Gt	Irradiance on a tilted plane	W/m ²
H.B.	Heating bath	-
Ht	Total irradiation on collector field (aperture)	kWh
$H_{\text{t_day_avg}}$	Specific average daily irradiation for “good” summer days	kWh/(m ² _{ap} d)
$m_{\text{available}}$	Available mass per day	kg/d
\dot{m}_{charge}	Charging loop specific mass flow	kg/h
\dot{m}_{solar}	Solar loop specific mass flow	kg/h
NC_Charge	Night cooling charging loop	kWh
NC_Discharge	Night cooling discharging loop	kWh
Q_Charge	Heat quantity charging the store	kWh
$q_{\text{available}}$	Specific available load	kWh/(m ² _{ap} d)
q_{charge}	Specific collector yield	kWh/m ² _{ap}
q_{design}	available load at a daily solar fraction just below 100 % on an average “good” summer day	kWh/(m ² _{ap} d)
Q_Discharge	Heat quantity discharging the store	kWh
$q_{\text{discharge}}$	System yield	kWh/m ²
$Q_{\text{process. day}}$	Daily total process heat demand	kWh/d
$q_{\text{sol_day_avg}}$	Specific system yield on an average “good” summer day	kWh/(m ² _{ap} d)
q_{store}	Specific heat store capacity	kWh/m ² _{ap}
ρ_{Water}	Density of water	kg/m ³
T _{0.9}	Store temperature at 90 % of store height	°C
T _{0.9_max}	Maximum heat store temperature	°C
T _a	Ambient temperature	°C
T _{BWF}	Brewing water loop flow temperature	°C
T _{BWR}	Brewing water return flow temperature	°C
T _{CF}	Charging loop flow temperature	°C
T _{col}	Collector temperature	°C
T _{CR}	Charging loop return temperature	°C

T_{DCF}	Discharging loop flow temperature	$^{\circ}\text{C}$
T_{DCR}	Discharging loop return temperature	$^{\circ}\text{C}$
T_m	Average temperature of solar loop	$^{\circ}\text{C}$
$T_{\text{process_flow_max}}$	Maximum process flow temperature	$^{\circ}\text{C}$
$T_{\text{process_return}}$	Process return temperature	$^{\circ}\text{C}$
T_{SF}	Solar flow temperature	$^{\circ}\text{C}$
T_{SR}	Solar return temperature	$^{\circ}\text{C}$
ua	Specific heat transfer capacity rate (per m^2 of aperture area)	$\text{W}/(\text{m}^2_{\text{ap}}\text{K})$
UA-value	Heat transfer capacity rate	W/K
U-value	Heat loss coefficient	$\text{W}/(\text{m}^2\text{K})$
\dot{V}_{BW}	Brewing water volume flow	m^3/h
\dot{V}_C	Charging loop volume flow	m^3/h
\dot{V}_{DC}	Discharging loop volume flow	m^3/h
\dot{V}_S	Solar loop volume flow	m^3/h
V_{store}	Heat store volume	m^3
v_{store}	Specific heat store volume	$\text{l}/\text{m}^2_{\text{ap}}$
V_{VVT}	Volume variable volume tank	m^3

References

- Aidonis, A., Drosou, V., Mueller, T., Staudacher, L., Fernandez-Llebrez, F., Oikonomou, A., Spencer, S., 2004.** *PROCESOL II – Phase 4 Part I (CRES)*. Interim Report, Pikermi, Greece.
- Aidonis, A., Drosou, V., Mueller, T., Staudacher, L., Fernandez-Llebrez, F., Oikonomou, A., Spencer, S., 2005b.** *PROCESOL II - Solar thermal plants in industrial processes: Design and Maintenance Guidelines*. Center for Renewable Energy Sources, Pikermi, Greece.
- Aidonis, A., Drosou, V., Mueller, T., Staudacher, L., Fernandez-Llebrez, F., Oikonomou, A., Spencer, S., 2005a.** *PROCESOL II – Solarthermische Anlagen in Industriebetrieben*. Planungs- und Wartungsrichtlinien, Pikermi, Greece.
- Anthrakidis, A., Faber, C., Kroker, J., Lanz, M., Backes, K., Adam, M., Dreher, M., Schramm, S., 2010.** *Solare-Prozesswärme-Standards*. Proceedings 20. Symposium thermische Solarenergie, Bad Staffelstein, Germany.
- Anthrakidis, A., Faber, C., Lanz, M., Adam, M., Schramm, S., Wirth, H.-P., 2013.** *Monitoring und Analyse solarer Prozesswärmeanlagen*. Proceedings 23. Symposium thermische Solarenergie, Bad Staffelstein, Germany.
- Aquametro AG, 2012.** *TOPAS PMW-basic: Hot water meter*. <http://www.aquametro.com/> accessed on 04.12.2012.
- Arbeitsgemeinschaft Fernwärme e.V., 2000.** *Pluralistische Wärmeversorgung—Zeithorizont 2005*, Frankfurt am Main, Germany.
- Austrian Institute of Technology, 2011.** *Summary of EN12975 Test Results: Registration No. 011-7S839F*. Annex to Solar Keymark Certificate, Vienna.
- Bastian, O., 2012.** *Steigerung der Wandlungs- und Energieeffizienz durch Kopplung von Biomassekonversionsverfahren und modulierend betriebene Biogasproduktion mit dezentraler Energiebereitstellung*. Dissertation, Kassel University Press, Kassel. ISBN 9783862193349.
- Benz, N., Gut, M., Ruß, W., 1998.** *Solar process heat in breweries and dairies*. Proceedings of the Second International ISES Europe Solar Congress, Portoroz, Slovenia.
- Bokhoven, T.P., van Dam, J., Kratz, P., 2001.** *Recent experience with large solar thermal systems in The Netherlands*. *Solar Energy* 71, 347–352.
- Brown, K.C., 1983.** *Reexamining the Prospects for Solar Industrial Process Heat*. *Annual Review of Energy* 8, 509–530.
- Bundesministerium für Wirtschaft und Technologie (BMWi), 2010.** *Energiedaten - Nationale und Internationale Entwicklung*, Berlin.
- Collares-Pereira, M., Gordon, J., Zarmi, Y., 1984.** *Design and optimization of solar industrial hot water systems with storage*. *Solar Energy* 32, 121–133.
- Croy, R., Mies, M., Rehrmann, U., Wirth, H.P., 2011.** *Solarthermie-2000, Teilprogramm 2 und Solarthermie2000plus: Wissenschaftlich-technische Programmbegleitung und Messprogramm (Phase 4)*. Teil 2: Systemtechnik und Planungshinweise. ZfS –Rationelle Energietechnik GmbH, Hilden, Germany.

- Croy, R., Wirth, H.P.**, 2006. *Analyse und Evaluierung großer Kombianlagen zur Trinkwassererwärmung und Raumheizung - Abschlussbericht zum BMU-Vorhaben 0329268B*. ZfS – Rationelle Energietechnik GmbH, Hilden, Germany.
- de Keizer, C.**, 2012. *Simulation-based long-term fault detection of solar thermal systems*. Dissertation, Kassel University Press, Kassel. ISBN 9783862194001.
- Deutsches Institut für Normung e. V.**, 2009. *DIN EN 60751:2009-05: Industrial platinum resistance thermometers and platinum temperature sensors*. German version. Deutsches Institut für Normung e. V., Berlin.
- Dr. Valentin EnergieSoftware GmbH**, 2013. *T*SOL*. <http://www.valentin.de/>.
- Drück, H.**, 2006. *MULTIPORT Store - Model for TRNSYS, Type 340 version 1.99F*. Institut für Thermodynamik und Wärmetechnik - Universität Stuttgart, Stuttgart, Germany.
- Drück, H., Schenke, A.**, 2007. *Systemuntersuchung großer solarthermischer Kombianlagen - Analyse und Evaluierung großer Kombianlagen zur Trinkwassererwärmung und Raumheizung*. Abschlussbericht zum BMU-Vorhaben Förderkennzeichen 0329268B - Bericht Teil 1. SWT Stuttgart, Stuttgart, Germany.
- Eikmeier, B., Gabriel, J., Schulz, W., Krewitt, W., Nast, M.**, 2005. *Analyse des nationalen Potenzials für den Einsatz hocheffizienter KWK einschließlich hocheffizienter Kleinst-KWK unter Berücksichtigung der sich aus der EU-KWK-RL ergebenden Aspekte*. Endbericht zum Forschungsvorhaben Projekt I A 2 – 37/05 des Bundesministeriums für Wirtschaft und Arbeit. bremer energie institut; DLR, Institut für Technische Thermodynamik, Abteilung Systemanalyse und Technikbewertung, Bremen, Germany.
- Eisenmann, W., Hess, S., Klemke, M., Kramp, G.**, 2011. *Entwicklung eines leistungsgesteigerten Flachkollektors mit Reflektoren für die Gewinnung von Prozesswärme bis 150 °C*. Final project report - Förderkennzeichen BMU 0329 280 C. Wagner & Co Solartechnik; Fraunhofer ISE, TIB Hannover, Germany.
- Energiesparverband O.Ö.**, 2011a. *Solar Process Heat-status reports on the regional pilot projects*. Intelligent Energy Europe Project, Linz, Austria.
- Eskin, N.**, 2000. *Performance analysis of a solar process heat system*. Energy Conversion and Management 41, 1141–1154.
- ESTIF**, 2013. *Solar Keymark Database*. <http://solarkey.dk/solarkeymarkdata>
- Eurostat**, accessed 2011. *Structural business statistics*.
- Forschungsstelle für Energiewirtschaft e.V.**, 1999. *Ermittlung von Energiekennzahlen für Anlagen, Herstellungsverfahren und Erzeugnisse*, München, Germany.
- German Federal Statistical Office (Destatis)**, 2009. *Erhebung über die Energieverwendung für 2006*, Wiesbaden, Germany.
- German Federal Statistical Office (Destatis)**, received 2011. *Unternehmen mit sozialversicherungspflichtig Beschäftigten (enterprises and employees with social insurance contribution) for 2009, private communication*, Wiesbaden, Germany.
- Gordon, J., Rabl, A.**, 1982. *Design, analysis and optimization of solar industrial process heat plants without storage*. Solar Energy, 519–530.
- Haller, M., Paavilainen, J., Dalibard, A., Perers, B.**, 2009. *TRNSYS Type 832 v3.07 Dynamic Collector Model by Bengt Perers. Updated Input-Output Reference*.

- Heimrath, R.**, 2004. *Simulation, optimization and comparison of solar assisted heating systems for the space heating of multi-family houses*. Dissertation. Graz University of Technology, Graz, Austria.
- Heimrath, R., Haller, M.**, 2007. *The Reference Heating System, the Template Solar System. A technical report of Subtask A. A Report of IEA-SHC Task 32*. Institute of Thermal Engineering, Division Solar Energy and Thermal Building Simulation, Graz University of Technology, Graz, Austria.
- Heinzen, R., Zaß, K., Luhmer, R., Meyer, R., Vajen, K.**, 2011. *Integration of Solar Thermal Systems into Gas Pressure Regulating Stations*. Proceedings ISES Solar World Congress Kassel, Germany.
- Henning, H.-M.**, op. 2004. *Solar-assisted air-conditioning in buildings*. A handbook for planners, Springer, Vienna [etc.], Austria. ISBN 3211006478.
- Hess, S., Oliva, A.**, 2011. *Solar process heat generation: Guide to solar thermal design for selected industrial processes*, Freiburg, Germany.
- Hofer, R.**, 1994. *Analyse der Potentiale industrieller Kraft-Wärme-Kopplung*, Ph.D. Thesis. 1., Resch Media Mail Verlag, Gräfeling, Germany. ISBN 3878061498.
- Institut für Solarenergieforschung Hameln (ISFH)**, 2008. *Summary of EN12975 Test Results: Registration No. 011-7S556 R*. Annex to Solar Keymark Certificate, Hameln, Germany.
- Institut für Solarenergieforschung Hameln (ISFH)**, 2012. *Summary of EN12975 Test Results: Registration No. 011-7S1750F*. Annex to Solar Keymark Certificate, Hameln, Germany.
- Institut für Thermodynamik und Wärmetechnik (ITW)**, 2009. *Summary of EN12975 Test Results: Registration No. 011-7S659 F*. Annex to Solar Keymark Certificate. University of Stuttgart, Stuttgart, Germany.
- Institut für Thermodynamik und Wärmetechnik (ITW)**, 2011. *Summary of EN12975 Test Results: Registration No. 011-7S1501 R*. Annex to Solar Keymark Certificate. University of Stuttgart, Stuttgart, Germany.
- Institut für Thermodynamik und Wärmetechnik (ITW)**, 2012a. *Summary of EN12975 Test Results: Registration No. 011-7S089 R*. Annex to Solar Keymark Certificate. University of Stuttgart, Stuttgart, Germany.
- Institut für Thermodynamik und Wärmetechnik (ITW)**, 2012b. *Summary of EN12975 Test Results: Registration No. 011-7S1890F*. Annex to Solar Keymark Certificate. University of Stuttgart, Stuttgart, Germany.
- Institut für Thermodynamik und Wärmetechnik (ITW)**, 2012c. *Summary of EN12975 Test Results: Registration No. 011-7S2031 R*. Annex to Solar Keymark Certificate. University of Stuttgart, Stuttgart, Germany.
- Institut für Thermodynamik und Wärmetechnik (ITW)**, 2012d. *Summary of EN12975 Test Results: Registration No. 011-7S212 R*. Annex to Solar Keymark Certificate. University of Stuttgart, Stuttgart, Germany.
- Institute for Solar Technology (SPF)**, 2011. *Summary of EN12975 Test Results: Registration No. 011-7S1804 R*. Annex to Solar Keymark Certificate, Rapperswil, Switzerland.
- International Energy Agency**, accessed 2011. *Energy Balance of OECD and non-OECD countries*, Paris.

- Kalab, O.** *Standardisierte Lastprofile*. without year. Wirtschaftskammer Oberösterreich (WKO), Linz, Austria.
- Kalogirou, S.**, 2003. *The potential of solar industrial process heat applications*. Applied Energy, S. 337–361.
- Karagiorgas, M., Botzios, A., Tsoutsos, T.**, 2001. *Industrial solar thermal applications in Greece - Economic evaluation, quality requirements and case studies*. Renewable and Sustainable Energy Reviews, 157–173.
- Kipp & Zonen**, 2011. *Pyranometers: For the accurate measurement of solar irradiance*, Delft, Netherlands.
- Klein, S., Beckman, W., Mitchell, J., Duffie, J., Duffie, N.**, 2009. *TRNSYS 17: A Transient System Simulation program*. Solar Energy Laboratory, University of Wisconsin, Madison, USA.
- Kovacs, P., Quicklun, H., Pettersson, U.**, 2003. *Solenergi i industriell processvärme - En förstudie av svenska möjligheter*. SP Rapport 2003. SP Technical Research Institute of Sweden, Borås, Sweden.
- Kulkarni, G., Kedare, S., Bandyopadhyay, S.**, 2008. *Design of solar thermal systems utilizing pressurized hot water storage for industrial applications*. Solar Energy, 686–699.
- Kusyy, O., Vajen, K., Jordan, U.**, 2008. *Application of Sensitivity Analysis to Parameters of Large Solar Water Heating Systems*. Proceedings Eurosun Graz, Austria.
- Kutscher, C., Davenport, R., Dougherty, D., Gee, R., Masterson, P., May, E.**, 1982. *Design Approaches for Solar Industrial Process Heat Systems*, Golden, USA.
- Kutscher, C.F., Davenport, R.L.**, 1980. *Preliminary operational results of the low-temperature solar industrial process heat field tests*, Golden, USA.
- Lambauer, J., Fahl, U., Ohl, M., Blesl, M., Voß, A.**, 2008. *Industrielle Großwärmepumpen - Potenziale, Hemmnisse und Best-Practice Beispiele*. Forschungsbericht. Institut für Energiewirtschaft und Rationelle Energieanwendung, Universität Stuttgart, Germany.
- Lauterbach, C., Schmitt, B., Vajen, K., Jordan, U.**, 2010. *Potential for solar process heat in Germany - Suitable Industrial sectors and processes*. Proceedings Eurosun Graz, Austria.
- Lauterbach, C., Javid Rad, S., Schmitt, B., Vajen, K.**, 2011a. *Feasibility assessment of solar process heat applications*. Proceedings ISES Solar World Congress Kassel, Germany.
- Lauterbach, C., Schmitt, B., Jordan, U., Vajen, K.**, 2011b. *Solare Prozesswärme in Deutschland - Potential und Markterschließung*. 21. Symposium Thermische Solarenergie, Bad Staffelstein, Germany.
- Lauterbach, C., Schmitt, B., Vajen, K.**, 2011c. *Das Potential solarer Prozesswärme in Deutschland*. Teil 1 des Abschlussberichtes zum Forschungsvorhaben "SOPREN - Solare Prozesswärme und Energieeffizienz". University of Kassel, Germany.
- Lauterbach, C., Schmitt, B., Jordan, U., Vajen, K.**, 2012a. *The potential of solar heat for industrial processes in Germany*. Renewable and Sustainable Energy Reviews 16, 5121–5130.

- Lauterbach, C., Schmitt, B., Vajen, K.,** 2012b. *Pilotanlage zur Bereitstellung solarer Prozesswärme bei der Hütt-Brauerei*, Proceedings of Gleisdorf Solar 2012, Gleisdorf, Österreich.
- Lauterbach, C., Schmitt, B., Vajen, K.,** 2014. *System analysis of a low-temperature solar process heat system*. Solar Energy 101, 117–130.
- McLeod, V., Annas, J., Stein, W., Hinkley, J.,** 2005. *Application of solar process heat to the commercial & industrial sectors*. Energetics Pty Ltd, Sydney.
- Meteotest,** 2009. *METEONORM Version 6.1.0.15*. <http://www.meteotest.ch>
- Mies, M., Rehrmann, U., Szablinski, D.,** 2006. *Abschlussbericht für das Projekt Neubaugebiet "Badener Hof" Heilbronn*. ZfS – Rationelle Energietechnik GmbH, Hilden, Germany.
- Müller, H., Zörner, W.,** 2013. *Potentiale solar-thermischer Anwendungen in der bayrischen Lebensmittelindustrie*. Proceedings OTTI Staffelstein, Germany.
- Müller, H., Zörner, W., Hanby, V.,** 2011. *Solar-thermal process heat - a low-temperature heating network in a dairy*. Proceedings ISES Solar World Congress Kassel, Germany.
- Müller, T., Weiß, W., Schnitzer, H., Brunner, C., Begander, U., Themel, O.,** 2004. *PROMISE - Produzieren mit Sonnenenergie*. Potenzialstudie zur thermischen Solarenergienutzung in österreichischen Gewerbe- und Industriebetrieben. Arbeitsgemeinschaft Erneuerbare Energien – Institut für Nachhaltige Technologien, Vienna.
- Nagaraju, J., Garud, S., Ashok Kumar, K., Ramakrishna Rao, M.,** 1999. *1 MW Industrial solar hot water system and its performance*. Solar Energy 66, 491–497.
- Nitsch, J., Pregger, T., Scholz, Y., Naegler, T., Sterner, M., Gerhardt, N., von Oehsen, A., Pape, C., Saint-Drenan, Y.-M., Wenzel, B.,** 2010. *Langfristszenarien und Strategien für den Ausbau der erneuerbaren Energien in Deutschland bei Berücksichtigung der Entwicklung in Europa und global – „Leitstudie 2010“*. im Auftrag des BMU. Deutsches Zentrum für Luft- und Raumfahrt; Fraunhofer Institut für Windenergie und Energiesystemtechnik-; Ingenieurbüro für neue Energien, Stuttgart, Kassel, Teltow, Germany.
- O.Ö. Energiesparverband,** 2011b. *WP5 – Second status reports on the regional pilot projects*, Linz, Austria.
- Peuser, F.A., Remmers, K.-H., Schnauss, M.,** 2001. *Langzeiterfahrung Solarthermie*. Wegweiser für das erfolgreiche Planen und Bauen von Solaranlagen, Solarpraxis, Berlin. ISBN 3934595073.
- Puente Salve, F.,** 2011. *WP2- Priority applications selection summary*. Project report. Downloaded from www.solar-process-heat.eu.
- Saltelli, A.,** 2004. *Sensitivity analysis in practice*. A guide to assessing scientific models, Wiley, Chichester, United Kingdom. ISBN 0470870931.
- Schmitt, B.,** 2014. *Integration thermischer Solaranlagen zur Bereitstellung von Prozesswärme in Industriebetrieben*. Dissertation, Shaker Verlag, Aachen, Germany.
- Schmitt, B., Lauterbach, C., Dittmar, M., Vajen, K.,** 2012a. *Guideline for the utilization of solar heat in breweries*. Proceedings Eurosun Rijeka, Croatia.

- Schmitt, B., Lauterbach, C., Jordan, U., Vajen, K.**, 2010. *Sustainable Beer Production by Combining Solar Process Heat and Energy Efficiency - Holistic System Concept and Preliminary Operational Experiences*. Proceedings Eurosun Graz, Austria.
- Schmitt, B., Lauterbach, C., Vajen, K.**, 2011. *Investigation of selected solar process heat applications regarding their technical requirements for system integration*. Proceedings ISES Solar World Congress Kassel, Germany.
- Schmitt, B., Lauterbach, C., Vajen, K., Reinl, K.-P.**, 2012b. *Pilotanlage zur Bereitstellung solarer Prozesswärme bei der Hütt-Brauerei*. Abschlussberichtes zum Forschungsvorhaben „Thermische Solaranlage zur Prozesswärmebereitstellung in Verbindung mit der Implementierung eines neuen, energieeffizienten Kochverfahrens“, FKZ 0329609E. University of Kassel, Germany.
- Schnitzer, H., Brunner, C., Taferner, K., Slawitsch, B., Giannakopoulou, K.**, 2006. *Solare Prozesswärme - Österreichische Beteiligungen an der Task 33 des IEA Solar Heating and Cooling Programms*, Graz, Austria.
- Schweiger, H., Mendes, J., Benz, N., Hennecke, K., Prieto, G., Cusi, M., Goncalves, H.**, 2000. *The potential of solar heat in industrial processes. A state of the art review for Spain and Portugal*. Proceedings Eurosun Copenhagen, Denmark.
- Schweiger, H., Mendes, J., Schwenk, C., Hennecke, K., Barquero, C., Sarvisé, A., Carvalho, M.**, 2001. *POSHIP - The Potential of Solar Heat for Industrial Processes*, Barcelona, Spain.
- SP Technical Research Institute of Sweden**, 2009. *Test of solar collector according to EN 12975-2:2006: Sunmark GJ 140D-001.5*, Borås, Sweden.
- Taibi, E., Gielen, D., Bazilian, M.**, 2012. *The potential for renewable energy in industrial applications*. Renewable and Sustainable Energy Reviews 16, 735–744.
- Taylor, J.R.**, 1997. *An Introduction to error analysis. The study of uncertainties in physical measurements*. 2, University Science Books, Sausalito, California, USA. ISBN 0935702423.
- TESS**, 2009. *TESS Component Libraries*. Thermal Energy System Specialists (TESS), Madison, USA.
- TÜV Rheinland - Energie und Umwelt GmbH**, 2011. *Summary of EN12975 Test Results: Registration No. 011-7S1520F*. Annex to Solar Keymark Certificate, Köln, Germany.
- TÜV Rheinland - Energie und Umwelt GmbH**, 2012. *Summary of EN12975 Test Results: Registration No. 011-7S1912F*. Annex to Solar Keymark Certificate, Köln, Germany.
- van de Pol, V., Wattimena, L.**, 2001. *Onderzoek naar het potentieel van zonthermische energie in de industrie*. KWA Bedrijfsadviseurs B.V.
- Vannoni, C., Battisti, R., Drigo, S.**, 2006. *SHIP – Plant Survey Report*. IEA SHC Task 33/IV. CIEMAT, Madrid, Spain.
- Vannoni, C., Battisti, R., Drigo, S.**, 2008. *Potential for Solar Heat in Industrial Processes*. Report within IEA SHC Task 33/IV. Department of Mechanics and Aeronautics - University of Rome “La Sapienza”, Rome, Italy.
- Vannoni, C., Battisti, R., Drigo, S., Corrado, A.**, 2006. *SHIP Potential Studies Report*. Report within IEA SHC Task 33/IV. Department of Mechanics and Aeronautics - University of Rome “La Sapienza”.

- Verband der Chemischen Industrie e.V. (VCI)**, 2009. *Chemiewirtschaft in Zahlen 2009*, Frankfurt am Main, Germany.
- Verein Deutscher Ingenieure**, 2004. *VDI 6002 Blatt 1: Solar heating for potable water - General principles - System technology and application in residential buildings*. Verein Deutsche Ingenieure, Berlin, Germany.
- Vogt, M., Blum, O., Hutter, A., Jung, H., Meyer, B., Kirschbaum, S., Schubert, A., Meyer, J.**, 2008. *Branchenleitfaden für die Papierindustrie*. Arbeitsgemeinschaft Branchenenergiekonzept Papier.
- Werner, S.**, 2006. *ECOHEATCOOL - workpackage 1. The European Heat Market*. Final Report IEE ALTENER Project. Euroheat&Power, Belgium.
- Westnetz GmbH**, 2013. *Standard-Lastprofile zur Belieferung von Letztverbrauchern*. <http://www.westnetz.de/web/cms/de/1772992/westnetz/netzstrom/netznutzung/lastprofile/standard-lastprofile-nach-vdew/>.
- Wirtschaftskammer Oberösterreich (WKO)**, 2003. *Energiekennzahlen und Energiesparpotentiale in der metallverarbeitenden Industrie*, Linz, Austria.
- Wutzler, M., Schirmer, U., Platzer, B.**, 2011. *Solar process heat application at the Hofmuehl brewery at Eichstaett/Germany*. Proceedings ISES Solar World Congress Kassel, Germany.

List of figures

Figure 3-1: Final energy consumption in Germany and distribution within industry in 2007.....	16
Figure 3-2: Breakdown of the industrial process heat demand between 100 and 500 °C.....	19
Figure 3-3: Technical potential of solar heat for industrial processes in European countries.	23
Figure 3-4: Heat demand below 300 °C of all and the selected promising sectors.....	24
Figure 3-5: Technical potential of the eleven selected sectors divided in temperature ranges.	28
Figure 3-6: Promising processes for the integration of solar heat.....	29
Figure 4-1: Initial state of the hot water supply of the brewhouse.....	32
Figure 4-2: Improved hot water supply of the brewhouse with integrated STS.	33
Figure 4-3: Hydraulic scheme of the STS with monitoring sensors	34
Figure 4-4: Irradiation on collector plane, specific collector and system yield.	37
Figure 4-5: Filling level of the variable volume tank and volume flows.	38
Figure 4-6: Efficiency of the collector field for selected stationary operating points.....	40
Figure 4-7: Temperatures within store, discharge return, and room temperature, volume flows ...	41
Figure 4-8: Monthly measured and simulated heat quantities for 2011.....	45
Figure 4-9: Simulated heat quantities for different faults.	46
Figure 4-10: Ranking of parameters by the Morris method.....	49
Figure 4-11: Results of local sensitivity analysis.....	52
Figure 5-1: Distinction between supply and process level and Integration on supply level.	56
Figure 5-2: Integration on process level.....	57
Figure 5-3: Heating cold water with plate heat exchanger and heating of bottle washing machine	59
Figure 5-4: System configuration for “heating of a fluid stream”/“heating of a bath/ vessel”	60
Figure 5-5: Average monthly irradiation and average monthly ambient air temperatures	62
Figure 5-6: Overview of the selected daily load profiles; values can be found in Annex A.....	64
Figure 5-7: Overview of weekly load profiles; values can be found in Annex A.....	65
Figure 5-8: Overview of different annual load profiles considered for the simulations.	66
Figure 5-9: Utilization ratio for good summer days and annual utilization ratio.....	68
Figure 5-10: Temperature levels of processes supplied by existing STS and promising applicat. .	70
Figure 5-11: Utilization ratio for good summer days for different flow and return temperatures ..	71
Figure 5-12: Efficiency curves for advanced collectors based on aperture area.....	73
Figure 5-13: Utilization ratio for good summer days for different collector types.....	73
Figure 5-14: Annual utilization ratio for different weekly profiles.....	77
Figure 5-15: Utilization ratio for good summer days for different storage volumes.	78
Figure 5-16: Simulated design values of q_{design}	80
Figure 5-17: Annual utilization ratio for different temperatures.....	81
Figure 5-18: Annual utilization ratio for different temperatures with high difference.	82
Figure 5-19: Annual utilization ratio for different temperatures and profiles.....	83
Figure 5-20: Change of annual system yield for different specific heat store capacities.....	85
Figure 5-21: Change of annual system yield for different temperatures/ heat store capacities.....	87
Figure 5-22: Annual utilization ratio for different specific heat store capacities; 15..60 °C	88
Figure 5-23: Annual utilization ratio for different specific heat store capacities; 60..90 °C,	89

Figure 5-24: Change of annual system yield for different annual load profiles.....	91
Figure 5-25: Annual utilization ratio for different annual load profiles.....	92
Figure 5-26: Change of annual system yield for different weekly load profiles.....	93
Figure 5-27: Change of annual system yield for different daily load profiles.....	93
Figure 5-28: Annual utilization ratio and system yield.....	95
Figure 5-29: Annual utilization ratio for different process temperatures and collector types.....	96
Figure A-1: Change of annual system yield for different annual load profiles; 40..70 °C.....	125
Figure A-2: Change of annual system yield for different weekly load profiles; 40..70 °C.....	125

List of tables

Table 3-1: Breakdown of industrial heat demand for the year 2009.....	17
Table 3-2: Breakdown of industrial heat demand with detailed temperatures (100 and 500 °C)....	20
Table 3-3: Suitable sectors mentioned in prior potential studies.....	25
Table 4-1: Heat quantities for charging, discharging and night cooling of the STS.....	36
Table 4-2: Main parameters of the simulation model.....	43
Table 4-3: Measured and simulated heat quantities for 2011.....	44
Table 4-4: Simulated heat quantities for validated, design, and model without faults.....	47
Table 4-5: Considered parameters for the global sensitivity analysis.....	48
Table 4-6: Investigated cases for sensitivity analysis of the load profile.....	50
Table 5-1: Meteorological data for the selected locations.....	62
Table 5-2: Investigated temperature levels for dimensioning of collector field.....	70
Table 5-3: Collector parameters for each collector type.....	72
Table 5-4: Influence of collector type on q_{design}	74
Table 5-5: Influence of orientation and slope on q_{design}	75
Table 5-6: Influence of daily load profile on q_{design}	76
Table 5-7: Specific store volumes for different temperature levels.....	84
Table A-1: TRNSYS types used for the simulations.....	117
Table A-2: Values of daily load profiles used within simulations.....	118
Table A-3: Values of weekly load profiles used within simulations.....	118
Table A-4: Values of annual load profiles used within simulations.....	118
Table A-5: Simulated design values of q_{design}	120
Table A-6: Detailed results for dimensioning of heat store, Constant, Wuerzburg.....	121
Table A-7: Detailed results for dimensioning of heat store, 5 days peak, Wuerzburg.....	122
Table A-8: Detailed results for dimensioning of heat store, Constant, Madrid.....	123
Table A-9: Detailed results for dimensioning of heat store, 5 days peak, MAadrid.....	124
Table A-10: Detailed results for annual system yield for locations Copenhagen and Wuerzburg.....	126
Table A-11: Detailed results for annual system yield for locations Toulouse and Madrid.....	127
Table A-12: Detailed results for system yield (HP collectors) for Cop/Wue.....	129
Table A-13: Detailed results for system yield (HP collectors) for Tou/Mad.....	130

Annex

A TRNSYS types

Table A-1: TRNSYS types used for the simulations.

Type	Description	Remarks
2	Differential controller	Standard TRNSYS (Klein et al., 2009)
5	Heat exchanger: counter flow	Standard TRNSYS (Klein et al., 2009)
9	Data reader: free format	Standard TRNSYS (Klein et al., 2009)
11	Flow mixer / diverter / tempering valve	Standard TRNSYS (Klein et al., 2009)
14	Forcing function	Standard TRNSYS (Klein et al., 2009)
23	PID controller	Standard TRNSYS (Klein et al., 2009)
24	Quantity integrator	Standard TRNSYS (Klein et al., 2009)
25	Printer	Standard TRNSYS (Klein et al., 2009)
31	Pipe / duct	Standard TRNSYS (Klein et al., 2009)
65	Online plotter	Standard TRNSYS (Klein et al., 2009)
93	Input Value Recall	Standard TRNSYS (Klein et al., 2009)
109	Weather data reading and processing	Standard TRNSYS (Klein et al., 2009)
340	Multiport store model	Non-Standard (Drück, 2006)
803	Variable flow pump	TESS library (TESS, 2009)
805	Domestic hot water heat exchanger	Non-Standard (Heimrath et al., 2007)
832	832v307 - Dynamic collector model	Non-Standard (Haller et al., 2009)

Table A-3: Values of weekly load profiles used within simulations.

Profile										
	7 days	6 days	Constant week	5 days	5 days peak	G1	4 days row	4 days	Variable	
Daily demand [%]	1	100	100	100	100	120	100	100	100	120
	2	100	100	100	100	100	100	100	100	59
	3	100	100	100	100	100	100	100	0	26
	4	100	100	100	100	100	100	100	100	89
	5	100	100	100	100	100	100	0	100	77
	6	100	100	94	10	0	21	0	0	38
	7	100	0	84	0	0	17	0	0	0

Table A-4: Values of annual load profiles used within simulations.

Profile							
	Constant	Summer peak	Space heating	Summer only	Summer break	Variable peak	
Daily demand [%]	1	100	100	120	0	100	59
	2	100	100	120	0	100	60
	3	100	100	120	0/100	100	82
	4	100	100	110	100	100	76
	5	100	100	100	100	100	74
	6	100	120	100	100	100	82
	7	100	120	100	100	100	100
	8	100	100	100	100	0	81
	9	100	100	110	100	100	73
	10	100	100	110	0/100	100	67
	11	100	100	120	0	100	70
	12	100	100	120	0	100	69

C Design values for dimensioning of collector field

Table A-5: Simulated design values of q_{design} for different temperature levels, collector types, daily load profiles and location. Specific heat store capacity of 5 kWh/m^2_{Col} for Daytime and Constant and 7 kWh/m^2_{Col} for Heating bath.

Temp.	Collector	G1				Heating bath				G3			
		Cop	Wue	Tou	Mad	Cop	Wue	Tou	Mad	Cop	Wue	Tou	Mad
15..60 °C	FPC	4.2	4.2	4.8	4.8	4.0	4.0	4.4	4.4	4.0	4.0	4.4	4.6
	FPC-DG	4.6	4.6	5.0	5.0	4.4	4.4	4.6	4.8	4.4	4.4	4.8	5.0
	ETC	4.6	4.6	5.0	5.0	4.4	4.4	4.8	4.8	4.6	4.6	5.0	5.0
	CPC	4.2	4.2	4.4	4.4	4.2	4.2	4.4	4.4	4.4	4.4	4.6	4.6
15..80 °C	FPC	3.4	3.4	4.0	4.2	3.4	3.4	4.0	4.0	3.4	3.4	3.8	4.0
	FPC-DG	4.0	4.0	4.6	4.6	4.0	4.2	4.4	4.4	4.0	4.0	4.4	4.4
	ETC	4.2	4.2	4.6	4.6	4.2	4.2	4.4	4.6	4.2	4.2	4.6	4.6
	CPC	4.0	4.0	4.2	4.2	4.0	4.0	4.2	4.2	4.0	4.0	4.4	4.4
30..60 °C	FPC	4.0	4.2	4.6	4.6	4.0	4.0	4.4	4.6	4.0	4.0	4.6	4.6
	FPC-DG	4.4	4.6	5.0	5.0	4.4	4.4	4.6	4.8	4.4	4.6	5.0	5.0
	ETC	4.6	4.6	5.0	5.0	4.4	4.6	4.8	4.8	4.6	4.6	5.0	5.0
	CPC	4.2	4.2	4.4	4.4	4.2	4.2	4.4	4.4	4.2	4.2	4.6	4.6
30..80 °C	FPC	3.4	3.4	3.8	4.0	3.4	3.4	4.4	4.2	3.2	3.4	3.8	4.0
	FPC-DG	4.0	4.0	4.4	4.4	4.0	4.0	4.0	4.6	4.0	4.0	4.4	4.6
	ETC	4.2	4.2	4.6	4.6	4.2	4.2	4.6	4.6	4.2	4.2	4.6	4.6
	CPC	4.0	4.0	4.2	4.2	4.0	4.0	4.2	4.2	4.0	4.0	4.4	4.4
40..70 °C	FPC	3.6	3.6	4.2	4.2	3.6	3.6	4.0	4.2	3.6	3.6	4.2	4.2
	FPC-DG	4.2	4.2	4.6	4.6	4.0	4.2	4.6	4.6	4.2	4.2	4.6	4.6
	ETC	4.0	4.4	4.8	4.8	4.2	4.4	4.6	4.6	4.4	4.4	4.8	4.8
	CPC	4.0	4.0	4.4	4.4	4.0	4.0	4.2	4.2	4.0	4.2	4.4	4.4
40..90 °C	FPC	2.8	2.8	3.4	3.4	2.8	3.0	3.4	3.6	2.8	3.0	3.4	3.6
	FPC-DG	3.4	3.6	4.2	4.2	3.6	3.8	4.2	4.2	3.6	3.8	4.2	4.2
	ETC	4.0	4.0	4.4	4.4	4.0	4.0	4.4	4.4	4.0	4.0	4.2	4.2
	CPC	3.8	3.8	4.0	4.0	3.8	3.8	4.0	4.0	3.8	3.8	4.2	4.2
50..80 °C	FPC	3.0	3.2	3.6	3.8	3.0	3.2	3.6	3.8	3.0	3.2	3.6	3.8
	FPC-DG	3.8	3.8	4.2	4.4	3.8	3.8	4.2	4.2	3.8	3.8	4.2	4.4
	ETC	4.0	4.2	4.4	4.4	4.0	4.0	4.4	4.4	4.0	4.2	4.6	4.6
	CPC	3.8	3.8	4.2	4.2	3.8	3.8	4.2	4.2	3.8	4.0	4.2	4.2
60..90 °C	FPC	2.6	2.6	3.0	3.2	2.4	2.6	3.2	3.2	2.6	2.6	3.2	3.2
	FPC-DG	3.4	3.6	4.0	4.0	3.4	3.4	3.8	4.2	3.4	3.6	4.0	4.0
	ETC	3.8	3.8	4.2	4.4	3.8	3.8	4.2	4.2	3.8	4.0	4.2	4.4
	CPC	3.6	3.6	4.0	4.0	3.6	3.6	4.0	4.0	3.6	3.8	4.0	4.0
70..90 °C	FPC	2.4	2.4	2.8	3.0	2.2	2.4	2.8	3.0	2.4	2.4	2.8	3.0
	FPC-DG	3.4	3.4	3.8	3.8	3.2	3.2	3.6	3.8	3.2	3.4	3.8	3.8
	ETC	3.8	3.8	4.2	4.2	3.6	3.6	4.0	4.0	3.8	3.8	4.2	4.2
	CPC	3.6	3.6	3.8	4.0	3.6	3.6	3.8	3.8	3.6	3.6	3.8	3.8
80..95 °C	FPC	2.0	2.2	2.6	2.6	1.8	2.0	2.4	2.6	2.0	2.0	2.4	2.4
	FPC-DG	2.6	2.6	3.4	3.4	2.6	2.6	3.4	3.4	2.8	3.0	3.4	3.4
	ETC	3.4	3.6	4.0	4.0	3.4	3.4	3.4	3.6	3.4	3.4	3.8	3.8
	CPC	3.4	3.4	3.8	4.0	3.4	3.4	3.4	3.6	3.4	3.6	3.8	3.8

D Detailed results for dimensioning of heat store

Table A-6: Detailed results for dimensioning of heat store for weekly profile Constant and location Wuerzburg.

Weekly profile	Daily profile	q_{design}	q_{store}	15..60 °C				40..70 °C				60..90 °C			
				FPC	FPC-DG	ETC	CPC	FPC	FPC-DG	ETC	CPC	FPC	FPC-DG	ETC	CPC
Constant week	Daytime	4	1	46	48	49	48	34	40	44	44	22	32	38	38
			3	50	54	55	53	36	43	48	46	22	32	39	39
			5	51	55	56	53	36	43	48	46	22	32	39	38
			7	51	55	57	53	35	43	48	46	22	32	39	38
			9	52	55	57	53	35	43	47	45	22	31	38	38
		6	1	55	58	59	55	36	44	49	47	23	33	40	40
			3	55	59	59	55	36	44	49	47	23	33	40	39
			5	56	59	60	55	36	44	49	47	22	32	39	39
			7	56	59	60	55	36	44	48	46	22	32	39	38
			9	56	59	60	55	36	43	48	46	22	32	39	38
		10	1	57	60	61	56	37	45	49	47	24	34	41	40
			3	57	61	61	56	37	44	49	47	23	33	40	40
	5		58	61	61	56	37	44	49	47	23	33	40	39	
	7		58	61	61	56	37	44	49	47	23	33	39	39	
	9		58	61	61	56	36	44	49	47	22	32	39	38	
	Heating bath	4	3	41	44	46	45	30	36	40	40	19	29	35	35
			5	46	50	53	50	32	40	45	44	20	30	37	37
			7	48	52	54	51	33	41	46	44	20	30	37	37
			9	49	53	55	52	33	41	46	44	20	30	37	37
			3	42	46	48	46	30	36	40	41	19	29	35	36
		6	5	48	53	55	51	33	41	46	44	21	31	37	37
			7	51	55	56	53	34	42	47	45	21	31	38	37
			9	52	56	57	54	34	42	47	45	21	30	37	37
			3	43	46	49	47	31	37	41	42	20	29	36	36
5			50	54	56	52	34	41	46	45	21	31	38	38	
10		7	53	57	58	54	34	42	47	45	21	31	38	38	
		9	54	58	59	55	34	42	47	45	21	31	38	38	
	1	36	37	38	38	26	29	31	32	19	24	27	29		
	4	3	48	51	54	52	35	42	46	46	22	32	39	39	
		5	51	55	57	54	36	43	48	46	23	33	39	39	
7		52	56	57	54	36	43	48	46	22	32	39	39		
9		53	56	58	54	36	43	48	46	22	32	39	38		
6		1	44	45	46	46	32	36	39	40	22	29	34	35	
	3	53	57	59	55	37	44	49	47	23	33	40	40		
	5	56	59	60	56	37	45	49	47	23	33	40	39		
	7	57	60	60	56	37	44	49	47	23	33	40	39		
	9	57	60	61	56	37	44	49	47	23	32	39	39		
10	1	56	59	60	56	38	45	50	48	24	34	41	41		
	3	58	61	61	57	37	45	50	48	24	34	41	40		
	5	59	62	62	57	37	45	50	47	23	33	40	40		
	7	59	62	62	57	37	45	49	47	23	33	40	39		
	9	59	62	62	57	37	44	49	47	23	33	39	39		

Table A-7: Detailed results for dimensioning of heat store for weekly profile 5 days peak and location Wuerzburg.

Weekly profile	Daily profile	q _{design}	q _{store}	15..60 °C				40..70 °C				60..90 °C				
				FPC	FPC-DG	ETC	CPC	FPC	FPC-DG	ETC	CPC	FPC	FPC-DG	ETC	CPC	
5 days peak	Daytime	4	1	36	37	39	38	27	31	34	34	18	25	29	30	
			3	41	43	44	42	30	35	39	38	20	26	30	31	
			5	43	46	47	45	31	37	41	39	21	28	33	33	
			7	44	47	48	46	32	38	41	41	21	29	35	35	
			9	45	48	49	47	33	39	42	41	21	30	36	36	
		6	1	42	44	45	42	28	33	37	36	18	26	31	31	
			3	46	48	48	46	31	37	40	39	20	28	34	34	
			5	48	51	52	49	33	39	43	42	21	29	34	34	
			7	50	53	54	51	34	40	45	43	22	31	36	36	
			9	51	54	55	52	35	41	46	44	22	31	38	37	
		10	1	43	46	46	43	28	34	38	36	19	26	31	31	
			3	48	50	50	47	31	37	41	40	21	29	35	34	
			5	51	54	54	51	34	40	44	43	22	31	36	36	
			7	53	56	56	53	35	41	45	44	22	31	37	37	
			9	54	57	58	55	35	42	47	45	22	32	38	38	
		Heating bath	4	3	32	35	36	36	24	28	31	31	16	23	27	28
				5	38	41	43	42	27	33	37	36	19	26	31	32
				7	41	44	46	44	29	35	39	38	19	28	33	33
	9			43	46	48	46	31	36	40	40	19	28	34	34	
	3			33	36	37	36	24	28	31	31	16	23	28	28	
	6		5	40	43	45	43	28	33	38	36	19	27	32	32	
			7	44	47	49	46	30	35	40	38	20	29	34	34	
			9	46	50	51	49	32	37	42	41	20	29	36	36	
			3	34	37	38	37	25	28	32	32	17	24	28	29	
			5	41	44	46	44	28	34	38	37	19	27	32	32	
	10		7	46	49	50	48	31	36	41	40	20	29	35	35	
			9	49	52	53	50	32	38	43	42	20	30	36	36	
			1	29	30	31	31	22	24	26	26	15	20	23	24	
			3	40	42	44	43	29	35	38	38	20	28	32	32	
			5	43	46	48	46	32	37	41	40	21	29	33	34	
	Constant		4	7	45	48	50	48	33	38	42	41	21	30	36	36
				9	46	49	51	49	34	40	43	43	22	31	37	37
				1	35	36	37	37	25	29	32	32	18	24	27	29
		3		44	48	49	46	29	37	41	40	21	29	35	34	
		5		48	51	52	50	31	40	44	42	21	30	35	35	
		6	7	51	54	54	51	33	41	45	43	22	31	37	37	
9			52	55	56	53	35	42	46	45	22	32	38	38		
1			43	46	46	43	29	34	38	37	19	26	31	31		
3			49	51	51	48	32	38	42	40	21	29	35	35		
5			52	55	55	52	34	40	45	43	22	31	37	37		
10		7	54	57	57	53	35	42	46	44	22	32	38	38		
		9	56	58	59	55	36	43	47	45	22	32	39	38		

Table A-8: Detailed results for dimensioning of heat store for weekly profile Constant and location Madrid.

Weekly profile	Daily profile	Q _{design}	Q _{store}	15..60 °C				40..70 °C				60..90 °C				
				FPC	FPC-DG	ETC	CPC	FPC	FPC-DG	ETC	CPC	FPC	FPC-DG	ETC	CPC	
Constant week	Daytime	4	1	41	43	43	43	38	39	41	42	30	35	38	39	
			3	52	54	55	53	44	48	50	49	32	41	46	45	
			5	54	56	56	54	44	49	52	50	32	41	46	45	
			7	54	56	57	54	44	50	52	50	31	41	46	44	
			9	54	57	57	54	44	50	52	50	31	41	46	44	
		6	1	56	58	59	56	44	50	53	51	32	42	47	45	
			3	60	63	62	57	45	52	55	51	32	42	48	45	
			5	61	63	63	57	46	52	55	51	32	42	48	45	
			7	61	64	63	57	46	52	55	51	32	42	47	45	
			9	61	64	63	57	45	52	55	51	31	41	47	45	
		10	1	61	64	63	58	45	52	55	52	33	42	48	46	
			3	62	65	64	58	46	52	55	52	32	42	48	46	
			5	63	65	64	58	46	52	55	52	32	42	48	45	
			7	63	65	64	59	46	52	55	52	32	42	48	45	
			9	63	66	65	59	46	52	55	51	32	42	47	45	
		Heating bath	4	3	39	40	41	41	34	37	39	39	27	34	38	37
				5	48	50	51	50	42	46	48	48	29	39	44	43
				7	51	54	55	52	42	48	51	49	29	39	45	43
	9			53	55	56	53	42	48	51	49	29	39	45	43	
	3			41	43	44	43	33	34	36	39	27	34	38	38	
	6		5	51	55	56	53	42	46	48	49	30	39	45	43	
			7	55	59	59	55	43	50	53	50	30	40	46	44	
			9	57	61	61	56	43	50	54	50	30	40	46	44	
			3	41	44	46	44	35	36	37	41	27	35	39	39	
			5	53	57	58	54	41	48	50	49	30	40	45	44	
	10		7	57	61	61	56	44	51	54	51	31	41	47	44	
			9	60	63	63	57	44	51	54	51	31	41	47	44	
			1	31	32	32	33	26	27	28	29	22	25	27	28	
			3	49	50	52	51	42	46	48	48	31	41	46	44	
			5	53	55	56	54	44	49	52	50	32	42	46	45	
	Constant		4	7	54	57	57	55	45	50	52	50	32	41	46	45
				9	55	57	58	55	45	50	53	50	32	41	47	45
				1	38	40	40	41	33	34	36	37	29	32	34	35
		3		58	61	61	57	46	52	55	52	33	43	48	46	
		5		61	64	63	58	47	53	56	52	33	43	48	46	
		6	7	62	65	64	58	47	53	56	52	33	42	48	46	
9			62	65	64	58	46	53	56	52	32	42	48	45		
1			60	60	60	58	47	52	55	52	34	43	49	47		
3			64	66	65	59	47	54	56	52	33	43	49	46		
5			65	67	65	59	47	53	56	52	33	43	49	46		
10		7	65	67	66	59	47	53	56	52	33	43	48	46		
		9	65	67	66	59	47	53	56	52	33	42	48	45		

Table A-9: Detailed results for dimensioning of heat store for weekly profile 5 days peak and location Madrid.

Weekly profile	Daily profile	Q _{design}	Q _{store}	15..60 °C				40..70 °C				60..90 °C			
				FPC	FPC-DG	ETC	CPC	FPC	FPC-DG	ETC	CPC	FPC	FPC-DG	ETC	CPC
5 days peak	Daytime	4	1	34	33	33	34	29	31	32	33	23	28	30	30
			3	41	42	43	41	35	38	40	39	26	33	36	35
			5	43	44	45	43	36	40	42	40	27	34	35	36
			7	44	45	46	44	37	41	43	41	28	34	38	37
			9	45	46	47	45	38	42	43	42	29	36	40	39
			1	43	45	45	42	34	38	40	38	24	32	36	34
			3	48	49	49	45	37	41	44	41	27	35	39	38
			5	51	52	52	48	40	44	46	44	29	36	39	39
			7	52	54	53	50	41	46	48	46	30	38	43	41
		9	53	56	55	52	42	47	49	47	31	39	44	41	
		1	46	48	47	43	34	39	41	39	25	32	36	35	
		3	50	52	51	47	38	42	44	42	28	36	40	38	
		5	54	55	55	51	40	45	48	45	30	38	42	41	
		7	56	58	58	53	42	48	50	47	31	39	44	43	
		9	58	60	59	55	43	48	51	48	31	40	44	43	
		3	30	30	31	31	25	28	29	29	21	26	28	28	
		5	38	39	40	39	32	36	38	37	24	31	35	34	
		7	41	43	44	42	34	38	40	39	26	33	38	36	
	9	43	45	46	44	36	40	42	41	27	34	38	37		
	3	31	32	33	32	26	26	27	29	21	26	28	28		
	5	40	42	43	41	33	36	37	37	25	32	36	35		
	7	45	47	47	45	36	40	42	40	27	35	39	38		
	9	48	51	51	48	38	42	44	42	28	36	41	40		
	3	31	33	34	32	27	27	28	30	21	27	29	29		
	5	42	44	45	42	33	37	39	38	25	32	36	35		
	7	47	49	49	46	36	40	43	41	28	35	40	38		
	9	51	53	53	50	39	43	45	43	29	37	42	40		
	1	27	26	26	26	22	22	22	23	18	20	22	22		
	3	39	40	41	41	34	37	38	39	26	33	36	36		
	5	43	45	45	44	37	40	41	41	28	34	35	37		
	7	45	46	47	45	38	41	43	42	29	36	39	38		
	9	45	47	47	46	39	42	44	43	30	37	40	39		
	1	34	32	32	32	28	27	28	29	23	26	27	29		
	3	47	49	49	46	38	42	44	42	28	36	40	39		
	5	51	53	53	49	41	45	47	45	30	38	41	40		
	7	53	55	55	52	42	47	49	47	31	39	43	41		
9	55	57	57	53	43	48	51	48	31	40	44	42			
1	46	47	47	44	36	40	42	40	26	33	37	36			
3	52	54	53	49	39	44	46	43	29	37	41	39			
5	56	58	57	52	42	47	49	46	31	39	44	42			
7	58	60	59	54	43	49	51	48	32	40	45	44			
9	60	61	61	56	44	50	52	49	32	41	46	44			

E Detailed results for utilization and yield

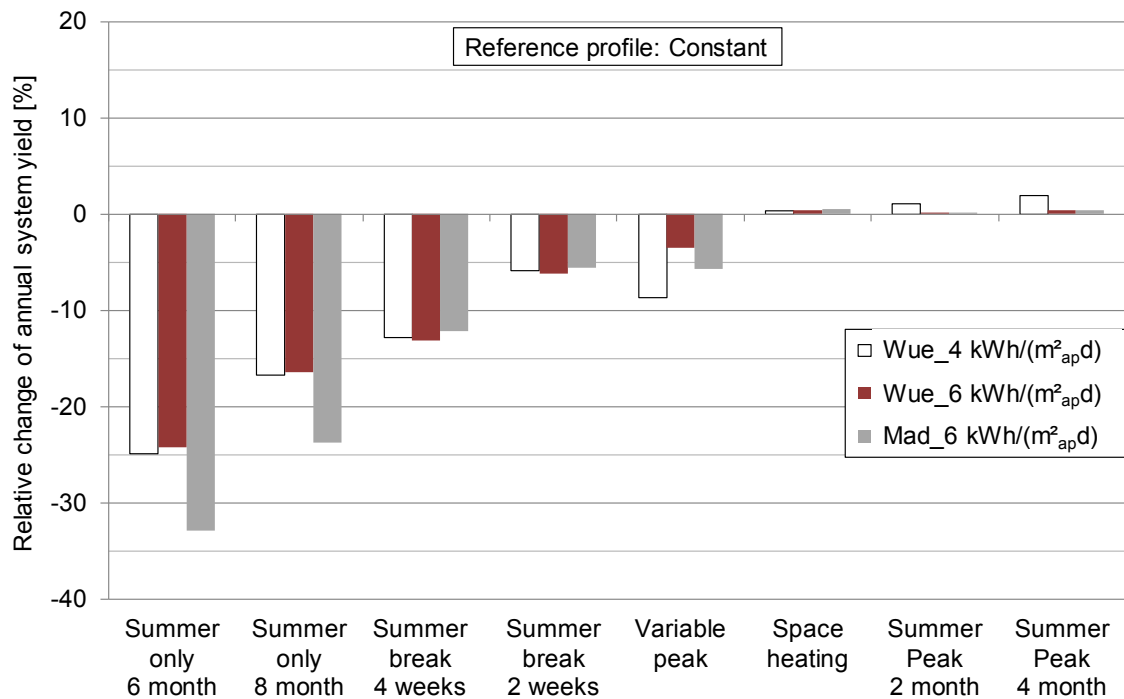


Figure A-1: Change of annual system yield for different annual load profiles, different available loads, process temperatures 40..70 °C, ETC_advanced and locations Wurzburg and Madrid.

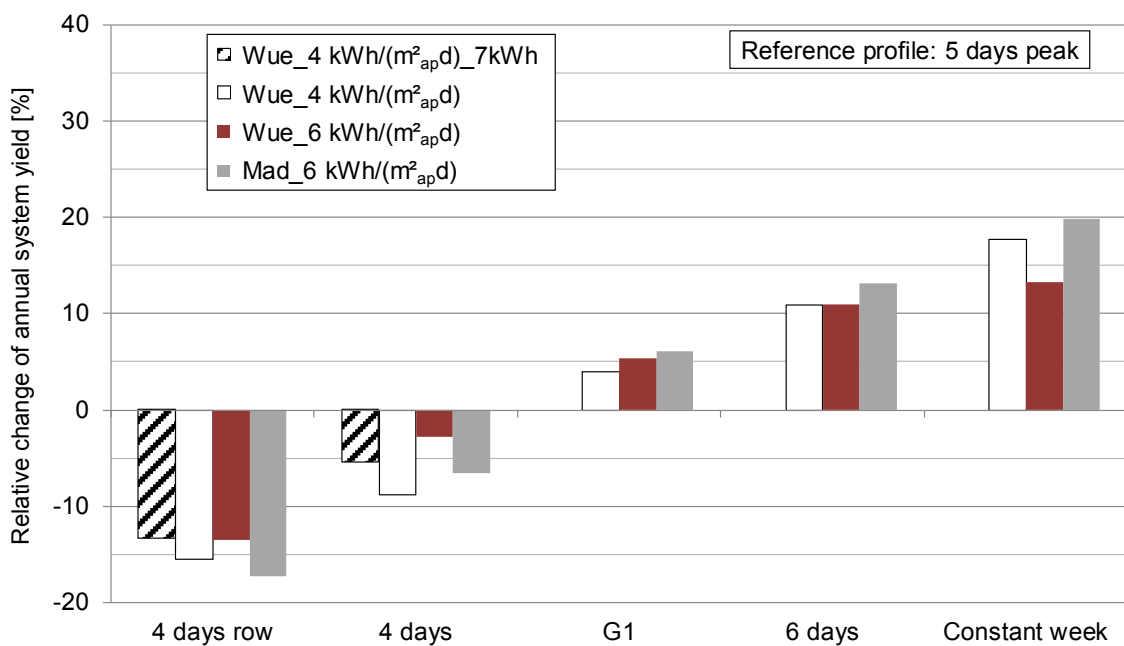


Figure A-2: Change of annual system yield for different weekly load profiles, different available loads, process temperatures 40..70 °C, ETC_advanced and locations Wurzburg and Madrid.

Table A-10: Utilization ratio for different daily and weekly profiles, constant annual profile, advanced collectors and locations Copenhagen and Wuerzburg; specific heat store capacity 3/5 kWh/m²_{ap} for daily profile Daytime and weekly profile Constant/5 days peak, 5 kWh/m²_{ap} daily profile Constant, and 7 kWh/m²_{ap} for daily profile Heating bath/vessel, a maximum temperature in the heat store of 110 °C was considered for maximum process flow temperatures 90 and 95 °C.

Temp.	Collector (advanced)	Copenhagen												Wuerzburg																							
		Constant week						5 days peak						Constant week						5 days peak																	
		Daytime	Heating b.	Constant	Daytime	Heating b.	Constant	Daytime	Heating b.	Constant	Daytime	Heating b.	Constant	Daytime	Heating b.	Constant	Daytime	Heating b.	Constant	Daytime	Heating b.	Constant															
30.0 °C	FPC	49	54	56	48	49	51	49	54	57	44	48	51	41	44	46	44	48	52	50	55	57	48	51	53	51	56	59	43	48	51	41	44	46	43	48	52
	FPC-DG	53	57	59	51	53	55	53	58	60	47	52	54	45	48	49	47	52	55	54	59	61	52	55	57	55	59	62	46	51	54	44	47	49	46	51	55
	ETC	55	58	60	53	55	57	55	59	60	48	52	55	47	50	51	49	53	56	55	59	60	54	56	58	57	60	62	47	51	54	46	49	50	48	52	55
30.80 °C	FPC	52	54	56	51	52	53	53	55	56	46	50	51	45	48	49	47	50	52	53	55	56	51	53	54	54	56	57	45	49	51	44	46	48	46	50	52
	FPC-DG	37	40	42	35	37	39	38	41	43	34	37	39	32	34	36	34	38	40	39	42	44	37	39	41	40	43	45	34	38	40	32	35	37	34	38	41
	ETC	44	47	48	42	44	46	44	47	49	39	42	45	37	40	42	39	43	45	45	49	50	44	46	47	46	49	51	38	42	45	37	39	41	39	43	46
40.70 °C	FPC	47	51	52	46	48	50	48	51	53	41	45	48	41	44	45	42	46	49	48	52	53	48	50	51	50	53	54	41	45	48	40	43	44	42	46	49
	FPC-DG	46	48	50	45	47	48	47	49	50	40	44	46	40	42	44	41	45	47	47	49	51	46	48	49	48	50	51	40	43	46	39	41	43	41	44	46
	ETC	33	34	35	31	32	32	34	35	35	31	32	33	29	30	30	31	33	33	36	36	37	33	34	34	36	37	37	32	33	34	29	30	31	32	34	34
40.90 °C	FPC	41	42	43	39	40	40	41	42	43	37	39	40	35	36	37	37	39	40	43	44	44	41	42	42	43	45	45	37	39	40	35	36	37	37	40	40
	FPC-DG	46	47	48	44	45	46	46	48	48	40	43	44	40	41	41	41	44	45	47	48	49	46	47	47	48	49	50	40	43	44	39	40	41	41	44	45
	ETC	45	46	46	43	44	44	45	46	46	40	42	43	39	40	41	40	43	43	46	47	47	44	45	45	46	47	47	40	42	42	38	39	40	40	42	43
50.80 °C	FPC	30	33	34	24	25	25	27	27	28	28	30	32	23	23	24	25	26	26	32	35	36	26	27	27	29	30	30	29	32	33	23	24	25	26	27	28
	FPC-DG	38	41	42	32	34	34	35	36	37	34	37	39	29	31	31	32	34	35	40	43	44	33	35	36	37	39	39	33	36	40	29	31	32	32	35	35
	ETC	43	46	47	37	39	40	41	43	43	38	41	43	33	36	37	37	39	40	45	47	48	38	41	42	43	44	45	37	40	43	32	35	36	37	39	40
50.90 °C	FPC	43	45	46	38	40	40	41	42	42	37	40	42	34	36	37	37	39	39	44	46	47	39	41	42	42	43	43	36	39	42	34	35	36	36	39	39
	FPC-DG	20	20	21	18	19	19	21	21	21	19	20	20	18	18	18	20	20	20	22	23	23	21	21	21	21	23	23	21	22	21	20	20	20	21	22	22
	ETC	30	31	31	28	29	29	30	31	31	28	28	29	27	27	28	28	29	30	32	33	33	30	31	31	33	33	33	28	29	31	28	29	29	28	30	31
60.90 °C	FPC	37	38	38	35	36	36	37	38	38	34	35	35	33	34	34	34	35	36	39	39	40	37	38	38	39	40	40	33	34	36	33	34	35	33	35	37
	FPC-DG	37	38	38	36	36	36	37	38	38	34	35	36	33	34	35	34	35	36	39	39	40	37	37	38	39	39	40	33	34	36	33	34	35	33	35	37
	ETC	10	10	11	9	9	9	10	10	10	10	10	10	8	9	9	10	10	10	12	12	13	11	11	11	11	11	12	12	11	12	12	10	10	10	12	12
80.95 °C	FPC	21	21	21	19	19	19	21	20	21	19	20	20	18	18	19	19	20	20	23	23	24	21	21	21	21	23	23	20	21	21	20	20	20	21	21	22
	FPC-DG	29	29	30	27	26	27	28	29	29	26	27	27	25	25	26	26	27	28	31	31	31	29	28	29	31	30	31	26	27	28	26	26	26	26	28	29
	ETC	30	30	31	28	28	28	30	30	30	27	28	28	26	27	27	27	28	29	32	32	32	29	29	30	31	31	31	27	27	29	27	27	27	27	28	29

Table A-11: Utilization ratio for different daily and weekly profiles, constant annual profile, advanced collectors and locations Toulouse and Madrid; specific heat store capacity 3/5 kWh/m²_{ap} for daily profile Daytime and weekly profile Constant/5 days peak, 5 kWh/m²_{ap} daily profile Constant, and 7 kWh/m²_{ap} for daily profile Heating bath/vessel. as described in Section 5.6, a maximum temperature in the heat store of 110 °C was considered for maximum process flow temperatures 90 and 95 °C.

Temp. °C	Toulouse												Madrid																								
	Constant week						5 days peak						Constant week						5 days peak																		
	Collector (advanced)	Daytime	Heating b.	Constant	Daytime	Heating b.	Constant	Daytime	Heating b.	Constant	Daytime	Heating b.	Constant	Daytime	Heating b.	Constant	Daytime	Heating b.	Constant	Daytime	Heating b.	Constant															
15, 60 °C	FPC	52	59	61	51	54	56	53	59	63	45	50	53	42	46	47	44	51	55	58	53	61	65	44	50	54	41	45	47	43	51	56					
15, 60 °C	FPC-DG	55	62	63	54	58	60	56	62	65	46	52	55	45	48	50	46	53	57	54	63	65	54	64	67	45	52	55	43	47	49	45	53	58			
15, 60 °C	ETC	56	61	62	56	59	60	57	62	64	47	52	55	46	49	50	48	53	56	56	61	63	55	59	61	45	51	54	44	47	49	45	53	57			
15, 60 °C	GPC	53	56	58	52	54	55	54	57	59	45	49	51	44	47	48	46	50	52	53	57	58	52	55	56	44	48	51	42	45	46	44	49	52			
15, 60 °C	FPC	42	47	49	41	44	46	43	48	50	36	41	43	35	37	39	37	41	44	44	49	51	43	47	49	46	51	54	35	38	41	37	43	47			
15, 60 °C	FPC-DG	47	52	54	47	50	52	49	53	56	40	45	47	38	41	44	40	45	49	47	55	57	48	52	55	50	56	58	40	45	48	38	41	44	40	46	50
30, 80 °C	ETC	50	54	56	50	53	55	52	56	58	42	46	49	41	44	46	42	47	50	51	56	57	50	55	57	52	58	60	41	46	49	40	43	45	41	47	51
30, 80 °C	GPC	48	51	53	48	50	51	50	52	53	40	44	47	39	42	44	41	45	48	49	53	54	49	51	53	50	54	55	39	44	47	39	41	43	40	45	48
30, 80 °C	FPC	40	41	42	38	39	40	41	42	43	35	37	38	33	34	34	35	38	38	44	45	46	42	43	44	44	44	47	37	39	40	34	36	37	41	42	
30, 80 °C	FPC-DG	46	49	49	45	47	47	47	49	50	40	42	43	38	39	39	40	43	44	48	52	52	48	50	51	49	53	53	40	44	45	38	40	40	40	45	47
40, 70 °C	ETC	50	52	52	49	51	51	51	53	54	42	45	46	40	42	43	42	46	47	52	54	54	51	53	54	52	56	56	42	46	48	40	42	43	41	47	49
40, 70 °C	GPC	48	49	50	47	48	48	49	50	50	41	44	44	39	41	41	41	44	45	49	51	52	49	50	51	50	52	52	40	44	45	39	40	41	41	45	46
40, 70 °C	FPC	36	40	41	30	32	33	34	35	35	31	35	37	26	28	29	30	31	32	39	43	45	33	36	37	38	39	40	32	37	40	27	30	31	32	35	36
40, 70 °C	FPC-DG	43	47	48	35	38	39	40	42	44	35	39	43	29	32	33	34	37	39	45	50	51	34	38	40	41	45	47	35	41	45	28	31	32	34	39	42
50, 80 °C	ETC	47	50	51	38	42	44	44	47	49	37	41	46	32	34	36	37	41	43	49	52	53	37	40	43	43	48	51	36	42	48	29	32	34	36	41	45
50, 80 °C	GPC	45	48	49	40	43	45	45	46	47	36	40	45	33	36	37	38	41	42	46	50	51	38	43	47	47	49	49	35	41	46	31	35	38	38	42	44
50, 80 °C	FPC	27	27	34	25	26	26	28	28	28	24	25	26	23	24	24	24	26	27	32	32	32	29	30	31	32	33	33	27	29	30	26	27	28	27	30	31
50, 80 °C	FPC-DG	37	38	52	35	36	36	38	38	39	31	33	35	31	32	33	31	34	36	41	42	42	39	40	41	42	43	43	33	37	38	33	35	35	33	38	39
50, 80 °C	ETC	43	43	44	42	42	43	44	45	45	35	37	40	36	37	38	35	38	41	46	46	47	45	46	47	46	48	49	35	39	42	38	39	40	35	41	44
50, 80 °C	GPC	42	43	49	41	41	42	42	43	43	34	36	39	35	37	37	34	38	40	45	45	46	43	44	44	44	45	46	34	39	41	36	38	38	35	40	42
60, 90 °C	FPC	16	16	17	14	14	14	16	16	16	14	15	15	14	14	14	14	15	15	21	20	21	19	19	19	20	20	21	18	19	19	18	18	18	19	20	
60, 90 °C	FPC-DG	28	28	29	26	26	26	28	28	28	24	25	26	23	24	24	24	26	26	33	33	33	31	31	31	31	33	33	27	29	29	27	27	27	27	30	30
60, 90 °C	ETC	35	35	35	33	33	33	35	36	36	29	30	32	29	29	29	30	32	33	39	39	39	35	35	36	40	40	40	31	33	35	31	31	32	31	35	36
60, 90 °C	GPC	36	36	36	34	34	34	35	35	36	29	31	33	30	30	30	30	31	33	39	39	39	37	37	38	39	39	39	31	34	35	32	32	31	34	36	

F Publications

The following publication list provides an overview of publications that result from the work for this thesis:

Lauterbach, C., Schmitt, B., Vajen, K., 2014. *System analysis of a low-temperature solar process heat system*. Solar Energy 101, 117–130.

Lauterbach, C., Schmitt, B., Jordan, U., Vajen, K., 2012a. *The potential of solar heat for industrial processes in Germany*, Renewable and Sustainable Energy Reviews, Volume 16, Issue 1, (pp. 5121 - 5130).

Schmitt, B., Lauterbach, C., Vajen, K., Reinl, K.-P., 2012b. *Pilotanlage zur Bereitstellung solarer Prozesswärme bei der Hütt-Brauerei*, Abschlussbericht zum Forschungsvorhaben „Thermische Solaranlage zur Prozesswärmebereitstellung in Verbindung mit der Implementierung eines neuen, energieeffizienten Kochverfahrens“, Förderkennzeichen: 0329609E.

Lauterbach, C., Schmitt, B., Vajen, K., 2012b. *Pilotanlage zur Bereitstellung solarer Prozesswärme bei der Hütt-Brauerei*, Proceedings of Gleisdorf Solar 2012, Gleisdorf, Österreich.

Schmitt, B., Lauterbach, C., Vajen, K., 2011. *Investigation of selected solar process heat applications regarding their technical requirements for system integration*. Proceedings ISES Solar World Congress Kassel, Germany.

Lauterbach, C., Javid Rad, S., Schmitt, B., Vajen, K., 2011a. *Feasibility assessment of solar process heat applications*. Proceedings ISES Solar World Congress Kassel, Germany.

Lauterbach, C., Schmitt, B., Jordan, U., Vajen, K., 2011b. *Solare Prozesswärme in Deutschland - Potential und Markterschließung*, 21. Symposium Thermische Solarenergie, Bad Staffelstein.

Lauterbach, C., Schmitt, B., Vajen, K., 2011c. *Das Potential solarer Prozesswärme in Deutschland*, Teil 1 des Abschlussberichtes zum Forschungsvorhaben „SOPREN – Solare Prozesswärme und Energieeffizienz“; Förderkennzeichen: 0329601T.

Lauterbach, C., Schmitt, B., Jordan, U., Vajen, K., 2010. *Potential for Solar Process Heat in Germany - Suitable Industrial Sectors and Processes*, Proc. EuroSun, Graz, Österreich.

Schmitt, B., Lauterbach, C., Jordan, U., Vajen, K., 2010. *Sustainable Beer Production by Combining Solar Process Heat and Energy Efficiency - Holistic System Concept and Preliminary Operational Experiences*, Proc. EuroSun, Graz, Österreich.

ISBN 978-3-86219-742-2